THESIS APPROVAL

GRADUATE SCHOOL, KASETSART UNIVERSITY

Doctor of Engineer (Environmental Engineering)

DEGREE

Environmental Engineering — **FIELD**

Environmental Engineering — **DEPARTMENT**

TITLE: Study of Fouling Mechanism and Fouling Indicators of Reverse Osmosis Membrane for Enhancing Reuse Potential of Wastewater from Textile Industry

NAME: Mr. Thirdpong Srisukphun

THIS THESIS HAS BEEN ACCEPTED BY

THESIS ADVISOR

(Associate Professor Chart Chiemchaisri, D.Eng)

COMMITTEE MEMBER

(Assistant Professor Monthon Thanuttamavong, Ph.D)

COMMITTEE MEMBER

(Associate Professor Wilai Chiemchaisri, D.Tech.Sc.)

COMMITTEE MEMBER

(Professor Kazuo Yamamoto, D.Eng.)

DEPARTMENT HEAD

(Assistant Professor Mongkol Damrongsri, D.Ing.)

APPROVED BY THE GRADUATE SCHOOL ON .....

DEAN

(Associate Professor Gunjana Theeragool, D.Agr.)

THESIS

STUDY OF FOULING MECHANISM AND FOULING INDICATORS OF REVERSE OSMOSIS MEMBRANE FOR ENHANCING REUSE POTENTIAL OF WASTEWATER FROM TEXTILE INDUSTRY

THIRDPONG SRISUKPHUN

A Thesis Submitted in Partial Fulfillment of
the Requirements for the Degree of
Doctor of Engineering (Environmental Engineering)
Graduate School, Kasetsart University
2009

Thirdpong Srisukphun 2008: Study of Fouling Mechanism and Fouling Indicators of Reverse Osmosis Membrane for Enhancing Reuse Potential of Wastewater from Textile Industry. Doctor of Engineering (Environmental Engineering), Major Field: Environmental Engineering, Department of Environmental Engineering. Thesis Advisor: Associate Professor Chart Chiemchaisri, D.Eng. 130 pages.

This research studied the fouling mechanism and developed mathematical model predicting flux decline during yarn and knit dyeing wastewater reclamation using reverse osmosis (RO) membrane. It was found that RO flux rapidly decreased at initial period of operation and slightly decreased in long-term. The main cause of fouling was the organic foulants and sequential cleaning using the alkaline solution followed by acid solution was the most effective procedure in this study. Flux decline corresponded to the mathematical expression using variable fouling index. The operation data of 7 days or more from bench-scale provided a promising agreement for predicting flux decline in long-term operation of larger scale system.

The non-ionic surfactant was found to be the major organic foulant. When its concentration was maintaining lower than the critical micelle concentration (CMC, 1.62 mM as C), permeate flux was influenced by the concentration. In contrary, the increasing surfactant concentration above CMC did not yield further flux decline due to the micellisation. The aggregation of effluent organic matters (EfOMs) & dye, EfOMs & surfactants, and dye & non-ionic surfactant enhanced flux. A mathematical model assuming competitive deposition of monomers and aggregates, which reduces fouling of monomers, could successfully predict RO flux. The important model parameters were the initial fouling time and the reduction of available site, which was proposed corresponding to the foulant concentration, and fouling coefficient.

_____ _____ ___ / ___ / ___

Student's signature Thesis Advisor's signature

ACKNOWLEDGEMENTS

I would like to grateful thank and am deeply indebted to Assoc. Prof. Chart Chiemchaisri, my thesis advisor, for advice, encouragement and valuable suggestions for completing the writing of this thesis. I would sincerely like to thank Asst. Prof. Monthon Thanuttamavong, Assoc. Prof. Wilai Chiemchaisri, and Prof. Kazuo Yamamoto, my thesis committees, and also Assoc. Prof. Thumrongrut Mungcharoen from Graduate School for their valuable comments and suggestions.

I gratefully thank Dr. Matsuo Kawasaki and WRPC's staff for kindly providing materials and experimental equipment for use in the first phase experiment. I am greatly indebted to Mr. Tetsuo Fujioka and Mr. Takeshi Sato for their advices and help.

I would like to sincerely thank Assoc. Prof. Taro Urase for his suggestions, encouragement and enthusiasm during study and research work of the second phase experiment in Japan. I give heartfelt thanks to my friends who made me feel alive in Japan: Dr. Pitiwat Watthanachai, Mr. Tanyanuparb Anantana, Dr. Korrakot Yaibuathet, Ms. Patima Sinthupinyo, and other Thai students in Tokyo.

This research was financially supported by Kasetsart University Research and Development Institute (KURDI) and by the Japan Society for the Promotion of Science (JSPS) Core university program in Environmental Engineering.

I deeply appreciate Dr. Nathiya Kreetachat, Dr. Torpong Kreetachat, Mr. Weerapong Rukapan, and Ms. Sukuma Chitapornpan, others friends in Environmental Engineering Laboratory, my parents, and my wife for their encouragement and help. Finally, I am deeply treasured to my daughter who always gives me heartfelt love during my graduate study.

Thirdpong Srisukphun

Febuary 2009

TABLE OF CONTENTS

LIST OF TABLES

LIST OF FIGURES

LIST OF FIGURES (Continued)

LIST OF FIGURES (Continued)

LIST OF ABBREVIATIONS

A	=	membrane area
ATP	=	adenosine tri phosphate
b	=	reduction rate of available site
BOD_5	=	biological oxygen demand for 5 days
C	=	cake concentration
C_b	=	concentration in bulk
C_m	=	concentration at membrane surface
C_p	=	concentration in permeate-water
COD	=	chemical oxygen demand
cm/s	=	centimeter per second
cm^2	=	square centimeter
CFU	=	colony forming units
CFV	=	cross-flow velocity
CMC	=	critical micelle concentration
D	=	diffusion coefficient
EC	=	electrical conductivity
EC_c	=	electrical conductivity of concentrate-water
EC_f	=	electrical conductivity of feed-water
EC_p	=	electrical conductivity of permeate-water
EDTA	=	ethylene diamine tetra acetic acid
EfOMs	=	effluent organic matters
EPS	=	extra-cellular polymeric substance
HCl	=	hydrochoric acid
HPC	=	heterotrophic plate counts
I	=	fouling index
I_o	=	initial fouling index
ICP-MS	=	inductively coupled plasma mass spectrometry
J	=	permeate flux
J_1	=	flux at 1 h
J_{24}	=	flux at 24 h

LIST OF ABBREVIATIONS (Continued)

J_s	=	solute flux
J_v	=	solvent flux
$J_{w, i}$	=	initial pure water flux of fresh membrane
$J_{w, f}$	=	initial pure water flux of fouled membrane
$J_{w, w}$	=	initial pure water flux of washed membrane
k	=	mass transfer coefficient
L	=	specific flux
L/min	=	liter per minute
m/d	=	meter per day
m/d-MPa	=	meter per day per mega pascal
m^{-1}	=	per meter
m^{-2}	=	per square meter
m^2	=	square meter
m^3/kg	=	cubic meter per kilogram
MBR	=	membrane bioreactor
mg/L	=	milligram per liter
min	=	minute
MF	=	micro-filtration
MFI	=	modified fouling index
MFI-NF	=	modified fouling index using nano-filtration membrane
MFI-UF	=	modified fouling index using ultra-filtration membrane
mL	=	milliliter
MWCO	=	molecular weight cut off
n	=	order of reaction rate
NaCl	=	sodium chloride
NaOH	=	sodium hydroxide
NF	=	nano-filtration
NFR	=	normalized fouling rate
R_a	=	hydraulic resistance due to adsorption
R_c	=	hydraulic resistance due to cake formation

LIST OF ABBREVIATIONS (Continued)

R_{cp}	=	hydraulic resistance due to concentration polarization
R_f	=	foulant resistance
$R_{f, f}$	=	foulant resistance before washing
$R_{f, w}$	=	foulant resistance after washing
R_m	=	hydraulic resistance due to membrane itself
$R_{m, 1}$	=	calculated hydraulic resistance of fresh membrane from pure water flux
$R_{m, 24}$	=	calculated hydraulic resistance of fouled membrane from pure water flux
R_p	=	hydraulic resistance due to plugging
R_t	=	total hydraulic resistance
RO	=	reverse osmosis
RR	=	resistance removal efficiency
SA	=	commercial soaping agent
SBS	=	sodium meta-bisulfite
SDI	=	silt density index
SDS	=	sodium dodecyle sulfate
SEM	=	scanning electron microscopy
SS	=	suspended solids
SSE	=	sum of square error
t	=	filtration time
t_o	=	initial fouling time due to adsorption
T	=	temperature, degree Fahrenheit
T_f	=	the second filtration time in SDI measurement
T_i	=	the first filtration time in SDI measurement
T_t	=	15 minute
TDC	=	total direct cell count
TKN	=	total kjeldahl nitrogen
TMP	=	trans-membrane pressure
TP	=	total phosphorus

LIST OF ABBREVIATIONS (Continued)

TX	=	triton X-100
UF	=	ultra-filtration
V	=	filtration volume
$\Delta J/\Delta V$	=	fraction of flux decline per accumulative volume
ΔP	=	net pressure
ΔR_F	=	irreversible resistance
$\Delta\pi$	=	net osmotic pressure
$\Delta\pi_{m,\,1}$	=	calculated net osmotic pressure at membrane surface from flux at 1 h
$\Delta\pi_{m,\,24}$	=	calculated net osmotic pressure at membrane surface from flux at 24 h
$\Delta\pi_{m,\,NaCl}$	=	net osmotic pressure at membrane surface due to sodium chloride
$\Delta\pi_{m,\,organic}$	=	net osmotic pressure at membrane surface due to organic foulant
$\Delta\pi_m$	=	total net osmotic pressure at membrane surface
α	=	specific cake resistance
β	=	fouling coefficient
γ	=	reduction coefficient
δ	=	boundary layer
η	=	dynamic viscosity
μm	=	micro meter
μS/cm	=	micro semen per centimeter
θ_T	=	total occupied site
$1-\theta_T$	=	total non-occupied site
π	=	osmotic pressure
σ	=	reflection coefficient

STUDY OF FOULING MECHANISM AND FOULING INDICATORS OF REVERSE OSMOSIS MEMBRANE FOR ENHANCING REUSE POTENTIAL OF WASTEWATER FROM TEXTILE INDUSTRY

INTRODUCTION

Fresh water shortage and land subsidence have been serious problems in middle and eastern region of Thailand. Huge requirement of industrial water consumption leads to substantial land subsidence because of excessive underground extraction. Textile industry is one of the major industries consuming approximately 26 % of total water quantity of industrial use. Underground water is pumped and used in every production processes i.e., desizing, scouring, bleaching, mercerizing, dyeing, and final finishing (Chen *et. al.,* 1997). Water consumption rate of textile industry ranges from 0.2 to 0.5 m^3/kg of finished product (Marcucci *et. al.*, 2001).

Presently, reclamation of wastewater is a foremost opportunity in solving these problems. Reverse osmosis (RO) membrane is widely used in water supply and industrial wastewater reuse including textile industry (Sójka-Ledakowicz, 1998; Suksaroj *et.al.*, 2005) because of its exceptional efficiency. Product from this system has high quality for use in many reclamation purposes such as cooling tower, boiler, cleaning, and dyeing etc. Nevertheless, this system still has an obstacle in membrane fouling issue that lead to short lifetime and high maintenance cost. Chemical cleaning cannot completely remove the foulant layer from the membrane surface, resulting in a long–term irreversible flux decline even if the textile effluents were treated by membrane bioreactor (MBR).

Membrane fouling has adversely affected plant performance both in terms of quantity and quality. It increases the operating cost of reuse system due to an increase in overall resistance as reflecting by increasing trans-membrane pressure (TMP), routine-cleaning cycles, channeling problems in hollow fiber bundles, corrosive by-

product from microorganism, and increased salt passage (Barker and Dudley, 1998; Al-Ahmad *et al.*, 2000; Brauns *et al.*, 2002; Chang *et al.*, 2002). Membrane elements can also be damaged by acid produced from an attached microorganism on membrane. Increasing biofilm on RO membrane lead to increasing salt passage through the membrane and poor quality permeate because it reduces turbulent flow and increases concentration polarization (Al-Ahmad *et al.*, 2000). In the case of hollow fiber bundles channeling problem is occurs when individual fibers become bound with foulant such as biofilm or scaling (Barker and Dudley, 1998).

In order to enhance reuse potential of wastewater from textile industry, study of fouling mechanism on reverse osmosis membrane is necessary. Moreover, in the past, many researchers studied effect of surfactants added in feed-water on efficiency of porous membrane like ultra-filtration (UF) and micro-filtration (MF). The micellisation and aggregation between surfactants and other impurities showed positive effect on pollutant rejection, membrane flux or both (Chilukuri *et.al.*, 2001; Purhait *et.al.*, 2004). Nevertheless, the mechanism of pollutant rejection and RO flux decline and fouling indicators have not been well described.

This research focuses on the study of the fouling mechanism, the effective cleaning procedure, the fouling cause, and the effect of interaction between organic foulant in textile wastewater on RO flux decline. Both real treated wastewater from textile industry and synthetic wastewater were used in the investigation.

OBJECTIVES

The objectives of this study are:

1. To study the fouling behavior and cause of RO membrane fouling during textile wastewater reclamation

2. To study the fouling mechanism and effect of foulant interaction on flux decline.

3. To develop a mathematical model for predicting RO membrane flux applied to textile wastewater.

SCOPES OF WORK

1. The experimental investigation for fouling behavior and cause of RO membrane fouling was conducted using real treated textile wastewater collected from the membrane bioreactor (MBR) of yarn and knit dyeing factory.

2. The experimental investigation for fouling mechanism and effect of foulant interaction on flux decline was conducted using synthetic wastewater representing treated wastewater by membrane bioreactor (MBR).

LITERATURE REVIEW

1. The constituents of textile wastewater

Wastewater from textile industry consists of two mainly parts i.e., 1) preparation process and 2) dyeing process. Most wastewater is discharged from preparation process and has variable constituents according to the type of products. The constituents of dyeing process wastewater consist of dyes, salts, and surfactants (Jiraratananon *et al.*, 2000; Koyuncu, 2002). The effluent from preparation process always contains oxidizing agent, surfactant, sodium hydroxide, and discarded fiber in wastewater. The variable constituents of wastewater from textile industries rely on types of product, surfactant, and dye. **Table 1** shows types of dye and physical/chemical characteristics (Buckley, 1992). **Table 2** shows the characteristic of textile wastewater from each process.

2. Membrane fouling during textile wastewater reclamation

Fouling on RO membrane during textile wastewater reclamation can be distinguished into four different types, i.e. organic fouling, particulate or colloidal fouling, scaling or inorganic fouling, and biofouling.

2.1 Organic fouling

Organic fouling occurs from attachment, plugging, and covering by organic matter from feed-water on membrane surface or wall of membrane pore (Judd and Jefferson, 2003). In the case of treated textile wastewater, surfactant, dye, and effluent organic matter (EfOMs) are the primary constituents. (Chen et al., 1997)

Table 1 Types of dye and product.

Type of dye	charge	Type of fiber	Dyeing process
1. Acid dye	Anionic charge	Nylon Woolen	- Soak fiber in acid solution (pH 3-5) - Dye anionic fiber at 50-110 ^{O}C
2. Metal complex acid dye	Anionic charge	Nylon Woolen	- Soak fiber in low strength acid solution (pH 5-7) - Dye anionic fiber at 50-110 ^{O}C
3. Direct dye	Anionic charge	Cotton Viscous	- Soak fiber in low strength alkaline solution - Add sodium chloride and sodium sulfate in solution - Dye at 98 ^{O}C
4. Basic or cationic dye	Cationic charge	Acrylic	- Soak fiber in acid solution (pH 4-6) - Add dyestuff and increase temperature to 100-105 ^{O}C
5. Disperse dye		Polyester Nylon Acrylic Cellulose Acetate	- Soak fiber in acid solution (pH 4-5) - Add dyestuff and increase temperature to 130 ^{O}C
6. Reactive dye	Anionic charge	Cotton Viscous Woolen	- Soak fiber in acid solution - Add sodium chloride for dispersing dyestuff to fiber - Add alkaline solution to occur reaction between dyestuff and fiber
7. Azoic dye		Cotton Viscous	- Dilute dyestuff in alkaline solution with sodium sulfate - Dyestuff disperse to fiber
8. Vat dye		Cotton Viscous	- Dilute dyestuff in alkaline solution with sodium sulfur - Dyestuff disperse to fiber
9. Mordant or Chrome	Anionic charge	Woolen	- Soak fiber in acid solution - Add sodium dichromate, dyestuff and increase temperature to 98 ^{O}C

Source: Adopted from Buckley (1992)

Table 2 Characteristic of textile wastewater.

Parameter	Wastewater from preparation process[1]			Textile wastewater[2]
	Bleaching	Mercerizing	Washing	
Temperature (^{O}C)	63	56.8	60.5	44.9
pH (-)	9.34	8.58	10.3	9.2
EC (µm/cm)	1,770	15,200	5,170	3,640
BOD_5 (mg/L)	N/A	855	57.5	148
COD (mg/L)	946	2,430	908	300
SS (mg/L)	26.6	82.7	67.8	30.9
Color (Pt-Co)	346	157	1,168	239
Cl^- (mg/L)	291	305	514	677
TDS (mg/L)	1,370	10,500	2,8400	2,250

Source: [1] Sirisongthum *et al.* (2004), [2] Saiviwat and Fujioka (2004)

1) Surfactants

(1) Surfactant in textile industry

Generally, surfactants can be separated into four categories i.e., anionic surfactant, cationic surfactant, nonionic surfactant, and Amphoteric surfactant or (Zwitterionics). Surfactant molecule can be separated into two parts i.e., hydrophilic head and hydrophobic tail (Doulia et al., 1997). In the case of textile industry, non-ionic and anionic, are commonly used in production process.

Non-ionic surfactant is difficult to be degraded by biological processes (Carvalho, et. al., 2002) therefore; it becomes a major foulant in treated textile wastewater. The hydrophilic property of surfactant molecule depends on amount of ethoxy group, $(CH_2CH_2O)_n$. Hydrophobic tail or lipophilic is a hydrocarbon chain (Muller, 1994; Doulia et al., 1997).

Anionic surfactant presents anionic charge on the hydrophilic head therefore; RO membrane fouling caused anionic surfactant is not severe due to the repulsive force of negative charge. Nevertheless, it can deposit on membrane surface by the hydrophobic adhesion (Kaya et al., 2006) because the hydrophobic adhesion always stronger than the anionic repulsive force (Childress and Elimelech, 2000). The fouled membrane caused by anionic surfactant becomes more hydrophilic due to the orientation of hydrophilic head towards the aqueous solution (Jőnsson and Jőnsson, 1991; Cornelis et. al., 2005).

(2) Surfactant properties affecting membrane fouling

The important properties of surfactant that affect fouling mechanism are critical micelle concentration (CMC) and could point. CMC is defined as the certain concentration that physico-chemistry properties of solution change such as detergency, density, surface tension, osmotic pressure, conductivity and interfacial tension (Adamson, 1990; Mietton-Peuchot and Ranisio. 1997) because the surfactant monomers associate each other and form aggregate namely micelle (Kim et al., 1998).

Could point is the temperature the solution containing non-ionic surfactant becomes heterogeneous and presents cloudy suspension form (Mietton-Peuchot and Ranisio. 1997). This temperature depends on hardness of solution.

(3) Mechanism of surfactant fouling on membrane surface

During reclamation of wastewater by RO membrane, surfactant forms a fouling layer on the membrane surface by hydrophobic interaction (Kim, et. al., 1998). Fouling mechanisms of surfactants rely on variable properties at CMC. When its concentration is below CMC, surfactant appears as monomer form in the wastewater (Adamson, 1990). Hydrophobic adhesion between surfactant monomers and the hydrophobic membrane always presents at high strength. Hence, the hydrophobic tails of the surfactant monomers easily associate themselves with the hydrophobic surface of membrane and turn the hydrophilic heads against the bulk. In

contrary, when its concentration is higher than CMC, it causes fouling by a concentration polarization and leads to colloidal formation in water (Mietton-Peuchot and Ranisio, 1997). The fouling mechanism of surfactant is illustrated in **Figure 1**. Møller and Maire (1993) reported that surfactant molecules adsorbed on membrane as monolayer. The adsorbed monolayer is illustrated into three characters as shown in **Figure 2**.

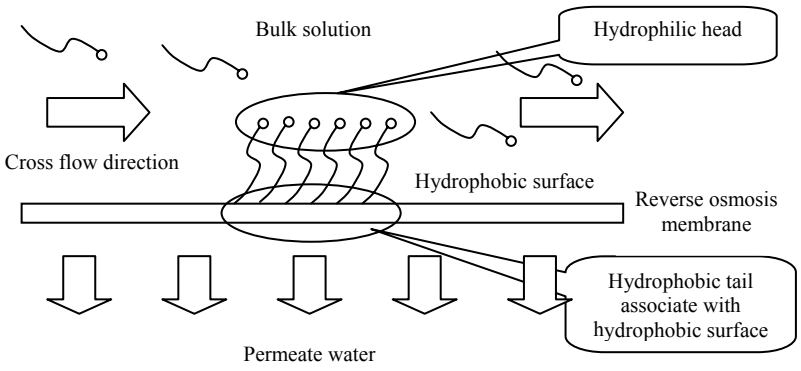

Figure 1 Organic fouling on reverse osmosis membrane due to surfactants

Source : Adopted from Thanuttamavong (2002a)

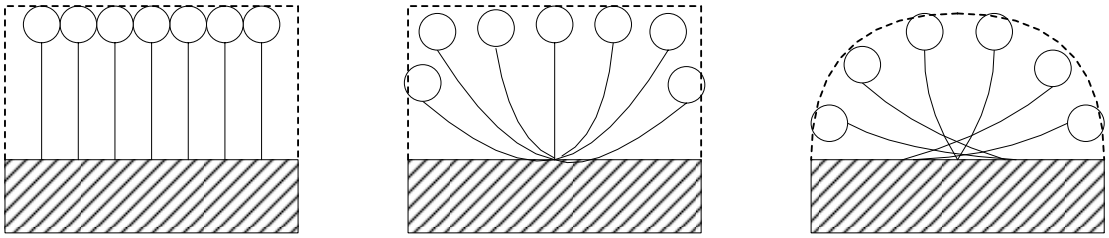

Figure 2 Adsorbed monolayer of surfactant molecule on membrane surface

Source: Adopted from Møller and Maire (1993)

(4) Rejection efficiency of surfactant

Rejection efficiency of surfactant relies on the hydrophobic property of membrane surface, size of surfactant, and trans-membrane pressure (TMP) (Kim et al., 1998). High rejection is obtained in the case where membrane with high hydrophobic property, low TMP, and large size of surfactant are applied.

2) Dyes

Dye is the major constituent of textile wastewater because up to 50% of the unfixed dye is discharged as wastewater (Jiraratananon et.al., 2000). The important dye contained in treated textile wastewater from MBR is reactive dye because of its solubility. The properties of reactive dye are soluble anionic dye which contains one or more reactive groups capable of forming a covalent bond with hydroxyl groups in the fiber (Sostar-Turk et.al., 2005).

Dye fouling is affected by charge properties, salt concentration, and cross-flow velocity (CFV) (Jiraratananon, *et.al.*, 2000; Koyuncu, 2002). High CFV decreases concentration polarization and increases percentage rejection (Chakraborty et. al., 2003). In wastewater containing low salt concentration, removal efficiency and permeate flux hinge upon CFV. In contrary, at high salt concentration, dye forms colloid and the role of CFV is decreased (Kim *et. al.*, 1998). Moreover, negatively charged membrane gives higher salt and dye removal efficiency than neutrally charged membrane but it yields rapid fouling due to the concentration polarization (Jiraratananon, *et.al.*, 2000). Furthermore, Tang and Chen (2002) reported that applying high pH water to NF membrane, the negatively charged property on membrane surface decreased but the neutral pH water and dye did not change its charged property. Increasing recovery ratio and operating temperature decrease salt rejection but do not affected COD and dye rejection (Sójka-Ledakowicz et. al., 1998).

3) Effluent organic matters (EfOMs)

EfOMs within treated textile wastewater from biological treatment process consist of microbial products such as an extra-cellular polymeric substance (EPS) and remaining non-biodegradable organic matters. EfOMs contain both hydrophobic and hydrophilic fractions. These organic matters tend to adsorb on the membrane surfaces and become a food supply for microorganisms especially in nutrient rich environments (Tansel *et.al.*, 2006). Fouling of EfOMs and surfactants were similar as shown in **Figure 1**.

The fouling and rejection mechanism of wastewater containing salt, inorganic, and dye is illustrated in **Figure 3**. Salt concentration in feed-water leads to higher fouling potential for dyeing wastewater due to cation species associate with negatively charged surface (Jiraratananon *et al.*, 2000). In addition, repulsive force between opposite species is reduced. Subsequently, this situation allows some small anion species to pass through membrane surface but larger anion species are filtrated by sieving mechanism. Then salt and color rejection decrease (Tang and Chen, 2002).

2.2 Particulate and colloidal fouling

Particulate and colloidal fouling occurs from accumulation of suspended solids from feed-water on membrane surface. Silt density index (SDI) is employed to evaluate the particulate fouling potential of feed-water. Pretreated unit such as slow-sand filter, coagulation, and MF is used to prevent this problem. Also, applying a turbulent condition around membrane surface can also reduce this problem (Judd and Jefferson, 2003) because of the increasing of shear force above membrane surface and dropping off concentration polarization (Chiemchisri *et al.*, 1992; Li *et al.* 1998; Chakraborty *et al.*, 2003).

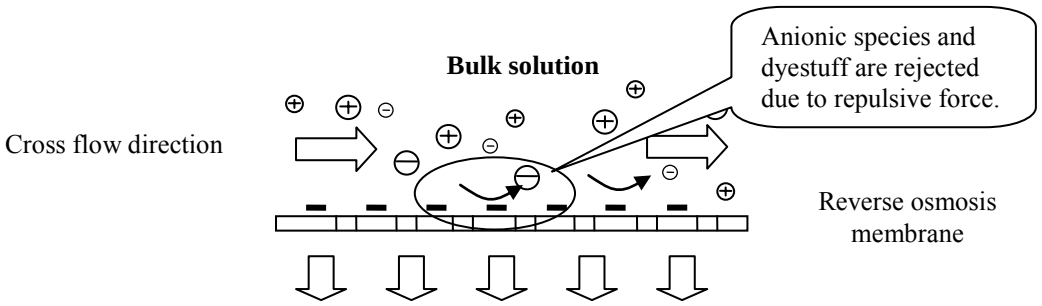

1. Anionic species and dyestuff are rejected due to repulsive force from charge of membrane.

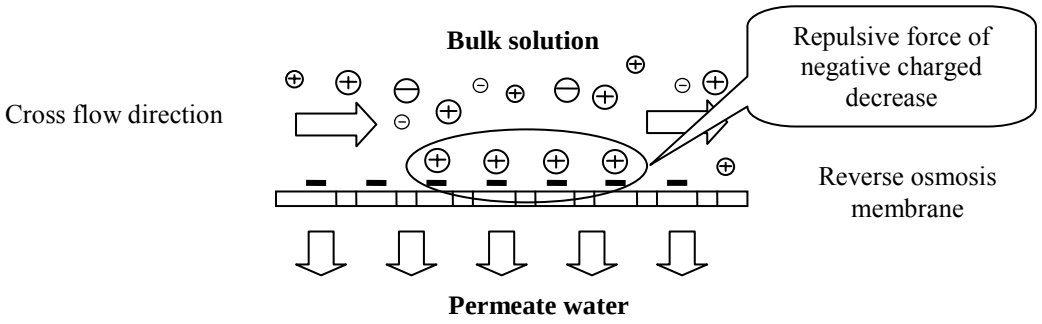

2. Cationic species associate with negative charged of membrane surface.

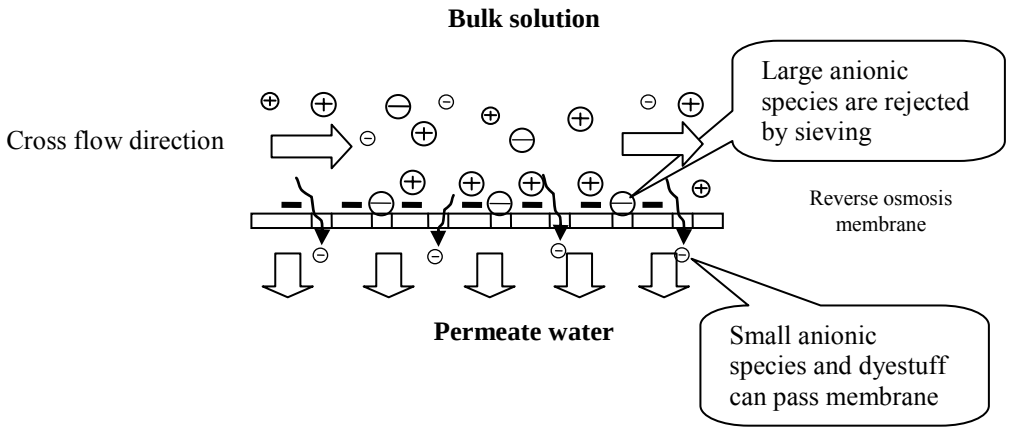

3. Salt and color rejection reduce due to decreasing of repulsive force.

Figure 3 Dye fouling and rejection on reverse osmosis membrane

Silt density index (SDI) is used to evaluate the amount of contaminated particles in feed water. Feed-water with high concentration of suspended solids yields high SDI-value and high fouling potential. It is used to ensure that particle and colloid from feed water do not affect RO and nano-filtration (NF) system (Osmoics Inc., 2003), RO feed water should have SDI lower than 3 (Metcalf & Eddy, 2003). But this indicator cannot predict the rate of flux reduction (Boerlage *et al.*, 2000) therefore, examinating only SDI-value is not enough for evaluating fouling potential of RO feed-water.

SDI can be measured by filtration of feed water through a 0.45 μm microfiltration membrane in a dead end membrane filtration unit and pressure is controlled at 2 bars (Hydranautics, 1998; Boerlage *et al.*, 2000). Record the time taken to fill a 500 mL graduated cylinder (T_i, min). Filtration continuous for another 15 minutes (T_t, min). Repeat the procedure and record the time for the second filtration (T_f, min). Calculate SDI using the following equation (Hydranautics, 1998; ASTM D4189-95).

$$SDI = \frac{100x\left(1-\frac{T_i}{T_f}\right)}{T_t} \qquad 1)$$

Another well-known indicator for assessment of the particulate fouling potential is the modified fouling index (MFI). MFI is developed from the resistance in series model and can be described as the flux decline in RO system caused by the hydraulic resistance (Schafer, *et al.*, 2005). The total hydraulic resistance (R_t) consists of the resistance due to membrane itself (R_m), the resistance due to concentration polarization (R_{cp}), the resistance due to adsorption (R_a), the resistance due to plugging (R_p), and the resistance due to cake formation (R_c) as shown in **Equation 2**.

$$J = \frac{\Delta P}{\eta(R_m + R_{cp} + R_a + R_p + R_c)} \quad 2)$$

Measurement of MFI can be done by recording permeate volume every 30 s over 15 min. MFI is determined from the gradient of the linear legion in the plot of t/V and V as presented in **Equations 3 and 4** (Boerlage *et al.*, 2000; Mulder, 2000; Metcalf & Eddy, 2003).

$$\frac{t}{V} = \frac{\eta R_m}{\Delta P A} + \frac{\eta I}{\Delta P A^2} V \quad 3)$$

$$MFI = \frac{\eta I}{\Delta P A^2} \quad 4)$$

Many researchers developed MFI to assess the fouling potential of feed water on RO/NF membrane. Modified fouling index using UF membrane (MFI-UF) is developed from conventional MFI by Boerlage *et al.* (2000) to assess fouling potential from smaller particles in treated feed water. This method is much more suitable to assess fouling potential for RO system (Vrouwenvelder *et al.*, 2003), because pretreated feed water usually has particle size smaller than average pore size of 0.45 μm MF (Boerlage *et al.* 2000). Moreover, Khirani, *et al.* (2006) proposes MFI-NF using NF membrane. Soluble foulant can also be assessed in this measurement.

2.3 Inorganic fouling and scaling

Scaling is the fouling caused by precipitation of low solubility inorganic foulant on membrane surface. The precipitation appears in conditions of high pH and concentration polarization (Judd and Jefferson, 2003), especially in case of a negatively charged membrane (Ghayeni *et al*., 1996). Scaling can be prevented by feeding antiscalant and acid into RO feed water.

Type of scaling can be investigated by autopsy. The fouled membrane is cut and the inorganic compounds concentration which deposit and accumulate on membrane surface are measured by ICP-MS (inductively coupled plasma mass spectrometry) analysis (Vrouwenvelder and van der Kooj, 2001). Also scanning electron microscopy (SEM) is used to identify deposits of crystal organic foulant and biofilm on membrane surface (Butt *et al.*, 1997; Khedr, 1998).

2.4 Biological fouling or biofouling

Biological fouling or biofouling occurs from coverage of biofilm on membrane surface. Vrouwenvelder and Van Der Kooij (2002) defined that "The biofouling is an accumulation of biomass on a surface by growth and/or deposition to such a level that is causing operational problems". Moreover, Dolan (2002) defined that "A biofilm is an assemblage of microbial cells that is irreversibly associated (not removed by gentle rinsing) with a surface and enclosed in a matrix of primarily polysaccharide material."

Biofouling decreases the overall performance of membrane filtration (Brauns *et al.*, 2002). Bacteria from feed water grow and develop a biofilm that covers the membrane surface leading to decreasing plant performance (Griebe and Flemming, 1998; Vrouwenvelder and Van der Kooij, 2001; Brauns *et al.*, 2002; Visvanathan, 2002). The important factors of biofouling development are the properties of membrane surface, the amount of microorganism, biodegradable compounds (substrate and nutrient), and hydrodynamics.

The mechanism of biofouling can be explained by the formation of biofilm on the membrane surface starting from clean a membrane to stabilized biofilm thickness. Mechanism of biofouling consists of four sizable phases: 1) adhesion phase, 2) reaction phase, 3) biofilm growth phase, and 4) detachment phase.

1) Adhesion phase

Adhesion phase is similar to particulate fouling and organic fouling, because this phase is caused by deposition of particles: microorganism and organic matters on membrane surface. Furthermore, it is the beginning step of biofilm development in which microorganism, substrates, and nutrients from feed water attach to rough membrane surface (Knoell, 1999; Al-Ahmad *et al.*, 2000; Visvanathan, 2002). Many researchers predict the biofouling potential of feed-water and membrane by study the behavior of adhesion phase using bio-adhesion assays. This phase usually occurs within two hours after operation of a clean membrane (Al-Ahmad *et al.*, 2000).

2) Reaction phase

The attached microorganisms on membrane surface utilize easy biodegradable compounds (substrates and nutrients) and start to produce biomass over the membrane surface (Knoell, 1999; Al-Ahmad *et al.*, 2000; Van Loosdrecht *et al.*, 2002; Visvanathan, 2002). In this phase, the chemical or microbial process can be calculated with standard reaction kinetics (van Loosdrecht *et al.*, 2002).

3) Biofilm growth phase

Dolan (2002) reported that microorganisms produce an EPS that is composed of polysaccharides covering them. Biofilm usually composed primarily of microbial cells and EPS. The amount of EPS in biofilm is about 50% to 90%. Types of bacteria stipulate types of polysaccharide. Gram-positive bacteria produces cation polysaccharide but gram-negative bacteria produces neutral and anion polysaccharide which leads to an association between biofilm and divalent cation, metal ion, and other macromolecule (difficulty-utilized substrates such as protein, lipids, humic substances, etc).

EPS (anion and neutral) provides binding force within and surrounding biofilm development. The slowly degradable compounds are gradually utilized by microorganism (Baker and Dudley, 1998; Dolan, 2002; Visvanathan *et al.*, 2002) in the biofilm matrix. This condition is also leading to regrowth of dead biomass and irreversible fouling (Griebe and Flemming, 1998; Knoell *et al.,* 1999). The biofilm formation occurs despite of using pretreatment and disinfection (Baker and Dudley, 1998), because EPS cover and protect biofilm from direct exposure to chemical biocide (Baker and Dudley, 1998; Knoell et al., 1999; Al-Ahmad *et al.*, 2000; Kreft and Wimpenny, 2001; Dolan, 2002; Visvanathan *et al.*, 2002).

4) Detachment phase

Detachment phase occurs by shear force from CFV and this phenomenon limits the biofilm thickness (Dolan, 2002; Van Loosdrecht *et al.*, 2002). High CFV detaches the accumulated cells out off hydrodynamic boundary layer from biofilm and cake layer (Li *et al*., 1998; Dolan, 2002), then controlling of high CFV is an essential operating condition for plant operators.

In filtration system, biofouling is inspected from physical appearance in all plant components as the biological accumulation takes place along membrane system operation of smell and color (Al-Ahmad, 2000). Quantity of biomass on membrane element can be determined by measuring of ATP (Adenosinetriphosphate), TDC (Total direct cell count), and heterotropic plate counts (HPC) on R2A medium (expressed in colony forming units, CFU). ATP is measuring for determination of total active microorganism quantity, while TDC includes active and non-active cells (Vrouwenvelder and van der Kooj, 2002).

3. Membrane properties affecting fouling

3.1 Roughness surface of membrane

Rough surface is normally found in high performance membranes, which have very narrow pore size corresponding to produce high quality products. To reduce the resistance of membrane and increase the quantity of product, membranes require a lot of filter area (effective area). Thus, high roughness surface is considered essential for increasing of passing area per total surface area. This development increases in membrane performance, whereas it leads to the attachment and accumulation of biomass and biodegradable compounds on membrane surface (Al-Ahmad *et al.*, 2000; Dolan, 2002; van Loosdrecht *et al.*, 2002; Al-Amoudi and Lovitt, 2007; Subramani and Hoek, 2008). The deposition of surfactant on polyamide (PA) membrane decreases roughness of membrane but increases roughness of cellulose acetate (CA) membrane (Wilbert et. al., 1998).

3.2 Charge properties of membrane

Normally, RO membranes present negative charge on their surface (Thanuttamavong, 2002a). The deposition of foulants on membrane surface changes charge property of membrane (Ghayeni et al., 1996). Most proteins and microorganism cell present negative charge thus the increasing negative charge of membrane increases electrostatic repulsive force and decreases deposition (Chen et. al., 1979). On the other hand, scaling or inorganic fouling is reduced when the negative charge is decreased. Fouling of anionic surfactant on membrane is lower than cationic surfactant (Chen et. al., 1979).

3.3 Hydrophilic and hydrophobic properties of membrane

The membrane with hydrophobic property is easily associated with organic matters and microorganisms than other hydrophilic substratum such as glass or metals (Dolan, 2002). Increase in hydrophilic property decreases deposition of organic and microorganism on membrane surface (Wilbert et. al., 1998; Subramani and Hoek, 2008).

3.4 Hydrodynamics

Hydrodynamic boundary layer means "the zone where flow velocity immediately adjacent to substratum liquid interface is negligible" (Dolan, 2002). The thickness is dependent on cross flow velocity. Higher cross flow velocity may appear thinner layer and limit the thickness of biofilm due to higher shear force detach the attached cells (Al-Ahmad *et al.*, 2000; Dolan, 2002). Then, high cross flow velocity needed to be maintained over the membrane surface in order to reduce fouling problem and maintain plant performance (Chiemchaisri *et al.*, 1994; Li *et al.* 1998).

4. Cleaning procedure

Physical cleaning can recover membrane flux by eliminating particulate fouling but are not effective for other types of fouling (Amjad *et.al.*, 1996). Therefore, chemical cleaning is needed to recover the membrane permeate flux in long-term operation. Chemical agents used in membrane cleaning can be classified into four categories consisting of acids, alkalies, chlelants, and formulated products (Amjad, 1993). Variety of chemical solutions as shows in **Table 3** are applied on used membrane for cleaning proposes.

Table 3 Chemical solution for cleaning RO membrane.

Cleaning solution	Foulant
1) 2.0 % (w) of citric acid (target pH of 4.0)	Calcium carbonate scale Metal oxides/hydroxides (Fe, Mn, Zn, Cu, Al) Inorganic colloidal
2) 0.5 % (w) of HCl (target pH of 2.5)	Calcium carbonate , barium, strontium, sulfate scale Inorganic colloidal
3) 0.1 % (w) of NaOH (target pH of 11.5)	Polymerized silica coating Biological matter Natural organic matters (NOMs)
4) 0.2 % (w) of Oxalic acid	Calcium carbonate and iron-based scale

Source: Adopted from David and Stephen (1996); Hydranautics (1998)

5. Relationship between flux decline and hydraulic resistance

Flux decline within the classical superior equation, resistance in series model, is influenced by the increase of foulant resistant (R_f) as shown in **Equation 5**. In case of long-term operation, fouling plays an important role for change in the total hydraulic resistance. Hence, the permeate flux can be assessed if the total hydraulic resistance can be estimated.

$$J = \frac{\Delta P}{\eta (R_m + R_f)} \quad 5)$$

where R_f (m^{-1}) is a foulant resistance, which is defined as the specific volume containing foulant (V/A, m^3/m^2) multiplied by the fouling index (I, m^{-2}). Furthermore, R_f is also defined as a function of specific cake resistance (α) multiplied by the cake concentration (C) as shown in **Equation 6**.

$$R_f = \frac{V}{A} I = \alpha C \quad 6)$$

Substituting the foulant resistance from **Equation 6** in **Equation 5**, the permeate flux can be estimated.

$$J = \frac{\Delta P}{\eta\left[R_m + \left(\frac{V}{A} xI\right)\right]} \quad 7)$$

Specific flux (L) or permeability is an important parameter which is useful for the operation with constant flux, a normal operation of RO system (Rabie et.al., 2001). The specific flux can be calculated from **Equations 8 and 9**.

$$L = \frac{J}{\Delta P} = \frac{1}{\eta R_t} \quad 8)$$

$$L = \frac{1}{\eta\left[R_m + \left(\frac{V}{A} xI\right)\right]} \quad 9)$$

The organic foulants contained in the textile wastewater adsorb on the membrane surface leading to a reduction of available site and consequently permeate flux decline. Braeken et. al (2006) proposed that the relationship between flux decline and filtration time (t) is considered as a function of a total non-occupied site ($1- \theta_T$) and a ratio of filtrated permeability to initial permeability (L/L_o) (Braeken et.al., 2006). Based on adsorption thermodynamics, the occupied site (θ_T) is a logarithmic function of time as shown in **Equations 10 and 11**.

$$\theta_T = b\ln(t) - b\ln(t_o) \quad 10)$$

$$L = L_o(1 - b\ln(t) + b\ln(t_o)) \quad 11)$$

where t_o is the initial time on which available site is reduce due to deposition (min) and b is the reduction rate of available site (min^{-1}). When this function is combined with Spiegler-Kedem equations ($J = L(\Delta P - \sigma\Delta\pi)$), and the permeate flux (J) can be estimated as follows (Braeken et.al., 2006).

$$J = L_o\left(1 - b\ln(t) + b\ln(t_o)\right)\left(\Delta P - \sigma\Delta\pi\right) \quad 12)$$

where σ is the reflection coefficient and $\left(\Delta P - \sigma\Delta\pi\right)$ is represented as TMP. To determined the model parameter, **Equation 12** was rewritten in term of normalized flux decline $(1 - \frac{J}{L_o x TMP})$ as shown in **Equation 13**.

$$1 - \frac{J}{J_o} = 1 - \frac{J}{L_o x TMP} = b\ln(t) - b\ln(t_o) \quad 13)$$

6. Aggregation of foulants

6.1 Aggregation of surfactant

In the case of non-ionic surfactant, the electrical effect is not involved in the aggregation. When surfactant concentration rises above CMC, total amount of surfactant appears into two forms i.e., monomer and micelle. The aggregate equilibrium constant (K_{eq}) can be determined as follows (Hamann, 1978).

$$nS \xleftrightarrow{K_{eq}} M \quad 14)$$

$$K_{eq} = \frac{C_M}{C_S{}^n} \quad 15)$$

where n is the number of surfactant monomer, S is the surfactant monomer, M is the surfactant micelle, C_S is the concentration of surfactant monomer, and C_M is the concentration of surfactant micelle. The required free energy of micellisation (ΔG^o) is given by (Hamann, 1978).

$$\Delta G^{o} = \ln(CMC)\, RT \qquad 16)$$

where R is the universal gas constant, 8.3145 J/mole.K, T is the temperature in Kelvin.

In the case of ionic surfactant, the counter ions are attracted onto the charged surface of micelle. The following equation is considered (Pisárčik et.al., 2003).

$$nS^{-} + (n-p)Na^{+} \xleftrightarrow{K_{eq}} M^{p-} \qquad 17)$$

where p is the effective charge of micelle, (n-p) is the number of counter ion. For dimeric surfactant, the free energy of micellisation per alkyl chain is estimated by (Pisárčik et.al., 2003).

$$\Delta G^{o} \approx RT\,(1.5-\alpha)\ln(CMC) \qquad 18)$$

where α is the ratio of slopes above and below CMC in the plot between conductivity and surfactant concentration.

6.2 Aggregation of foulants contained in the mixture

In the mixture containing organic matters and surfactant, they aggregate with micelle. The aggregate equilibrium constant and total organic solubility (C_T) can be determined from stoichiometry (Chidambaram and Burgess, 2000) as follows.

$$C_w + SAA \xleftrightarrow{K_{eq}} C_M \qquad 19)$$

$$K_{eq} = \frac{[C_m]}{[C_w][SAA]} \qquad 20)$$

$$[C_T] = [C_w](1 + K_{eq}[SAA]) \qquad 21)$$

where C_w is the organic matter in mixture, C_M is the organic matter in the micelle, SAA is the total surfactant concentration, and C_T is the total organic solubility. In the case of mixture containing non-ionic surfactant and ionic surfactant, micellisation decreases the electrostatic repulsive force between charged head of surfactant and it leads to increase in micelle formation (Gharibi et. al., 2004)

MATERIALS AND METHODS

Materials

The analytical materials used in this research are:

1. Total organic carbon analyzer, Shimadzu model TOC-5000A
2. Incubator 20 ^{O}C
3. Desiccators
4. Suction pump
5. SDI analytical tool
   - Filter holder, Advantec type KS-47
   - Pressure vessel, Advantec type DV 20, capacity 20 litres
   - Air pump, Jun Air model OF 301, maximum pressure 8 bars
6. pH meter
7. EC meter
8. Hot air oven 105^{O}C
9. Digestion Unit
10. Spectrophotometer
11. Scanning electron microscope, JEOL model JSM-5600 LV
12. High performance liquid chromatography, Agilent Technologies model HP 1100, Column:ZORBAX Eclipse XDB-C18 (Altech Associates)
13. Surface tension meter (Fisher Surface Tensionmat model 21).

Methods

This research consists of three-phase experiments, with different objectives. The fouling mechanism was studied using real wastewater from textile industry and synthetic wastewater was respectively used in the first and second experimental phase. Flux decline with time dependency model was studied in the third phase

experiment. The schematic diagram of overall experimental plan is shown in **Figure 4**. The research plan of each experimental phase is describes as follows.

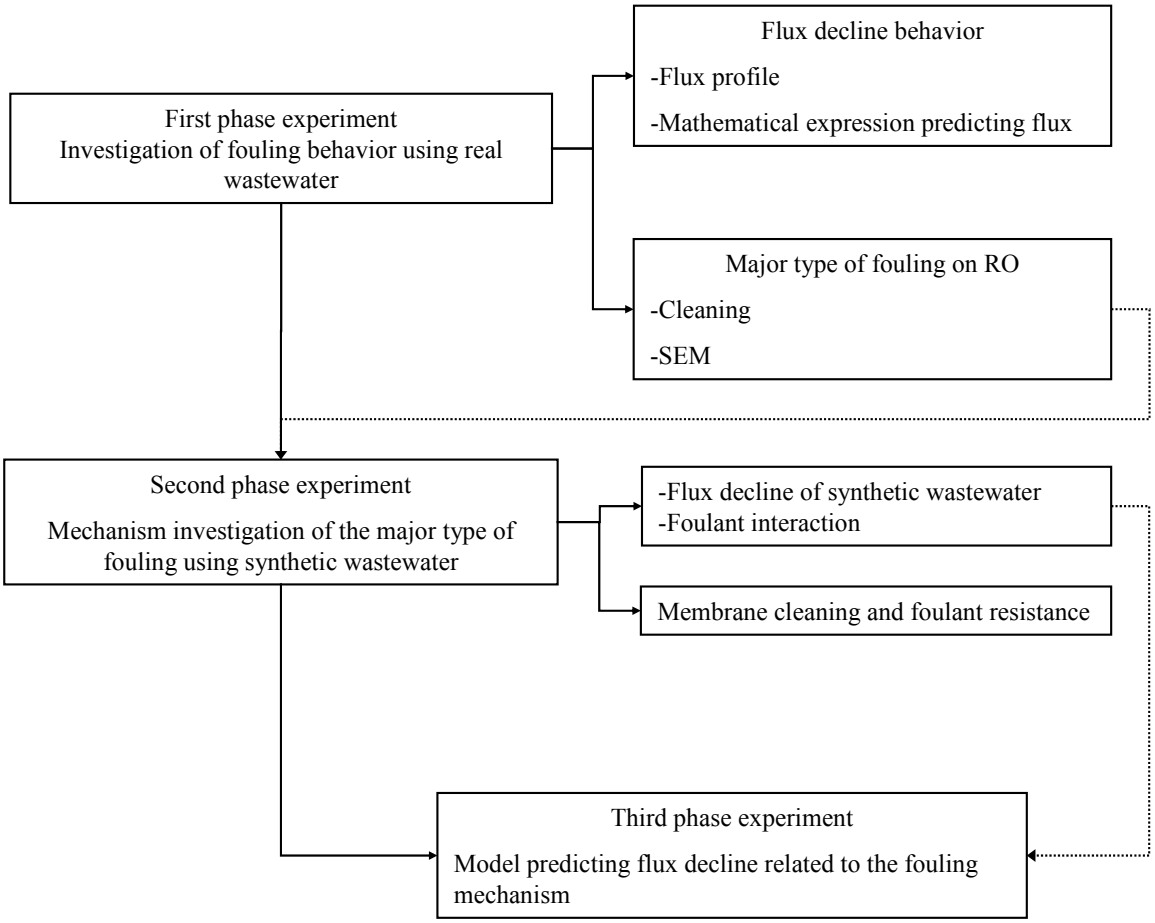

Figure 4 Overall experimental plan

1. First phase experiment

The first phase experiment was conducted to survey and understand the behavior and cause of membrane fouling under different operating conditions. The behavior of membrane fouling was studied by comparing of the operating data of textile wastewater reclamation in bench-scale and pilot-scale. The efficiency of chemical additives, antiscalant, and biocide in preventive membrane fouling were also studied.

The fouling type was also investigated through the cleaning experiment and direct observation through SEM micrographs. The effluent from MBR treating real textile wastewater from the production process of yarn and knit dyeing factory was used in the experiment.

1.1 Experimental equipment

1.1.1 Pilot-scale of textile wastewater reclamation

Pilot-scale of wastewater reclamation in yarn and knit dyeing factory, the hybrid process between membrane bioreactor (MBR) and RO system, was studied. The raw wastewater was obtained from the production process i.e., bleaching, mercerizing, dyeing, and washing. Flat-sheet micro-filtration membranes (MF, Kubota Corp.), which have average pore size of 0.4 μm and total membrane area of 20 m^2, were installed in MBR. The treatment capacity was 18 m^3/d. The temperature of raw wastewater was controlled by a cooling tower and adjusted to a pH of around 7.0 using hydrochloric acid (HCl) prior to MBR tank. Fine bubble air-diffuser tubes aerated the bioreactor continuously. Post treatment, RO unit, improved the quality of treated wastewater from MBR with the capacity of 200 L/h. The membrane model XLE-4040 (Film Tech Corp.) with active membrane area of 8.1 m^2 was applied. The biocide solution (Kuriverter EC 503, Kurita Water Industry LTD.) and antiscalant solution (Kulifloat, Kurita Water Industry LTD) were continuously added for preventing biofouling and scaling. Moreover, the feed-water was adjusted to a pH of 6.5 using HCl. RO unit was operated with a recovery ratio of 50%. This plant was monitored the permeate flux and salt rejection for 6 months. The schematic diagram of the reclamation system and the operating conditions of RO are shown in **Figure 5** and **Table 4**, respectively.

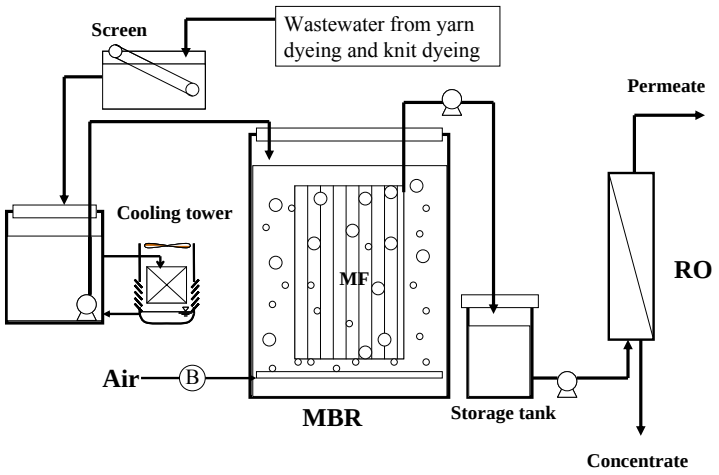

Figure 5 Schematic diagram of the reclamation system

Table 4 Operating condition of pilot-scale RO

Operating conditions	Details
1. recovery ratio	0.5 (200 L/h)
2. number of vessel	2 vessels/plant
3. number of elements	2 (1 element/ vessel)
4. feed direction	brine to feed
5. membrane size	4 inchs
6. chemical addition	biocide (5 mg/L)
	antiscalant (5 mg/L)
7. pH controlled	~6.5 (using HCl)
8. applied pressure	1.0-1.5 MPa

1.1.2 Bench-scale experimental units

Two types of RO units, a spiral wound membrane filtration unit and a stirring membrane filtration unit, were used in the first experimental phase. The details of these units were informed as following.

1) Spiral-wound membrane filtration unit

The behavior of membrane fouling under different operating conditions was studied using a spiral-wound membrane filtration unit (**Figure 6a**). The real treated wastewater from MBR (so called secondary effluent) was reserved in a storage tank with volume of 500 liters. Chemical additives for prevention of fouling were added into pipeline prior to a feed pump by a solenoid driven metering pump. The feed pump served as a booster and an in-line mixer. A cartridge filter with average pore size of 5 μm separated the large particles from the feed-water as a fine screen. A spiral-wound RO element with negatively charged surface and diameter of 1.8 inches was fitted in the pressure vessel.

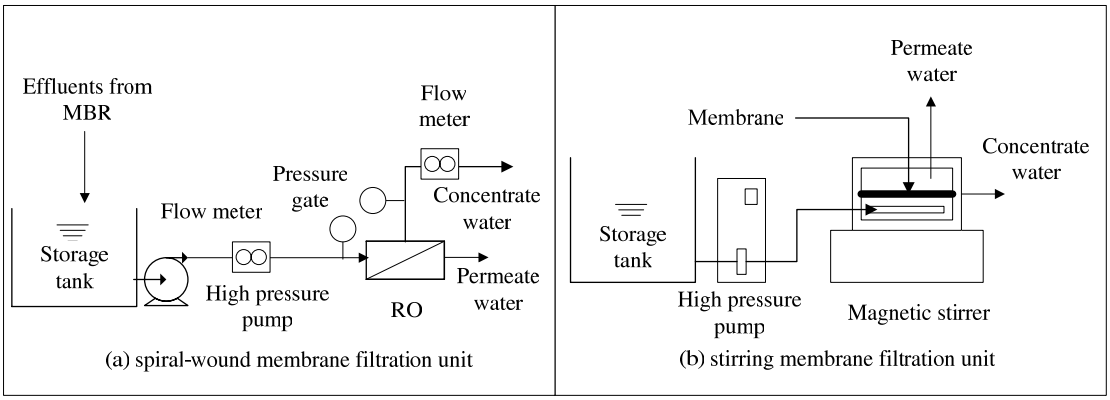

Figure 6 Schematic diagram of the experimental units

2) Stirring membrane filtration unit

Stirring membrane filtration unit (**Figure 6b**) was employed to investigate the effective cleaning procedure and the cause of membrane fouling after applied to the real treated textile wastewater. The fouled membrane elements from the spiral wound membrane filtration unit were taken out of the pressure vessel. They were cut off as a circle sheet with area of 8.04 cm^2 and studied for effective cleaning procedures and type of deposited foulant. The operating pressure and feed flow rate

was controlled by a high-pressure pump. CFV above the membrane surface was produced using a magnetic stirrer.

1.1.3 RO membrane

The spiral wound RO membrane, model BW-PA-2012-60 (Ultratek, USA), with diameter of 1.8 inches and area of 0.4 m^2 were used in this research. The membrane were tested with 1,500 mg/L of NaCl feed solution at applied pressure of 15 bars, and CFV of 8.6 cm/s using a stirring membrane filtration unit for examining its properties. Average values of EC rejection, permeate flux, and clean membrane resistance (R_m) were 96.22 %, 1.11 m/d, and $1.311x10^{14}$ m^{-1}, respectively.

1.2 Experimental methods

1.2.1 Study of membrane fouling due to real treated textile wastewater

1) Raw and treated wastewater from MBR unit

The characteristics of raw and treated wastewater from MBR unit were analyzed with the parameters of electrical conductivity (EC), silt density index (SDI), pH, chemical oxygen demand (COD), suspended solids (SS), biological oxygen demand (BOD_5), color, total kjeldahl nitrogen (TKN), and total phosphorus (TP). The analytical methods are shown in **Table 5**.

Table 5 Analytical parameters and methods

Parameter	Standard	Method
1. Electrical conductivity (EC)		EC meter
2. Silt density index (SDI)	D 4189 – 95[1]	Filtration method
3. pH	4500H[2]	pH meter
6. Chemical oxygen demand (COD)	5220[2]	Close reflux method
7. Biological oxygen demand (BOD_5)	5210B[2]	5-day BOD test
6. Suspended solids (SS)	2540D[2]	Total suspended solids dried at 103-105^{o}C
7. Color		Spectrophotometer
8. Total kjeldahl nitrogen (TKN)	420A[2]	Micro Kjeldahl and titrimetric method
9. Total phosphorus (TP)	4500P[2]	Phosphorus

Source: [1] = ASTM

[2] = Standard method for examination of water and wastewater 20th Edition (APHA, 1998)

2) Fouling behaviors due to secondary effluent

The effect of chemical additives, antiscalant and biocidein preventing RO fouling were studied. Antiscalant and biocide agent were added into the secondary effluent to prepare three different types feed-water i.e., 1) without chemical addition, 2) addition with antiscalant 5 mg/L, and 3) addition with antiscalant 5 mg/L and biocide 5 mg/L. The filtration system was operated at a feed flow rate of 1.6 L/min (average CFV of 8.6 cm/s), and applied pressure of 3.5 bars for 30 days. Salt rejection was recorded to evaluate the efficiency of membrane as shown in **Equation 22**. The operating results of the spiral-wound membrane filtration unit were compared with the operating results of the pilot-scale system.

$$\text{EC rejection, \%} = \left(1 - \frac{Q_P \,.\, EC_P}{Q_f \,.\, EC_f}\right)100 \qquad 22)$$

where EC_f, EC_c, and EC_p are the electrical conductivity of feed-water, concentrate-water, and permeate-water, respectively.

3) Mathematical expression of flux decline using variable fouling index

Generally, the fouling index is assumed to be a constant parameter and the permeate flux (J) is dependent upon the foulant resistant (R_f) and the specific volume (V/A) as defined in the theory of modified fouling index (MFI). According to the MFI concept, the specific flux (L) can be determined by the rearrangement of **Equation 9** as shown in **Equation 23**.

$$\frac{1}{L} = \eta R_m + \eta I \frac{V}{A} \qquad 23)$$

In the case of a spiral wound membrane filtration unit, the fouling rate or fouling index always decreases with filtration time because of a cross-flow velocity and a decrease of adhesion of foulant on membrane, hydrophobicity, hydrophilicity, and ionic strength. The cross-flow velocity limits the thickness of the foulant layer at the membrane surface by a detachment of particle and a back diffusion of solute (Bian et.al., 2000). The hydrophobicity and hydrophilicity between membrane and foulant are changed when the membrane surfaces are occupied by the foulant (Wilbert et.al., 1998; Cornelis et.al., 2005). The ionic strength between membrane and foulant are changed by Donnan equilibrium and this equilibrium prevents the diffusion of the ion between membrane and bulk solution (Thanuttamavong et.al., 2002b).

According to **Equation 23**, the dynamic viscosity (η), the resistance due to fresh membrane (R_m), and the foulant concentration contained in wastewater are assumed as constant parameters. Hence the change in specific flux is effected by the change in specific volume (V/A) and fouling index (I). The specific volume is determined by multiplying permeate flux and filtration time. In addition, in

this research, the fouling index is defined as a variable parameter. The variable fouling index is a function of an initial fouling index (I_o) and a reduction coefficient (γ). The n-order rate law is considered to estimate the model parameters as shown in **Equation 24**.

$$\frac{dI}{d(V/A)} = -\gamma I^n \qquad 24)$$

The n-order rate law is integrated from $I = I_o$ to $I = I$ and $V = 0$ to $V = V$. The integrated rate law becomes:

$$\frac{1}{I^{(n-1)}} = \frac{1}{I_o^{(n-1)}} + (n-1)\gamma \frac{V}{A} \qquad 25)$$

According to the **Equation 25**, the reduction coefficient (γ) is determined by linear plot between $1/I^{(n-1)}$ and V/A. Consequently, **Equations 9 and 25** are combined and the specific flux profile is determined by **Equation 26** as variable fouling index (VFI) model. The variable fouling index model is appropriate for both the constant flux operation and the constant pressure operation.

$$L = \frac{1}{\eta \left\langle R_m + \left[\frac{V}{A} \left\{ \frac{I_o^{(n-1)}}{1 + [(n-1)\gamma \frac{V}{A} I_o^{(n-1)}]} \right\}^{\left(\frac{1}{n-1}\right)} \right] \right\rangle} \qquad 26)$$

The empirical parameters were determined from three operating periods of bench-scale experiment i.e., 1 day, 7 days, and 30 days of operation. The specific flux ($L_{calculation}$), which were calculated from three sets of model parameters, were compared with the experimental data ($L_{experiment}$) to determine appropriate operation period for the modeling. The sum of square error (SSE) as

shown in Equation 13 was used to evaluate the accuracy of models. The operating period, which provided the smallest amount of difference in specific flux between model and experiment, the minimum SSE, was selected to be the optimum operation period.

$$SSE = \sum (L_{experiment} - L_{calculation})^2 \quad 27)$$

This mathematical expression can be applied for assessing the RO membrane flux of full-scale plant using short-term data of lab-scale experiment. The procedure for developing mathematical expression is shown in **Figure 7**.

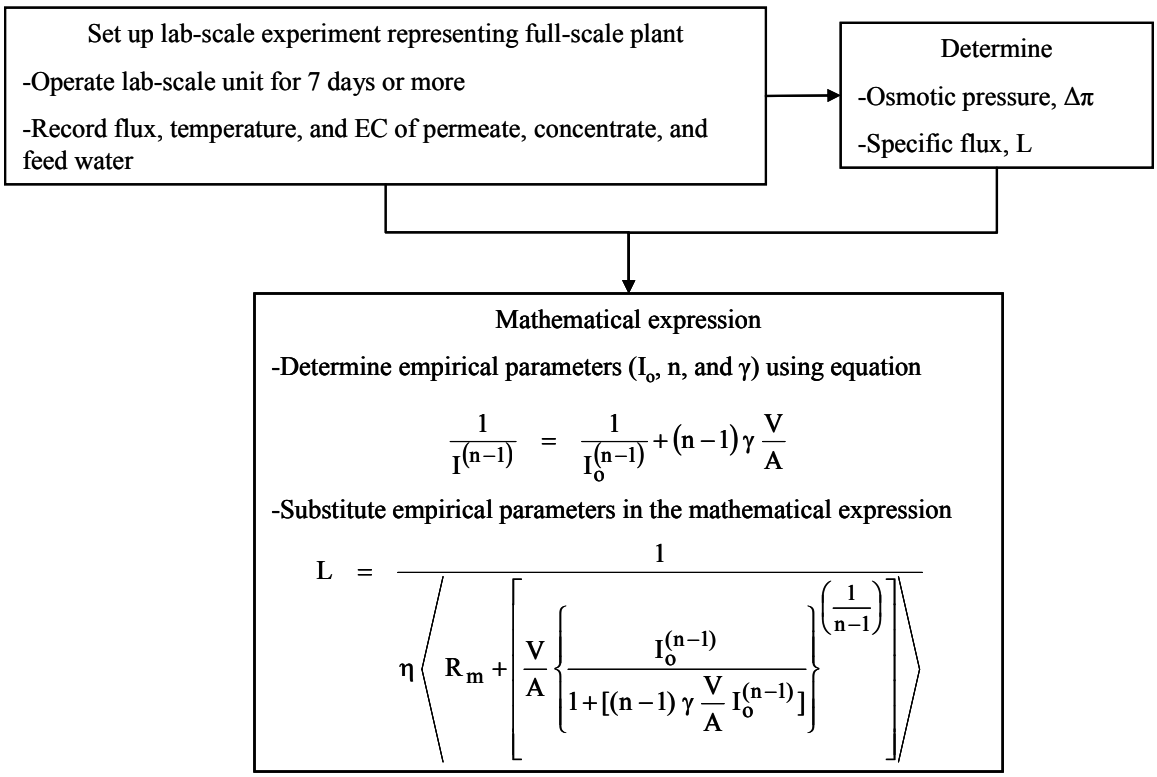

Figure 7 Procedure for developing mathematical expression

1.2.2 Study of fouling cause by real treated textile wastewater

The fouled membranes obtained from the spiral-wound membrane filtration unit were taken out of the pressure vessel and cut into small pieces for the investigation of fouling layer on the membrane surface. A cleaning study and SEM observations were used to illustrate the deposition of foulant on the membrane surface.

1) Physical and chemical cleaning

The samples of fouled membrane were washed by different physical and chemical procedures. Acid solution, hydrochloric acid (HCl), citric acid and oxalic acid were selected to evaluate extent of inorganic fouling of the fouled membrane. Alkaline solutions, sodium hydroxide (NaOH), sodium-EDTA (Na-EDTA) and sodium metabisulfite (SBS) were selected to evaluate extent of organic fouling of the fouled membrane. The fouled membranes were washed with the cleaning agents by cleaning time of 60 min and applied pressure of 0.3 MPa. CFV above membrane surface was created using a magnetic stirrer. The resistant removal efficiency (RR) definable by Madaeni *et. al.* (2001) was determined to evaluate the cleaning efficiency and the types of fouling as shown in **Equation 28**. The experimental plan for cleaning study is shown in **Tables 6 and 7**.

$$RR(\%) = \frac{R_{f,f} - R_{f,w}}{R_{f,f}} x100 \qquad 28)$$

where $R_{f,f}$ is the foulant resistance before washing as calculated from the pure water flux of the fouled membrane ($J_{w,f}$). $R_{f,w}$ is the foulant resistance after washing as calculated from the pure water flux of the washed membrane ($J_{w,w}$).

$$R_{f,f} = \frac{\Delta P}{\eta J_{w,f}} - R_m \qquad 29)$$

$$R_{f,w} = \frac{\Delta P}{\eta J_{w,w}} - R_m \quad 30)$$

where R_m is the hydraulic resistance of membrane as calculated from the initial pure water flux of fresh membrane ($J_{w,i}$) as following:

$$R_m = \frac{\Delta P}{\eta J_{w,i}} \quad 31)$$

2) Scanning electron microscope (SEM).

The deposited foulants on the fouled membranes were observed using SEM micrographs taking from scanning electron microscope (SEM), JEOL model JSM-5600 LV. Both of the fouled membrane samples and the washed membrane samples were cut into small pieces and liberated of moisture in a desiccator overnight. The dried samples were coated with gold mineral prior to be taken their images.

2. Second phase experiment

The main purpose of second phase experiment is to study the fouling mechanism on RO membrane due to the organic foulant contained in secondary effluent. The synthetic wastewater simulating treated textile wastewater from MBR was used this phase.

Table 6 Experimental condition to determine the effect of CFV on membrane cleaning efficiency

Run	Membrane samples	CFV (cm/s)	Cleaning solution
1	case 1: without chemical addition	5	pure water
2		15	
3		25	
4		35	
5		45	
6		55	
7	case 2: addition with antiscalant	5	pure water
8		15	
9		25	
10		35	
11		45	
12		55	
13	case 3: addition with antiscalant and biocide	5	pure water
14		15	
15		25	
16		35	
17		45	
18		55	

Note : 1. The operating pressure was controlled at 0.3 MPa.

2. The feed flow rate was 1 mL/min.

3. The washing time was 1 h.

Table 7 Experiments to determine the efficiency of chemical cleaning

Run	Membrane samples	CFV (cm/s)	Cleaning solution
19	case 1: without chemical addition	35	NaOH pH12
20			HCl pH 2
21			Citric acid 2%
22			Oxalic acid 0.2 %
23			EDTA 2 %
24			SBS 0.2 %
25			NaOH pH12+HCl pH2
26			HCl pH2+ NaOH pH12
27			Citric 2%+NaOH pH12
28	case 2: addition with antiscalant	35	pure water
29			NaOH pH12
30			HCl pH 2
31			NaOH pH12+HCl pH2
32			HCl pH2+ NaOH pH12
33	case 3: addition with antiscalant and biocide	35	pure water
34			NaOH pH12
35			HCl pH 2
36			NaOH pH12+HCl pH2
37			HCl pH2+ NaOH pH12

Note : 1. The operating pressure was controlled at 0.3 MPa.

2. The feed flow rate was 1 mL/min.

3. The washing time was 1 h.

2.1 Experimental materials

2.1.1 Membrane filtration unit

The permeate flux of RO membrane applied to wastewater composing of salt, EfOMs, SA and dye was investigated using a cross-flow membrane filtration unit (C10-T, Nitto Denko) and RO membrane model ES-20 and LF-10 (Nitto Denko). The schematic diagram of experimental unit is shown in **Figure 8**.

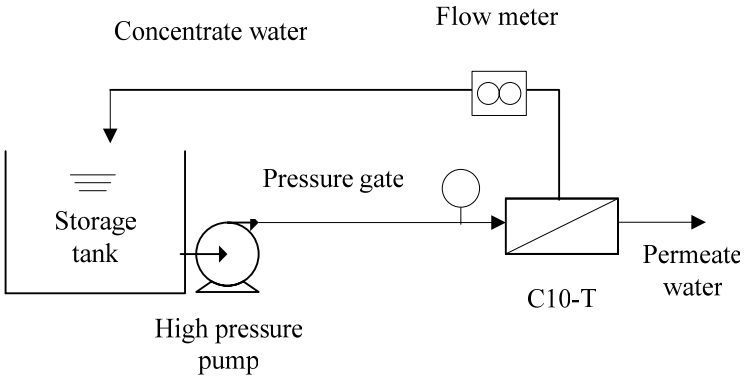

Figure 8 Schematic diagram of cross-flow membrane filtration unit

2.1.2 Synthetic wastewater

Since, half of all textiles worldwide are cotton dying by reactive dye (Sójka-Ledakowicz, 1998) hence reactive dye was used in this research. In addition, non-ionic surfactant and anionic surfactant are added in the synthetic wastewater for they are wildly used in textile industry. The synthetic wastewater was prepared by adding NaCl (2,000 mg/L) and organic foulants (reactive dye, surfactants and EfOMs) in pure water. The reactive dye model Marine E-EL (Nippon Kayaku Corp.), commercial soaping agent (SA) namely Sunmoor RC 700E which contains 4% of the anionic surfactant and 20% of the non-ionic surfactant (Nikka-Kagaku Corp.), non-ionic surfactant (Triton X-100, TX), and anionic surfactant (sodium dodecyl sulfate, SDS) were selected to simulate reactive dye and surfactants in the

secondary effluent. The effluents from an activated sludge process were filtrated by MF membrane with a pore size of 0.45 μm to simulate the treated wastewater containing EfOMs. CMC of the surfactant, SA, TX, and SDS, were measured by the ring method using a surface tension meter (Fisher Surface Tensionmat model 21) as 1.62, 7.37, and 19.34 mM as C mM as C at 30 ^{O}C respectively. The concentrations of SA, TX, and reactive dye were measured in term of mM as C using total organic carbon analyzer (Shimadzu model TOC-5000 A). The constitutes of synthetic wastewater are shown in **Table 8**.

2.1.3 Membrane

The fouling mechanism was studied using two types of flat sheet RO membrane, ES20 and LF10 (Nitto Denko Corp.). ES20 represents a negatively charged surface and low hydrophilic membrane. LF10 represents a neutrally charged surface and high hydrophilic membrane (Nitto denko, 1998). The membrane permeability (L_P) measured by pure water of ES-20 and LF-10 were 1.714±0.069 and 1.034±0.068 m/d-MPa respectively.

2.2 Experimental methodology

2.2.1 Fouling potential determination

Synthetic wastewater was applied continuously for 24 hours in recirculation mode. The feed flow rate and the applied pressure were controlled at 0.2 L/min and 0.5 MPa, respectively. The water temperature was controlled at 30 ^{O}C using a temperature controller. Triplicate experiments were conducted to confirm the experimental results.

Flux decline in term of $\Delta J/\Delta V$ were calculated from the data between the end (24 hour) and the initial time of operation (1 hour) as shown in **Equation 32**.

Table 8 Characteristic of synthetic textile wastewater

Run	Membrane	Feed water (mM as C)
1	ES-20	SA 0.78 mM as C
2	ES-20	SA 1.43 mM as C
3	LF-10	SA 1.43 mM as C
4	ES-20	SA 4.08 mM as C
5	ES-20	SA 6.72 mM as C
6	ES-20	EfOMs 0.83 mM as C
7	LF-10	EfOMs 0.83 mM as C
8	ES-20	SA 1.43 mM as C + EfOMs 0.83 mM as C
9	ES-20	SA 6.72 mM as C + EfOMs 0.83 mM as C
10	ES-20	Dye 7.23 mM as C
11	LF-10	Dye 7.23 mM as C
12	ES-20	Dye 7.23 mM as C + EfOMs 0.83 mM as C
13	ES-20	TX 0.25 mM as C
14	LF-10	TX 0.25 mM as C
15	ES-20	SDS 3.95 mM as C
16	LF-10	SDS 3.95 mM as C
17	ES-20	SDS 3.95 mM as C + EfOMs 0.83 mM as C
18	ES-20	TX 0.25 mM as C + EfOMs 0.83 mM as C
19	ES-20	SA 1.43 mM as C + Dye 1.53 mM as C
20	ES-20	SA 1.43 mM as C + Dye 7.23 mM as C
21	ES-20	SA 1.43 mM as C + Dye 7.23 mM as C + EfOMs 0.83 mM as C
22	ES-20	SA 6.72 mM as C + Dye 1.53 mM as C
23	ES-20	SA 6.72 mM as C + Dye 7.23 mM as C
24	ES-20	SA 6.72 mM as C + Dye 7.23 mM as C + EfOMs 0.83 mM as C
25	ES-20	TX 0.25 mM as C + Dye 7.23 mM as C
26	ES-20	TX 0.25 mM as C + Dye 7.23 mM as C + EfOMs 0.83 mM as C
27	ES-20	SDS 3.95 mM as C+ dye 1.53 mM as C
28	ES-20	SDS 3.95 mM as C + dye 7.48 mM as C
29	ES-20	SDS 3.95 mM as C + dye 7.48 mM as C + EfOMs 0.83 mM as C

Note: NaCl 2,000 mg/L was added in all runs

$$\frac{\Delta J}{\Delta V} = \frac{J_{v,1} - J_{v,24}}{V_{24} - V_1} \quad 32)$$

where $J_{v,1}$ and $J_{v,24}$ are the permeate flux at 1 and 24 hour respectively. V_1 and V_{24} are the accumulative flux at 1 and 24 hour.

2.2.2 Determination of trans-membrane pressure (TMP) at membrane surface

Theoretical osmotic pressure of solution can be calculated using Van't Hoff model as $\pi = vc_j RT/M$ (van der Bruggen *et.al.*, 2001). In non-porous filtration system like RO membrane, solute rejection and concentration polarization phenomena lead to an increase in foulant concentration at membrane surface as compare to bulk solution. The resistance in series model and osmotic pressure model can be modified to estimate the osmotic pressure at the membrane surface and the actual TMP.

The resistance in series model describes flux decline in RO system caused by the hydraulic resistance (Schafer *et.al.*, 2005). The osmotic pressure model (Wijmans *et.al.*, 1985) is similar to the resistance in series model but it includes the term of R_{cp} in $\Delta\pi$. These models are assembled together to estimate the osmotic pressure using the monitored flux data. To eliminate experimental errors, average value of the osmotic pressure that be calculated from the flux at 1 h ($\Delta\pi_{m,1}$) and the osmotic pressure that be calculated from the flux at 24 h ($\Delta\pi_{m,24}$) are determined as shown in **Equations 33 to 34**.

$$\Delta\pi_m = \frac{\Delta\pi_{m,1} + \Delta\pi_{m,24}}{2} \quad 33)$$

$$\Delta\pi_{m,1} = \Delta P - (J_1 \eta R_{m,0}) \quad 34)$$

$$\Delta\pi_{m,24} = \Delta P - (J_{24}\eta R_{m,24}) \quad 35)$$

where $R_{m,0}$ is calculated from the pure water flux of fresh membrane. $R_{m,24}$ can be calculated from the data of pure water flux of fouled membrane at the operating time of 24 h. Finally, TMP can be calculated from the difference between the net applied pressure osmotic pressure at membrane surface.

2.2.3 Determination of net osmotic pressure at membrane surface due to organic foulant ($\Delta\pi_{m,\ organic}$)

The film model assumed one-dimensional flow and completely developed boundary layer (Sutzkover *et.al.*, 2000) was considered to determine. Mass balance of solute transport in boundary layer is considered as a relationship between convective flow towards membrane surface and back-diffusion flow as shown in **Equation 36**.

$$J_s = C_p J_v = C J_v - D\frac{dC}{dy} \quad 36)$$

where J_S is the net solute flux, C_p is the solute concentration in permeate, C is the solute concentration at distance y away from the membrane surface within the boundary layer, J_v is the solvent flux. Mass transfer coefficient (k) definable as a ratio of diffusion coefficient (D) and boundary layer (δ) was assembled with the film model. Subsequent to the integration from y = 0 to y = δ, and C = C_m to C = C_b, **Equation 37** was given.

$$C_m = C_b e^{(J_v / k)} \quad 37)$$

The theoretical osmotic pressure definable by the Van't Hoff model was substituted in **Equation 37**. Relationship between the net osmotic pressure at membrane surface ($\Delta\pi_m$) and the net osmotic pressure in bulk ($\Delta\pi_b$) was acquired.

$$\Delta\pi_m = \Delta\pi_b e^{(J_v / k)} \quad 38)$$

According to the experiment with NaCl solution of 2,000 mg/L, the measured flux at 30 ^oC was 0.55 m/d. The calculated $\Delta\pi_{b,\ NaCl}$ using the Van't Hoff model was 0.172 MPa. The calculated $\Delta\pi_{m,\ NaCl}$ using **Equation 33** was 0.213 MPa. The mass transfer coefficient (k) of NaCl was obtained as 2.62 m/d. The net osmotic pressure of organic foulant ($\Delta\pi_{m,\ organic}$) can be determined by the difference between $\Delta\pi_m$ and $\Delta\pi_{m,\ NaCl}$ as shown in **Equation 39**.

$$\Delta\pi_{m,organic} = \Delta\pi_m - 0.172\, e^{(J_v / 2.62)} \quad 39)$$

2.2.4 Irreversible resistance evaluation

The fouled membranes after 24 hours of operation were determined for irreversible fouling using cleaning technique. The fouled membranes were cleaned with pure water and NaOH solution (pH 10.5). They were employed to evaluate the reversible fouling due to cross-flow velocity and removable organic foulant (Ang *et.al.*, 2006). The operating pressure and feed-flow rate of chemical cleaning were controlled at 0.3 MPa and 1 L/min, respectively. After cleaning, the pure water flux was recorded and the irreversible resistance was determined by **Equation 40**.

$$\Delta R_F = R_{f,w} - R_m \quad 40)$$

2.2.5 Measurement of aggregate concentration

In order to qualify aggregate and monomer concentrations in the wastewater, an experiment filtering synthetic wastewater containing surfactant, reactive dye, EfOMs, and their mixtures through UF membrane (PLBC07610, MWCO of 3,000, Millipore Corp). A dead-end membrane filtration unit (C40-B, Nitto Denko Corp.), a stirring batch-type cell, was used for this propose. Nitrogen gas was applied to control pressure in the pressure vessel. A stirrer bar was used to

simulate CFV above the membrane surface and to prevent the formation of concentration polarization. The stirrer bar was rotated at a speed of 200 rpm using magnetic stirrer. The aggregates were retained in C40-B cell above UF where the monomers passed through the membrane within permeate. The concentrations of surfactant, EfOMs, and reactive dye within permeate and within wastewater were analyzed using high performance liquid chromatography (Agilent Technologies model HP 1100, Column: ZORBAX Eclipse XDB-C18, Altech Associates).

3. Third phase experiment

The purpose of third phase experiment is the study of mathematical model for predicting flux decline of textile wastewater reclamation at different composition. The experimental result from the second experimental phase was employed to determine the model parameter and test the model accuracy.

The procedure of model development consists of two steps i.e. 1) determination of reduction of available site and initial fouling time, 2) determination of fouling coefficient and total occupied sited.

3.1 Determination of reduction of available site and initial fouling time

The parameters of reduction of available site and initial fouling time can be determined as the procedure in **Figure 9**. In this step, the synthetic wastewater is monitored flux during RO filtration for 24 hours. The reduction of available site is determined from the slope of linear plot between normalized flux decline and filtration time.

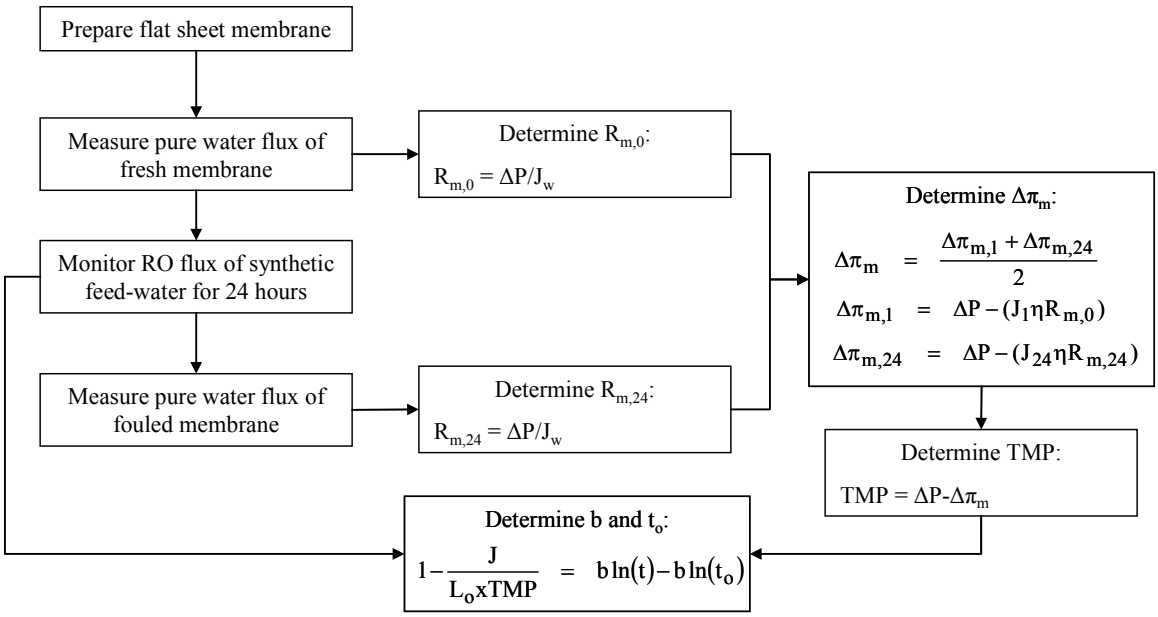

Figure 9 Determination procedure of reduction of available site (b) and initial fouling time (t_o)

3.2 Determination of fouling coefficient and total occupied site

The parameter of fouling coefficient and total occupied site can be determined as the procedure in **Figure 10**. The synthetic wastewater containing multiple foulants is filtered through UF membrane and the concentration of feed-water and permeate-water are measured for evaluating aggregation equilibrium constant (K_{eq}). Afterward, the fouling coefficient (β) is determined by divide the reduction of available site by foulant concentration. The aspect of these determinations is shown as follows.

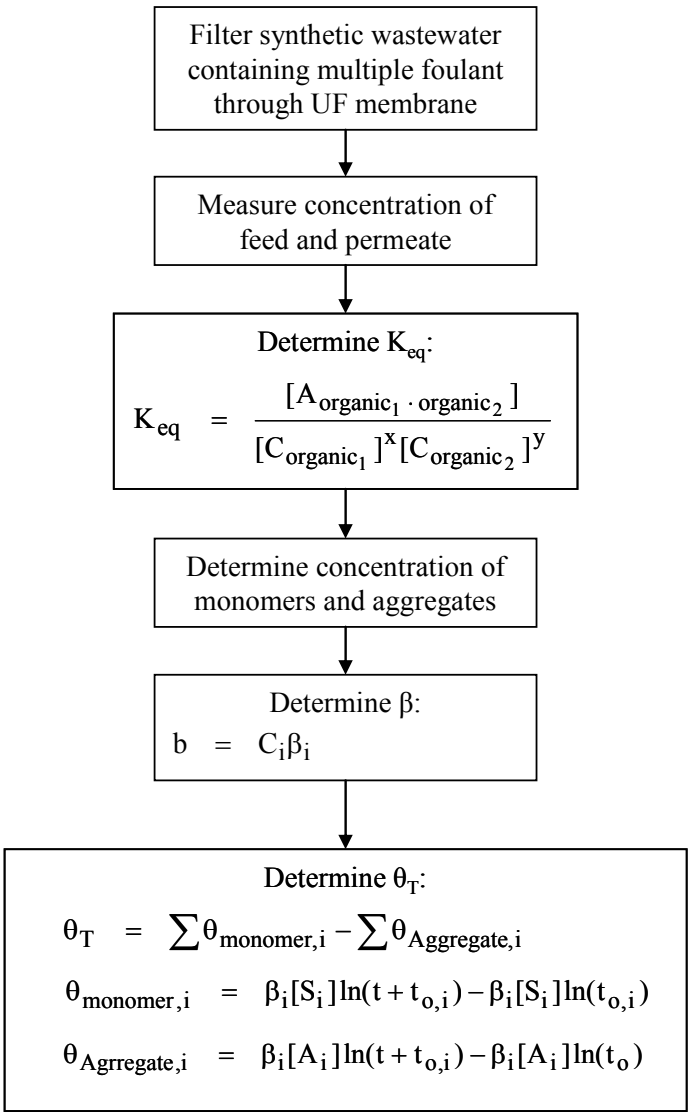

Figure 10 Determination procedure of fouling coefficient (β) and total occupied site (θ_T)

Interaction between foulants contained in wastewater provides two type of aggregates i.e., monomer-monomer and monomer-micelle. The concentrations of aggregates and monomers in the wastewater after foulant interaction are derived from aggregate equilibrium. Generally, the maximum concentration of surfactant monomer in the solution equals CMC when the solution contains pure surfactant. In addition, the micelles appear when the surfactant concentration raises higher than CMC.

The aggregation between organic foulants ([organic$_i$], mM as C) is mainly caused by hydrophobic adhesion. When the molar ratio in aggregate are x and the aggregate reaction is shown in **Equation 41**.

$$x[\text{organic}_1] + y[\text{organic}_2] \Leftrightarrow [\text{organic}_{1_x}.\text{organic}_{2_y}] \quad 41)$$

According to the aggregate reaction at equilibrium, the aggregation is represented by $[A_{\text{organic}_1 \cdot \text{organic}_2}]$. The total concentration of organic foulants is $[C_{\text{organic}_i}]$. The aggregate equilibrium constant (K_{eq}) becomes;

$$K_{eq} = \frac{[A_{\text{organic}_1 \cdot \text{organic}_2}]}{[C_{\text{organic}_1}]^x [C_{\text{organic}_2}]^y} \quad 42)$$

The reduction of available site (b) is specific to foulant and membrane surface properties and relate to the concentration of foulant in the wastewater. Larger b value means high fouling potential. Moreover, b is proposed as a function of concentration (C_i) and fouling coefficient (β_i) as shown in **Equation 43**. Fouling coefficient can be determined Therefore, permeate flux of RO membrane from **Equation 12** can be rewritten in **Equation 44**.

$$b = C_i \beta_i \quad 43)$$

$$J = L_o \left(1 - C_i \beta_i \ln(t + t_o) + C_i \beta_i \ln(t_o)\right) \text{TMP} \quad 44)$$

The total occupied site due to deposition of monomer and aggregate forms on the membrane surface are determined from the assumption that monomer form decreases flux but aggregate form enhances flux. **Equations 45- 47** show the relationships between fouling coefficient, filtration time, and occupied site of monomer, aggregate, and total.

$$\theta_T = \sum \theta_{monomer,i} - \sum \theta_{Aggregate,i} \quad 45)$$

$$\theta_{monomer,i} = \beta_i[S_i]\ln(t + t_{o,i}) - \beta_i[S_i]\ln(t_{o,i}) \quad 46)$$

$$\theta_{Agrregate,i} = \beta_i[A_i]\ln(t + t_{o,i}) - \beta_i[A_i]\ln(t_o) \quad 47)$$

RESULTS AND DISCUSSION

1. Fouling of RO membrane applied to textile wastewater

The fouling behaviors of RO system treating effluent from MBR were investigated using bench-scale and pilot-scale unit in this section.

1.1 Characteristic of raw wastewater and treated wastewater

The experiment was conducted continuously over 90 days. **Table 9** shows the characteristic of raw wastewater and secondary effluent. MLSS in bioreactor was controlled approximately 25,000 mg/L. It was found that MBR achieved excellent removal efficiency of particle and organic matter from wastewater. The removal efficiency of BOD_5 and SS were more than 99 %. In addition, the removal efficiency of COD, TKN, TP were 88.0, 62.8, and 6.2 %, respectively. MBR showed low effective removal of color. Because reactive dye contained in wastewater are non-degradable under the typical aerobic conditions of conventional biological treatment systems, and its adsorption capacity is very poorly on biological solids, resulting in residual color in discharged effluents association with fiber (Epolitoa ***et. al.***, 2005). Despite its high particle and organic removal efficiencies, the secondary effluent with an average SDI of 3.55 still contained potential foulants. Moreover, minute amounts of these nutrients, including TP of 6.1 mg/L and TKN of 4.5 mg/L, may be causing biofouling on RO surface (Vrouwenvelder and van der Kooij, 2001).

Table 9 Influent and effluent characteristic

Parameter	Unit	Raw wastewater		Secondary effluent	
		Range	Average	Range	Average
EC	µs/cm	-	-	3,580-5,150	4,343
SDI	%/min	-	-	1.87-4.54	3.55
pH	-	7.95-9.76	9.00	7.89-8.53	8.24
COD	mg/L	229-476	367	27.6-48.6	44
BOD_5	mg/L	89.3-202	146	ND	ND
SS	mg/L	24-55	32	ND	ND
Color	mg/L as Pt-Co	17.8-379	117	43-273	138
TKN	mg/L	8.9-20.8	12.1	2.1-12.5	4.5
TP	mg/L	1.82-10.9	6.5	1.48-8.16	6.1

Note: ND was not detect

1.2 RO flux profiles

Flux decline during RO filtration was explained using experimental data of the bench-scale experiment in this topic. Moreover, the mathematical expression was investigated to assess the long-term flux profile of larger-scale system from short-term data of bench-scale experiment. The long-term flux profile of pilot-scale was compared with the predicted flux profile to test the accuracy.

1.2.1 Experimental data of flux decline profile

The treated wastewater was fed into the bench-scale of spiral wound membrane filtration unit to study its fouling potential. The three experiments consist of the case i.e., no chemical addition, antiscalant addition, and antiscalant and biocide addition.

The specific flux (L) and relative hydraulic resistance (R_T/R_{To}) of spiral-wound membrane filtration unit are shown in **Figures 11 and 12**. In all cases, specific flux dropped rapidly during the early stage of operation and slightly decline further until the end of the experiments. In the case where antiscalant was added, R_T/R_{To} was found decreasing significantly compared to the case where the chemical was not added. However, the addition of biocide reduced R_T/R_{To} slightly. According to results from **Table 10**, the specific flux at the end of operation (30 days) was 0.213, 0.244, and 0.261 m/d-MPa respectively. The average real EC-rejection values were 91.3, 92.3, and 92.8 %. The additive chemical, antiscalant and biocide, could slightly reduce the fouling on membrane surface and increased the EC-rejection.

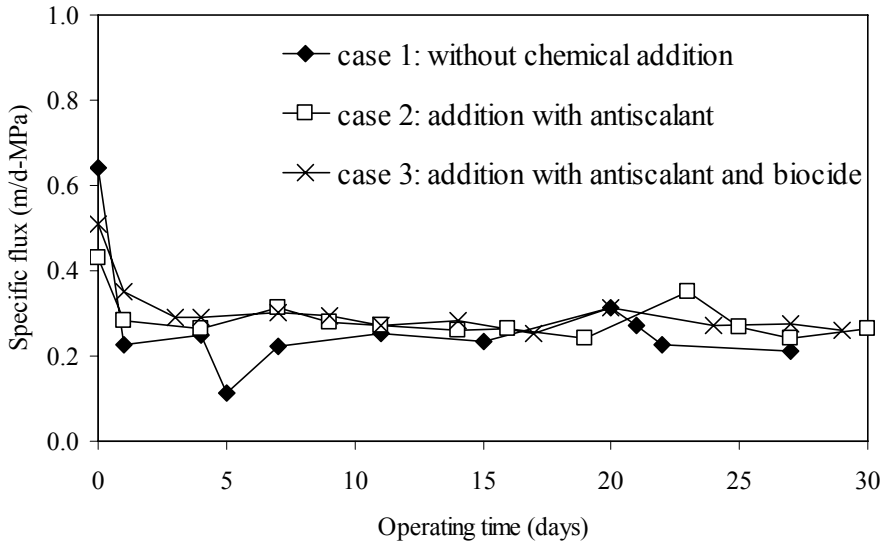

Figure 11 Variation of specific flux with operating time

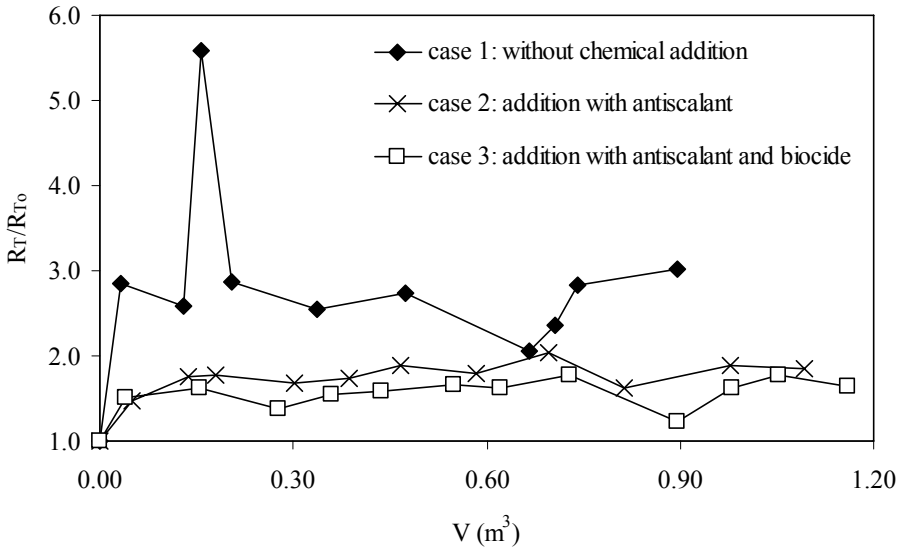

Figure 12 Variation of relative hydraulic resistance (R_T/R_{To}) with time

Table 10 Experimental results of bench-scale

Parameters	Experimental conditions		
	Case 1	Case 2	Case 3
Specific flux (m/d-MPa)			
$L_{1\ hour}$	0.511	0.430	0.511
L_{1day}	0.225	0.285	0.349
L_{7days}	0.224	0.314	0.303
L_{30days}	0.213	0.244	0.261
Fouling index (m^{-2})			
$I_{1\ hour}$	$5.62x10^{15}$	$1.50x10^{16}$	$7.89x10^{15}$
I_{1day}	$2.54x10^{15}$	$1.80x10^{15}$	$9.63x10^{14}$
I_{7days}	$5.51x10^{14}$	$2.52x10^{14}$	$2.41x10^{14}$
I_{30days}	$1.42x10^{14}$	$1.01x10^{14}$	$8.15x10^{13}$
Average EC-rejection (over 30 days)			
EC_{feed} (µS/cm)	3,844±340	3,986±284	3,944±150
$EC_{concentrate}$ (µS/cm)	3,917±349	4,066±290	4,030±154
$EC_{permeate}$ (µS/cm)	156±42	134±16	118±19
Rejection (%)	95.97	96.67	97.04

1.2.2 Mathematical expression for predicting RO flux

The resistance in series model with cake formation ($J = \Delta P/(\eta[R_m + (I\,V/A)])$) were modified to asses the specific flux decline during membrane filtration. In case of dead-end filtration system, the fouling index is constant hence the specific flux can be determined from $L^{-1} = \eta R_m + (\eta I V/A)$. In case of spiral wound filtration system, the fouling index varies with specific volume ($dI/d(V/A) = -\gamma I^n$). After integration, the mathematical expression of flux decline during RO filtration using concept of variable fouling index was obtain as $\frac{1}{I^{(n-1)}} = \frac{1}{I_o^{(n-1)}} + (n-1)\gamma\frac{V}{A}$.

In this topic, mathematical expression of flux decline using variable fouling index was applied to the experimental data. Empirical parameters were determined and were analyzed their sensitivity on change in flux decline. In addition, the accuracy of mathematical expression using concept of variable fouling index on assessment of flux decline profile in long-term operation was compared with the concept of constant fouling index.

1) Determination of empirical parameters

The specific flux data of bench-scale experiment from all cases were used to determine fouling index parameters. Subsequently, three sets of fouling index data obtained from the different operation periods (1 day, 7 days, and 30 days) were plotted against the specific volume (V/A) to determine the initial fouling index (I_o) and reduction coefficient (γ). Consequently, the estimated specific flux profiles were calculated from these empirical parameters. The accuracies of these empirical parameters obtained in predicting RO flux under different operating periods were compared.

The empirical parameters and the calculated profiles of specific flux are shown in **Table 11** and **Figure 13**, respectively. It was found that the appreciate order of reaction rate was 2.2 for all conditions. Moreover, similar profiles were achieved from all of the expression calculated from different operation periods. The values of SSE of case 1 were 0.0402, 0.0259, and 0.0234, for the operation periods of 1 day, 7 days, and 30 days, respectively. In addition, SSE values of case 2 were 0.0275, 0.0573, and 0.0243. The values of SSE of case 3 were 0.0253, 0.0128, and 0.00936. From these results, the best-fit expressions were achieved from the period of 30 days judging from the lowest SSE of all conditions. However, the models that were calculated from 1 day and 7 days data are also in good agreement with the experimental data as shown by SSE values. Therefore, it can be concluded that bench-scale operation data of 7 days or more provided a promising accuracy for estimation of flux decline in long-term operation of larger scale system using variable fouling index model. The model derived from case 3, the normal operating condition of pilot-scale plant, which was calculated from the period of 30 days, is showed as shown in **Equation 48**.

Table 11 Comparison of I_o and γ data between 1 d-data, 7 d-data, and 30 d-data

Parameter	Experimental case		
	without chemical addition	addition with antiscalant	addition with antiscalant and biocide
1 d			
n	2.2	2.2	2.2
I_o (m^{-2})	5.517×10^{15}	3.779×10^{16}	5.244×10^{15}
γ (m^{-1})	2.928×10^{-18}	3.537×10^{-18}	6.711×10^{-18}
SSE	**0.0402**	**0.0275**	**0.0253**
7 d			
n	2.2	2.2	2.2
I_o (m^{-2})	7.222×10^{15}	1.118×10^{16}	2.445×10^{16}
γ (m^{-1})	3.636×10^{-18}	6.570×10^{-18}	6.523×10^{-18}
SSE	**0.0259**	**0.0573**	**0.0128**
30 d			
n	2.2	2.2	2.2
I_o (m^{-2})	8.185×10^{15}	1.118×10^{16}	2.501×10^{16}
γ (m^{-1})	4.000×10^{-18}	4.600×10^{-18}	5.900×10^{-18}
SSE	**0.0234**	**0.0243**	**0.00936**

$$L = \frac{1}{\eta\left\langle R_M + \left[\frac{V}{A}\left\{\frac{\left(2.501\times10^{16}\right)^{1.2}}{1+[(1.2)\times5.900\times10^{-18}\,\frac{V}{A}\left(2.501\times10^{16}\right)^{1.2}]}\right\}^{\left(\frac{1}{1.2}\right)}\right]\right\rangle} \quad 48)$$

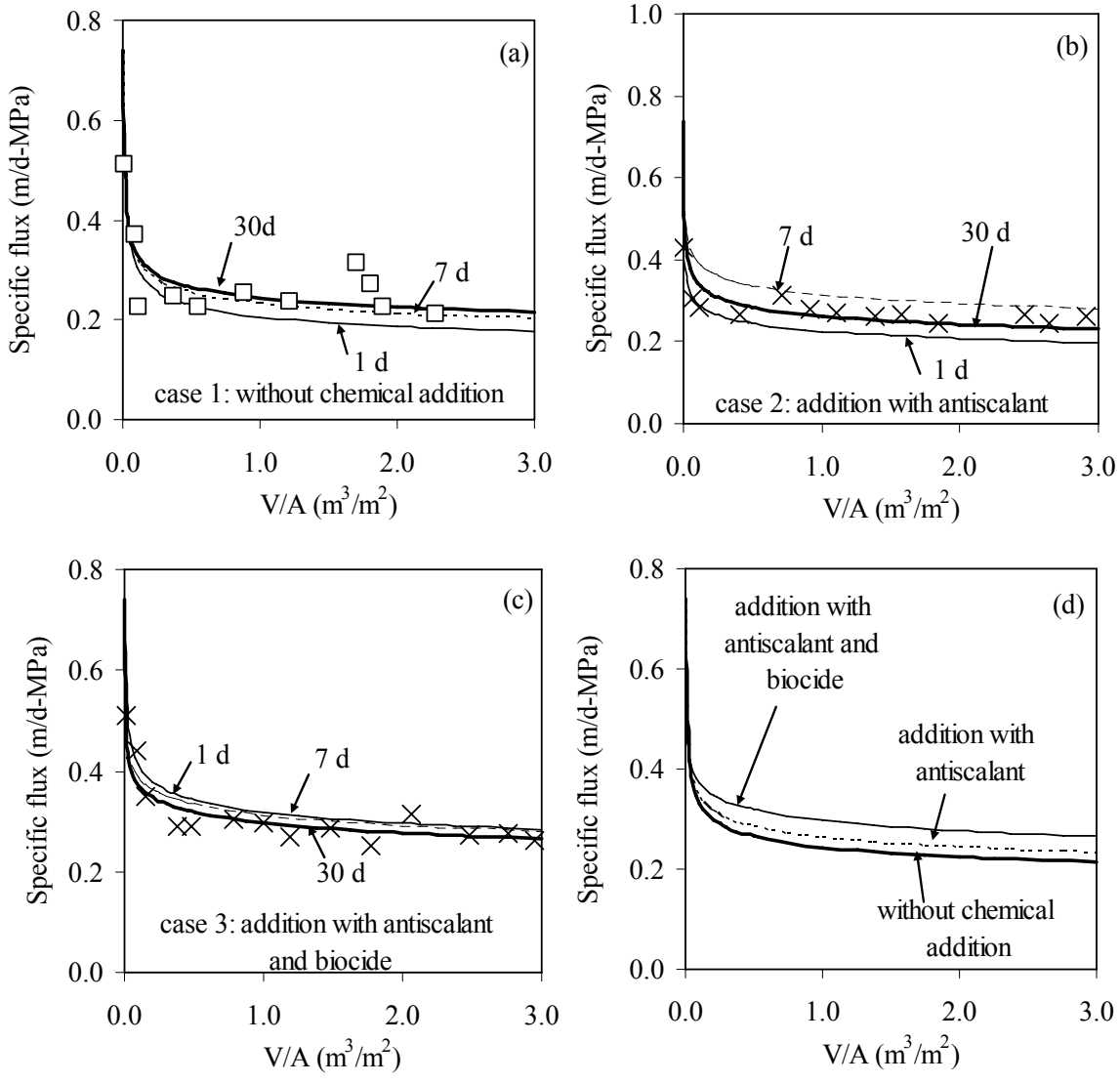

Figure 13 Comparison of the calculated specific flux profile between different operating periods (a) 1day, (b) days, and (c) 30 days) and (d) comparison of the flux profile between different operating conditions derived from data of 30 days.

2) Sensitivity analysis

Figures 14 and 15 show the effect of reduction coefficient (γ), initial fouling index (I_o), and the rate-order (n). It was found that the change in reduction coefficient led to change in fouling index and specific flux profile. An increase in reduction coefficient decreased fouling index and led to increase of specific flux. On the other hand, the decrease in reduction coefficient gave opposite results. The initial fouling index affected the specific flux only during the initial stage of operation. In long-term operation, the specific flux was not influenced by this parameter. The rate-order results in significant change of specific flux profile. A minute increase of rate-order from 2.20 to 2.25 (~ + 2.7%) yielded almost constant profile of specific flux throughout the operation. In addition, a small decrease of rate-order from 2.20 to 2.15 (~ - 2.7%) caused the large drop in specific flux.

3) Compatibility analysis for predicting long-term flux

The empirical parameters derived from the case 3 of bench-scale reclamation plants, in which antiscalant and biocide were added, were tested for their accuracy with long-term data of the pilot-scale plant. The operating data of the pilot-scale reclamation plant were recorded by WRPC since July 2004 unit the end of December 2004. The specific flux profiles which were determined from the model using constant fouling index concept were also compared.

Table 12 shows the empirical parameters comparing between constant fouling index model and variable fouling index model. **Figure 16** shows the comparison of specific flux and pressure profiles derived from constant fouling index and variable fouling index models with pilot scale operation data. In the comparison, the variable fouling index model previously described in **Equation 48** is used whereas the constant fouling index as shown in **Equations 49** is used.

$$\frac{1}{L} = 0.1184 + 3.3689\frac{V}{A} \qquad 49)$$

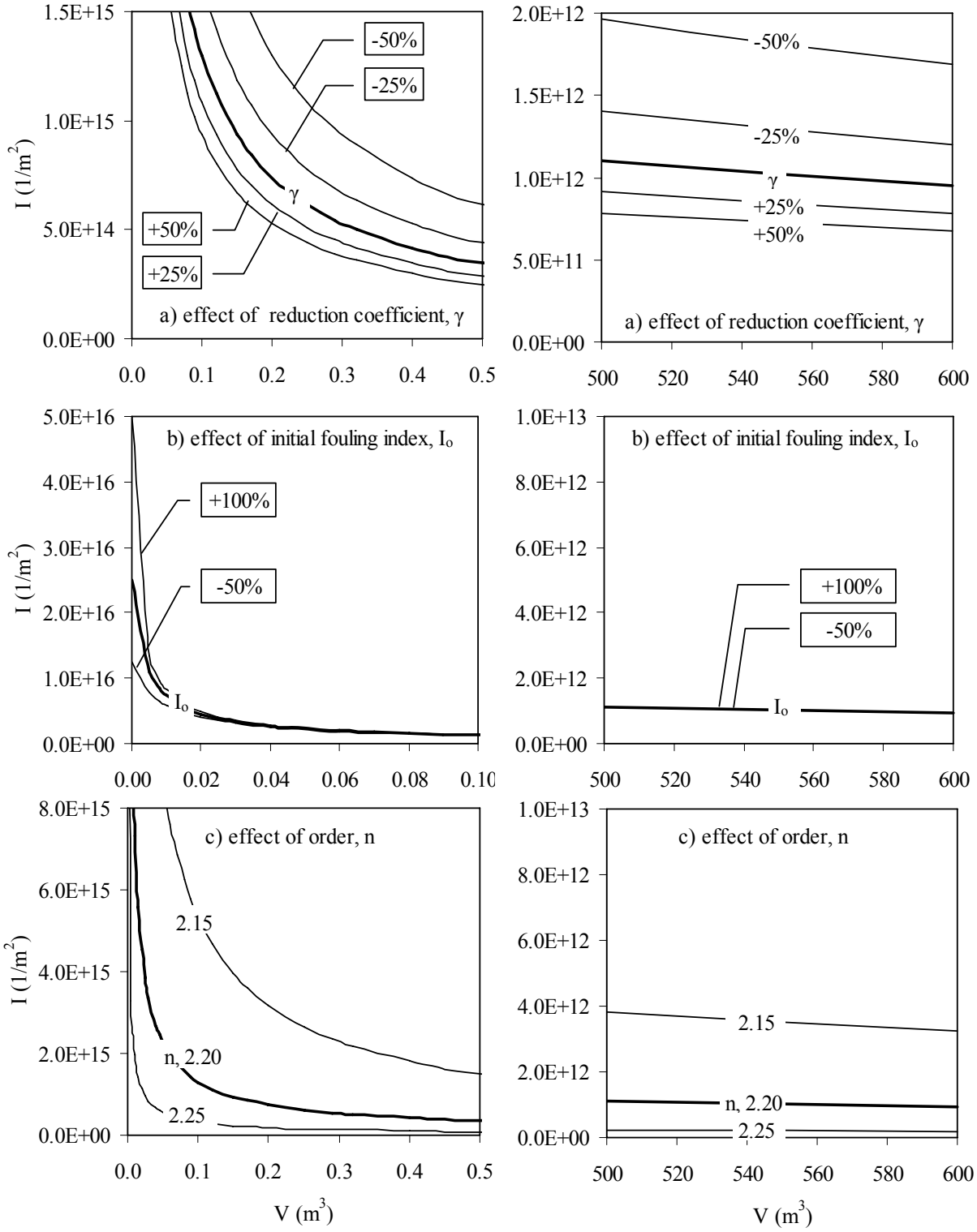

Figure 14 Model sensitivity analysis on fouling index (I) of the real treated textile wastewater using the data of bench-scale plant (case 3)

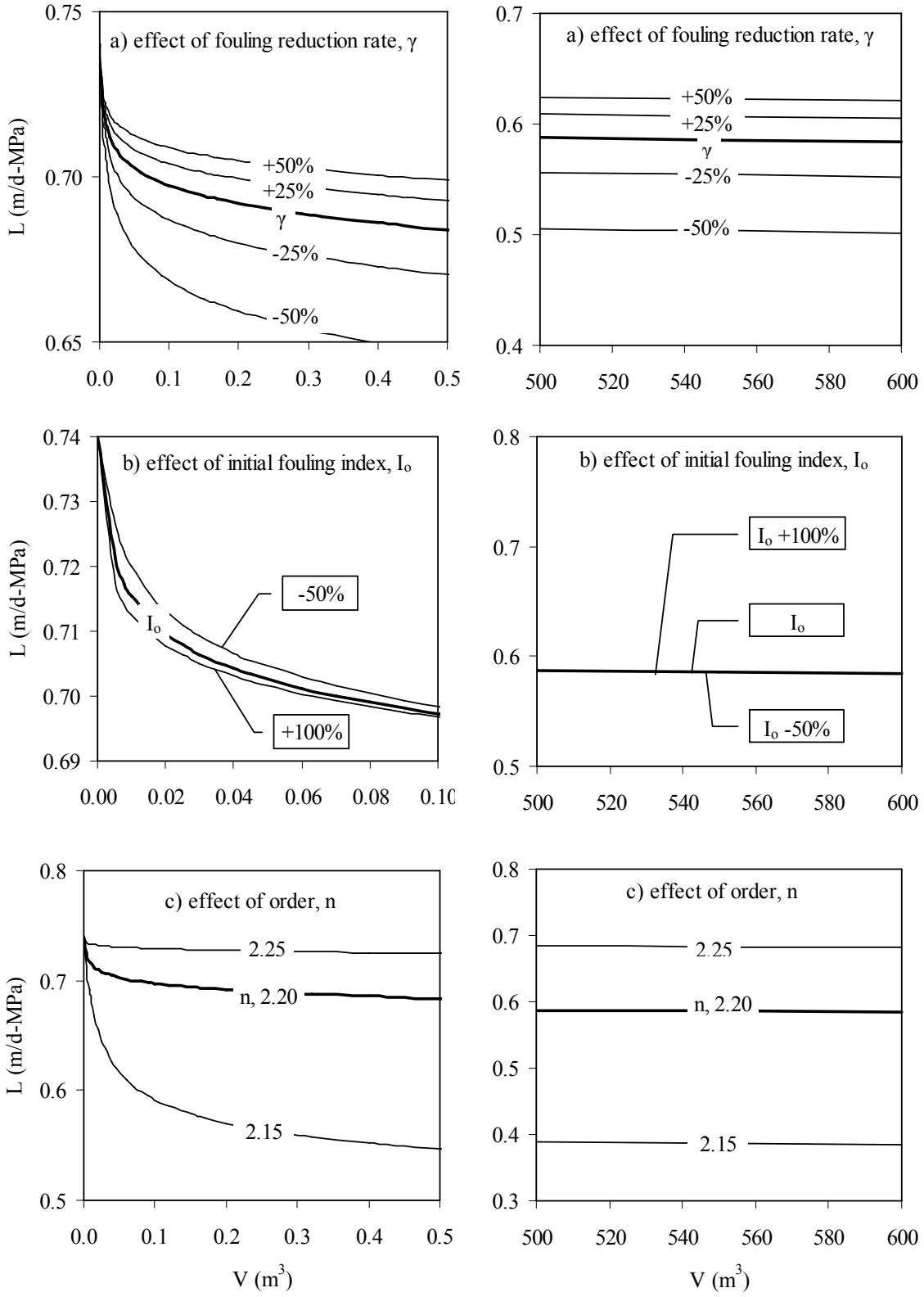

Figure 15 Model sensitivity analysis on specific flux (L, J/ΔP) of the real treated textile wastewater using the data of bench-scale plant (case 3)

Table 12 The empirical parameters comparing between model with constant fouling index and model with variable fouling index

Mathematical expression	Parameters	Data
Constant I	$1/L_o = \eta R_M$ (d.MPa.m^{-1})	0.1184
	ηI (d.MPa.m^{-2})	3.3689
	SSE	**0.399**
Variable I	n (-)	2.2
	I_o (m^{-2})	2.501x10^{16}
	γ (m^{-1})	5.900x10^{-18}
	SSE	**0.1231**

Note: The models with constant fouling index were calculated from Equation 9.

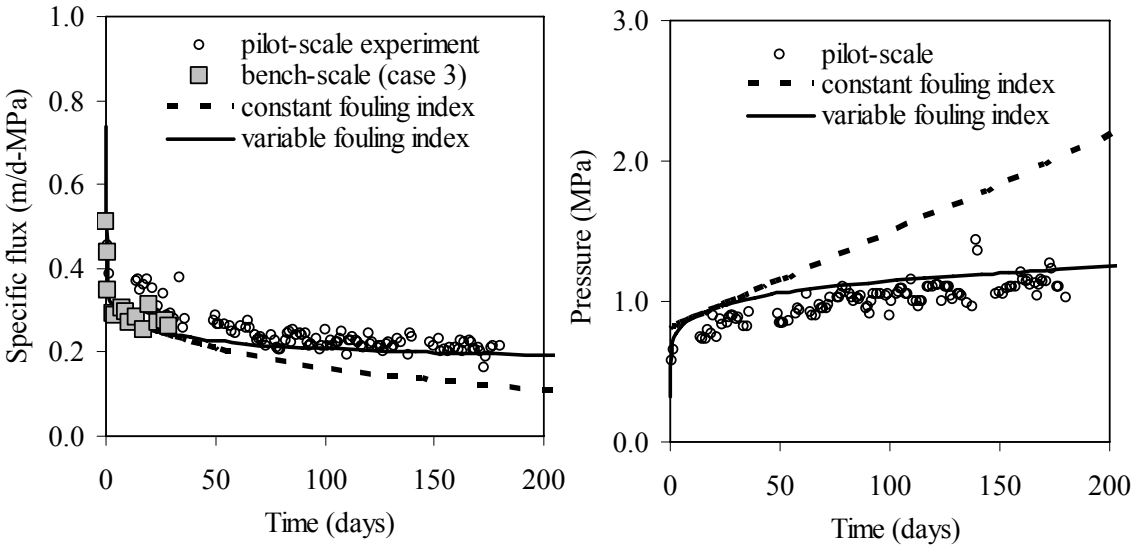

Figure 16 Comparison of the specific flux profiles and net driving pressure profiles between the constant fouling index model and the variable fouling index model

It was found that, SSE values of model with constant fouling index and model of variable fouling index were 0.3990 and 0.1231 m^{-2} respectively. Hence, the

model with variable fouling index provided more accurate estimation of specific flux and pressure in RO system judging from the lower value of SSE. Moreover, the membrane area and element size do not significantly affect the accuracy of proposed model in this study. Short-term operation in small-scale experimental set-up was successfully applied to assess a productivity of a larger plant in long-term operation.

1.3 Membrane cleaning study

Cause of fouling due to the treated textile wastewater was study using cleaning technique and SEM micrograph.

1.3.1 Cleaning procedure

The fouled membrane samples, which were took out off the spiral-wound membrane filtration unit, were washed with different cleaning procedures using the stirring membrane filtration unit. The fractions of foulant were separated into 4 categories i.e. the particulate foulant or loosed foulant, the organic foulant, the inorganic foulant, and the irreversible foulant. The fraction of particulate foulant or loosed foulant was evaluated by washing with pure water at high CFV. The fraction of organic foulant and inorganic foulant were evaluated by washing with alkaline and acid respectively.

The particulate foulant or loosed foulant was study by washing with pure water. Membrane samples were washed at different CFV of 5, 15, 25, 35, 45, and 55 cm/s, respectively to investigate the effective CFV for removal of the particulate foulant. The results from **Figure 17** show that the minimum effective CFV was 25 cm/s. Hence, in normal operation, feed flow rate should be controlled to maintain CFV at a minimum of 25 cm/s in order to prevent the particulate fouling. With CFV of 25 cm/s, the RR values of all cases, without chemical addition, addition with antiscalant, and addition with antiscalant and biocide, were 8.71, 17.54 and 28.41 %, respectively. The RR values illustrated that the most serious fouling occurred in the case where without chemical was added. Moreover, even if addition of biocide

could not increase the specific flux comparing with the case where only antiscalant was added but it increased the cleaning efficiency of pure water. The biocide probably decreased the viable microbial cell and decreased the biofouling potential of wastewater. Hence, the dead cell played a role as particulate foulant instant of biological foulant and it was easier to be removed by pure water.

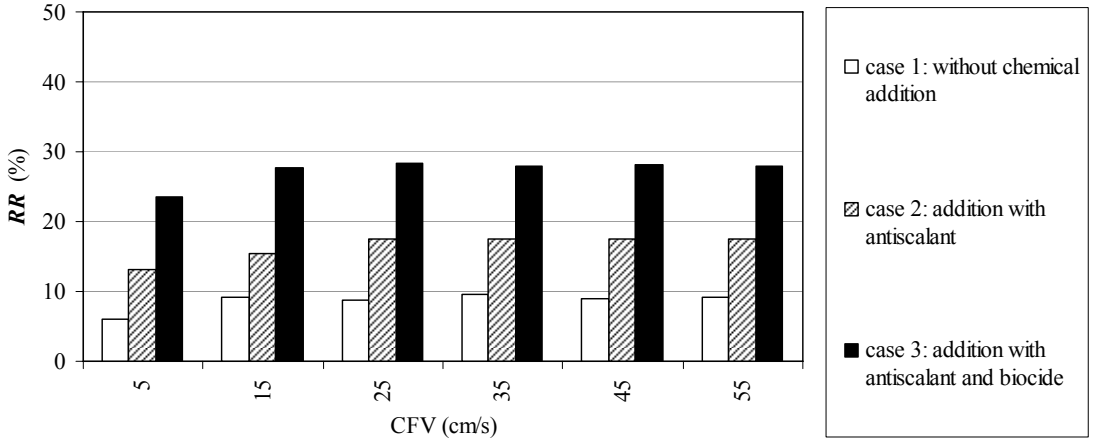

Figure 17 Effect of CFV on the total hydraulic resistance removal efficiency (RR)

The other types of foulant, organic foulant, inorganic foulant, and irreversible foulant were investigated by chemical cleaning. NaOH, HCl, citric acid, oxalic acid, EDTA, and SBS were study their cleaning efficiency on the fouled membrane where without additive chemical was added. **Figure 18** shows that excellent resistance removal efficiency data were achieved from the case where the sequential cleaning of NaOH (pH 12) following by HCl (pH 2) were applied. Hence, they were selected to represent the alkaline and acid in the chemical cleaning study and were applied to wash all of the membrane sample cases. **Figure 19** shows the removal efficiency of foulant resistance of all cases. It was found that NaOH achieved better removal efficiency than HCl hence; there was higher fraction of organic foulant than inorganic foulant on the fouled membrane. Moreover, the sequential cleaning of NaOH following by HCl was better than cleaning with HCl following by NaOH.

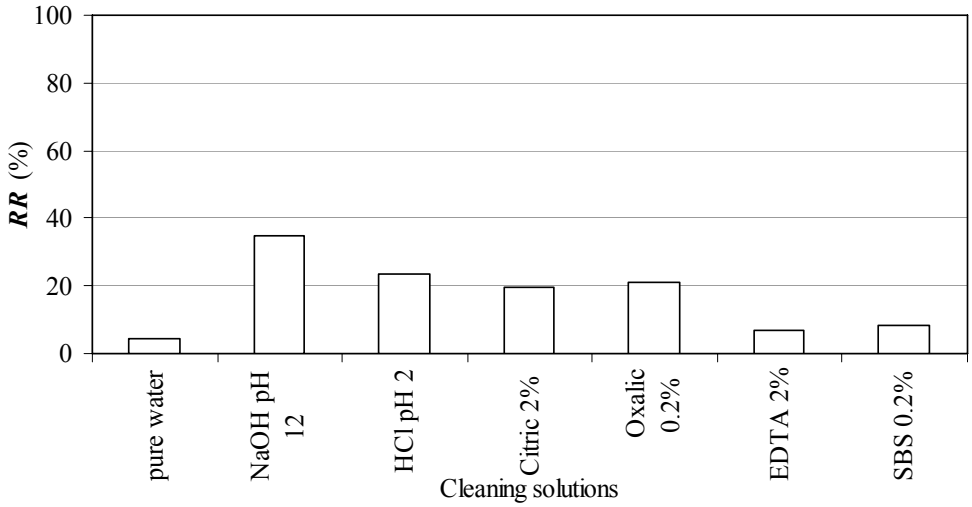

Figure 18 Resistance removal efficiency due to chemical cleaning for the case where without chemical was added

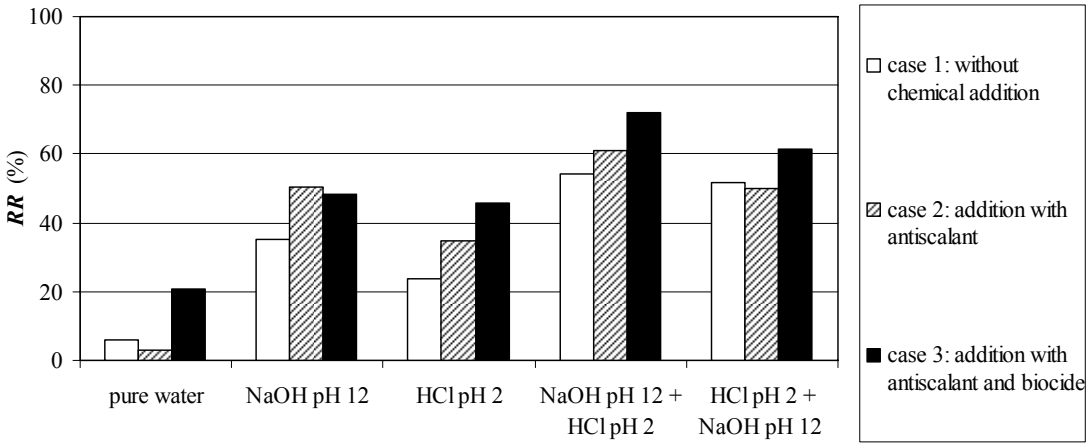

Figure 19 Resistance removal efficiency due to chemical cleaning comparing between cases 1 to 3

The fraction of foulant resistance **(Figure 20**) shows that the remained irreversible foulant on membrane after cleaning by the sequential cleaning, NaOH following by HCl, was 45.82, 38.96, and 27.83 %, respectively. Therefore, the additive chemical increased the cleaning efficiency significantly. Consideration of the total reversible foulant fraction, the organic foulant was the major cause of fouling in

this study. Hence, the organic foulants of the treated wastewater from MBR were considered to study deeply more detail in next experimental phase.

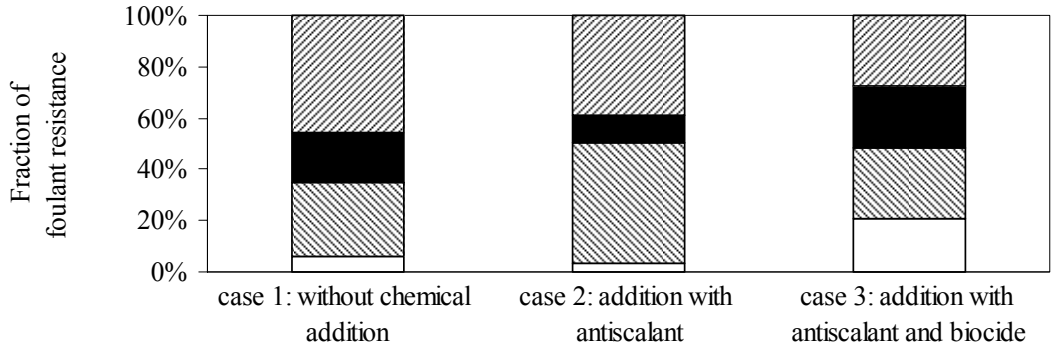

	case 1: without chemical addition	case 2: addition with antiscalant	case 3: addition with antiscalant and biocide
▨ irreversible fouling	45.82	38.96	27.83
■ inorganic fouling	19.15	10.58	23.76
▧ orgaic fouling	28.89	47.33	27.60
□ particulate fouling	6.14	3.14	20.82

Figure 20 Fraction of the foulant resistance

1.3.2 Deposit foulant

Figures **21a-23a** show the SEM-micrographs of the deposited foulant on fouled membranes and the remained foulant on the washed membrane. The various foulants; organic, scaling, and biofouling, were observed in all cases. The cake layers on each fouled membrane were not identical types and thickness. SEM micrographs from cases where antiscalant was added, and where antiscalant and biocide were added, showed that antiscalant and biocide solution could not prevent scaling and biofouling on the membrane surface.

From the membrane cleaning results, the most effective cleaning agents, sequential cleaning of NaOH (pH 12) following by HCl (pH 2), were applied on membrane samples from all cases. SEM micrographs of these samples (**Figures 29b-23b**), illustrated the performance of antiscalant and biocide solutions in supporting cleaning efficiency as shown in the cleanest membrane of **Figure 23b**.

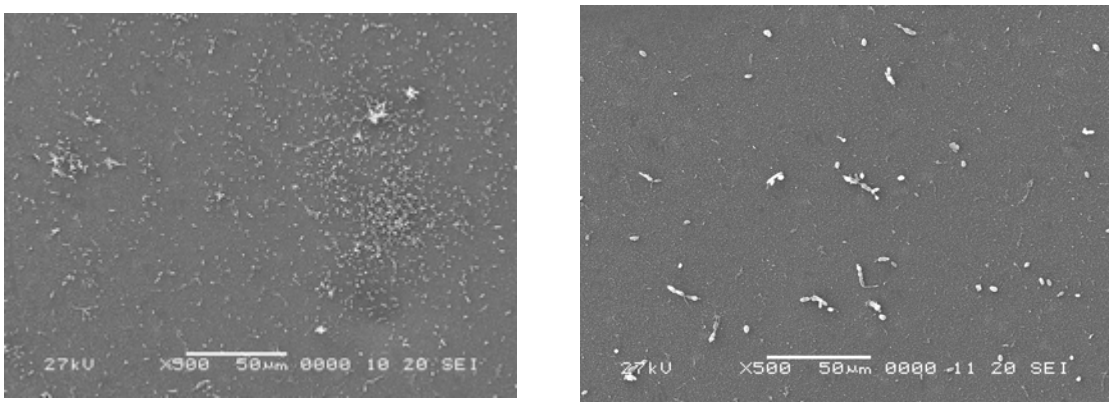

(a) before cleaning *(b) after cleaning*

Figure 21 SEM micrographs fouled and cleaned membrane applied to wastewater without chemical addition

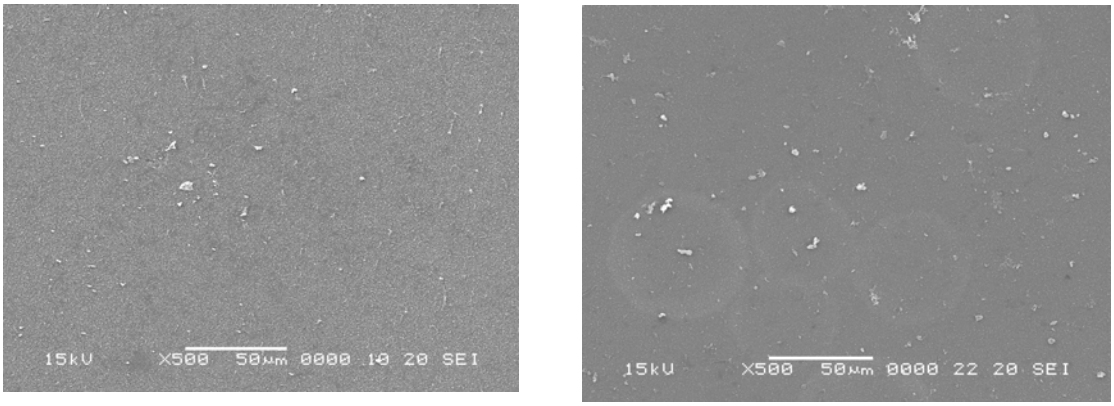

(a) before cleaning *(b) after cleaning*

Figure 22 SEM micrographs of fouled and cleaned membrane applied to wastewater with antiscalant

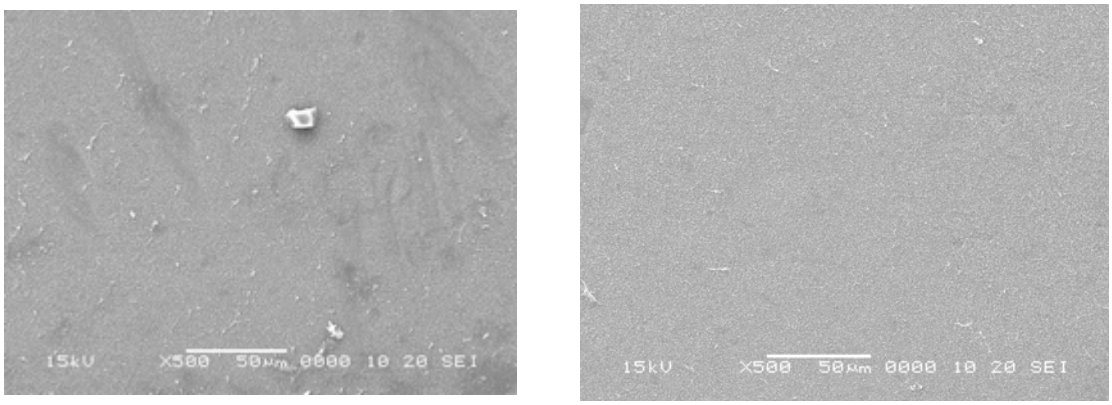

(a) before cleaning *(b) after cleaning*

Figure 23 SEM micrographs of fouled and cleaned membrane applied to wastewater with antiscalant and biocide

2. Experiment of organic foulant interaction and RO fouling

Organic fouling, the main cause of fouling of RO filtrated treated textile wastewater, was studied in this section. Synthetic wastewater composed salt, surfactants, reactive dye, and EfOMs were filtrated using C10-T cell. Fouling potential was determined in term of the fraction of flux decline and permeate volume (ΔJ/ΔV). Moreover, the fouled membranes were washed with pure water and alkaline solution to determine the irreversible foulant resistance.

2.1 Effect of single organic foulants on RO fouling

Synthetic wastewater composed salt (NaCl of 2,000 mg/L) and different organic foulants, i.e. 1) EfOMs of 0.83 mM as C, 2) dye of 7.48 mM as C, 3) SA of 1.43 mM as C, 4) TX of 5.26 mM as C, and 5) SDS of 3.95 mM as C, were tested for their fouling potential. RO membrane model of ES-20 and LF-10 representing negatively charged membrane with low hydrophilic property and neutrally charged membrane with higher hydrophilic property were selected in this study (Nitto Denko, 1998).

2.1.1 Flux decline

Flux profile and flux decline in term of ΔJ/ΔV during RO filtration using ES-20 and LF-10 are shown in **Figures 24**. The term of ΔJ is defined as a difference between flux at 1 hour and 24 hours of operation and the term of ΔV is defined as a cumulative volume from 1 hour to 24 hours of operation. It was found that the surfactants decreased flux more than dye, EfOMs and especially much more than NaCl for both membranes. In the case of ES-20 filtered SA, TX, SDS, dye, and EfOMs, ΔJ/ΔV were 96.7, 64.4, 30.80, 26.0, and 16.3 m/d-m^3 respectively. In the case of LF-10, ΔJ/ΔV were 69.5, 41.4, 23.09, 20.1, and -14.8 m/d-m^3.

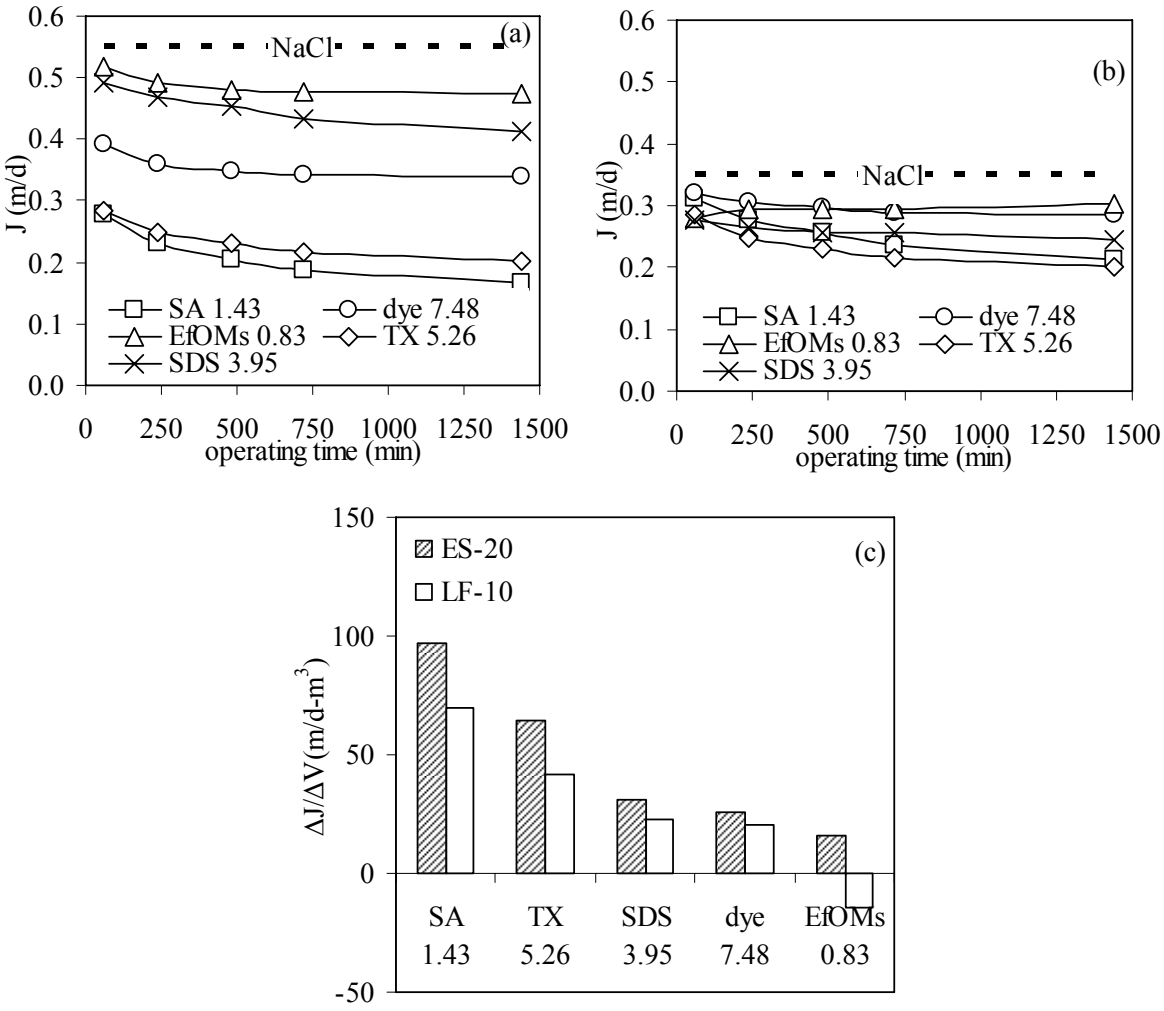

Figure 24 Flux profile of wastewater containing single foulant on (a) ES-20 and (b) LF-10, and (c) comparison of flux decline between ES-20 and LF-10

2.1.2 Calculated osmotic pressure at membrane surface

The total osmotic pressure at membrane surface ($\Delta\pi_{m,\ total}$), the osmotic pressure of organic foulant at membrane surface ($\Delta\pi_{m,\ organic}$), and the osmotic pressure of NaCl at membrane surface ($\Delta\pi_{m,\ NaCl}$) were calculated and are shown in **Table 13**. It was found that $\Delta\pi_{m,\ total}$ of ES-20 applied to the filtration of SA, TX, SDS, dye, and EfOMs were determined as the range from 0.226 to 0.302 MPa respectively and $\Delta\pi_{m,\ organic}$ ranged from 0.019 to 0.104 MPa. In the case of LF-10,

$\Delta\pi_{m,\ total}$ ranged from 0.201 to 0.245 MPa and $\Delta\pi_{m,\ organic}$ ranged from 0.011 to 0.059MPa.

Table 13 Osmotic pressure at membrane surface of wastewater containing single organic foulant

Wastewater	Osmotic pressure at membrane surface ($\Delta\pi_m$, MPa)		
	$\Delta\pi_{m,\ NaCl}$	$\Delta\pi_{m,\ organic}$	$\Delta\pi_{m,\ total}$
ES-20			
SA 1.43 mM as C	0.191	0.092	0.283
TX 5.26 mM as C	0.198	0.104	0.302
SDS 3.95 mM as C	0.207	0.019	0.226
dye 7.48 mM as C	0.199	0.047	0.246
EfOMs 0.83 mM as C	0.197	0.035	0.232
LF-10			
SA 1.43 mM as C	0.193	0.026	0.219,
TX 5.26 mM as C	0.187	0.059	0.245
SDS 3.95 mM as C	0.190	0.011	0.201
dye 7.48 mM as C	0.193	0.015	0.208
EfOMs 0.83 mM as C	0.191	0.011	0.202

2.1.3 Foulant resistance

The foulant resistance of fouled membranes, washed membrane by pure water, and washed membrane by alkaline solution were determined to evaluate the irreversible fouling potential of organic foulants contained in textile wastewater. The results from **Figure 25** show that SA and TX caused the irreversible fouling on ES-20. Physical cleaning using high CFV and pure waster could completely remove foulant resistance caused by EfOMs. Alkaline solution could entirely remove foulant resistance caused by the anionic species like dye and anionic surfactant as SDS.

Nevertheless, it could remove some of foulant resistance caused by non-ionic surfactant as TX and mixed surfactant as SA. The irreversible fouling caused by SA and TX decreased the membrane permeability (L_P) of 30.44 and 18.17 %. In case of LF-10, only SA performed irreversible fouling layer on the membrane surface. The membrane permeability was decreased 15.38 %.

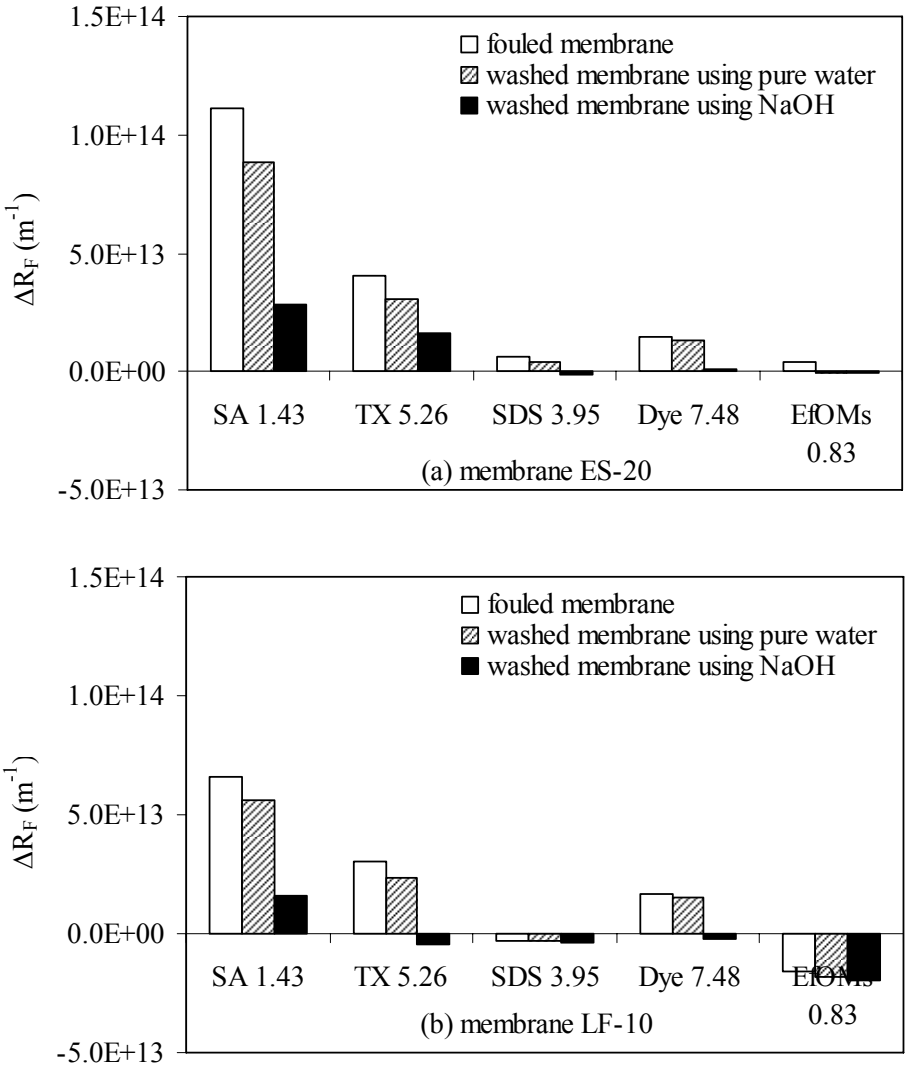

Figure 25 Foulant resistance on ES-20 and LF-10

2.1.4 Fouling of single organic foulant

According to the results, it was found that the surfactants yielded the highest fouling potential. In addition, NaCl contained in the wastewater was the main constituent contributing to osmotic pressure as the range from 56.6 to 95.6 %, even if the highest flux profile was obtained from the case where only NaCl was added. In contrary, osmotic pressure at membrane surface due to organic matter were mainly contributed from TX and SA. Hence, RO flux was influenced by the fouling due to non-ionic surfactant much more than the osmotic pressure of NaCl.

Lower fouling occurred on the membrane that contained higher hydrophilic property as LF-10. Since the ordinary fouling mechanism of surfactant monomers is influenced by the hydrophobic adhesion. They associated with membrane surface by their hydrophobic tail and presented the hydrophilic head against water stream (Mietton-Peuchot and Ranisio, 1997; Schulz, 1999; van der Bruggen, 2005). Therefore, lower hydrophobic adhesion and lower fouling occurred at the membrane with higher hydrophilic property.

The highest and lowest osmotic pressures at membrane surface were provided by TX and SDS respectively. High hydrophobic adhesions of non-ionic surfactant monomers draw themselves from the bulk and advance towards the surface of ES-20. In contrary, the higher hydrophilic property of LF-10 decreased the hydrophobic adhesion between membrane and organic foulants resulting in the lower $\Delta\pi_{m,\ organic}$. In the case of anionic surfactant, repulsive force due to anionic charge deflected the surfactant away from by the membrane surface. Therefore, osmotic pressure of anionic surfactant was minimized and flux decline was lower than the non-ionic surfactant and the mixed surfactant as SA.

The fouling mechanism of EfOMs was explained by the hydrophobic adhesion. It adsorbed onto the membrane surface by their hydrophobic tail (Thanuttamavong, 2002b) the same as the surfactant. In the case of the dye, it

fouled on the negatively charged membrane by colloidal formation at the membrane surface (Jiraratananon, *et.al.*, 2000).

Physical cleaning using high CFV and pure waster could completely remove foulant resistance caused by EfOMs. Alkaline solution could entirely remove foulant resistance caused by the anionic species like dye and anionic surfactant as SDS. Nevertheless, it could remove some of foulant resistance caused by non-ionic surfactant as TX and mixed surfactant as SA.

2.2 Effect of surfactant micellisation on RO fouling

Synthetic wastewaters composed of salt and varying concentration of SA of 0.78, 1.43, 4.08, and 6.72 mM as C were tested through the influence of micellisation on fouling potential of surfactant. Seriously fouled membrane, ES-20, was used in this study.

2.2.1 Flux decline

The experimental result from **Figure 26a** shows that flux profile at SA of 0.78 mM as C was similar to SA of 6.72 mM as C and flux profile at SA of 4.08 mM as C was similar to SA of 1.43 mM as C. From **Figure 26b**, at SA lower than CMC, $\Delta J/\Delta V$ increased from 77.4 to 96.7 m/d-m^3. In addition, at SA higher than CMC, $\Delta J/\Delta V$ decreased from 92.6 to 67.9 m/d-m^3.

2.2.2 Calculated osmotic pressure at membrane surface

Osmotic pressure at membrane surface, bulk concentration, and mass transfer coefficient are shown in **Table 14**. It was found that $\Delta\pi_{m,\ total}$ at SA of 0.78, 1.43, 4.08, and 6.72 mM as C were 0.266, 0.283, 0.276, and 0.255 MPa respectively. $\Delta\pi_{m,\ organic}$ were, 0.070, 0.092, 0.086, and 0.059 MPa. In addition, mass transfer coefficient of SA increased from 0.300 to 1.125 m/d. In relation to the normal behavior of surfactant, the concentration of SA monomer (S_{SA}) in the bulk increases

equally according to the increasing total concentration (C_{SA}) and it becomes constant at 1.62 mM as C when C_{SA} rises higher than CMC. The SA micelles appear when the C_{SA} is higher than CMC. The concentrations of SA micelle (M_{SA}) in the bulk at C_{SA} of 4.08 and 6.72 were 2.46, and 5.10 mM as C.

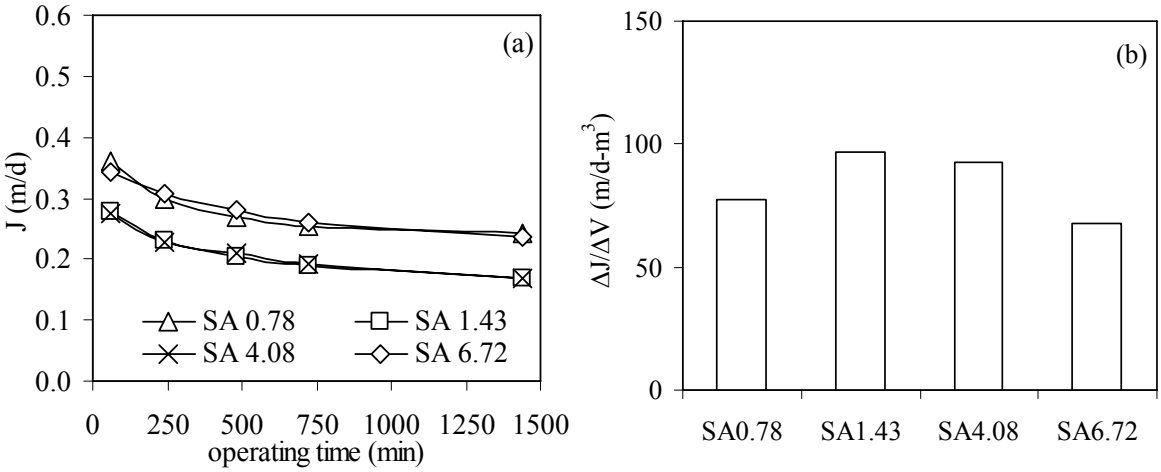

Figure 26 (a) Flux decline and (b) ΔJ/ΔV of wastewater containing different concentration of SA

Table 14 Osmotic pressure at membrane surface ($\Delta\pi_m$), the bulk concentration (C_b), and the mass transfer coefficient (k) of the wastewater containing different SA concentration

SA (mM as C)	Osmotic pressure at membrane surface, $\Delta\pi_m$ (MPa)			Bulk concentration, C_b (mM as C)		Mass transfer coefficient, k (m/d)
	$\Delta\pi_{m,\ NaCl}$	$\Delta\pi_{m,organic}$	$\Delta\pi_{m,\ total}$	monomer	micelle	
0.78	0.197	0.070	0.267	0.78	-	0.300
1.43	0.190	0.092	0.282	1.43	-	0.347
4.08	0.190	0.086	0.276	1.62	2.46	0.441
6.72	0.195	0.059	0.254	1.62	5.10	1.125

2.1.3 Foulant resistance

The foulant resistant of fouled membranes, washed membrane by pure water, and washed membrane by alkaline solution were determined to evaluate the irreversible fouling potential of surfactant at different concentration. The results from **Figure 27** show that SA produced the irreversible fouling in all of cases even if the alkaline solution was applied. The decreasing membrane permeability fluctuated in the narrow range between 26-37 %. It probably caused by the covered surfactant micelles were easy to remove by pure water and by alkaline solution due to the high hydrophilicity of washing solution could penetrate through a stern layer connecting with the hydrophilic micelle and the membrane surface. Moreover, the fouling remained on membrane surface related to the content of adsorbed surfactant monomer.

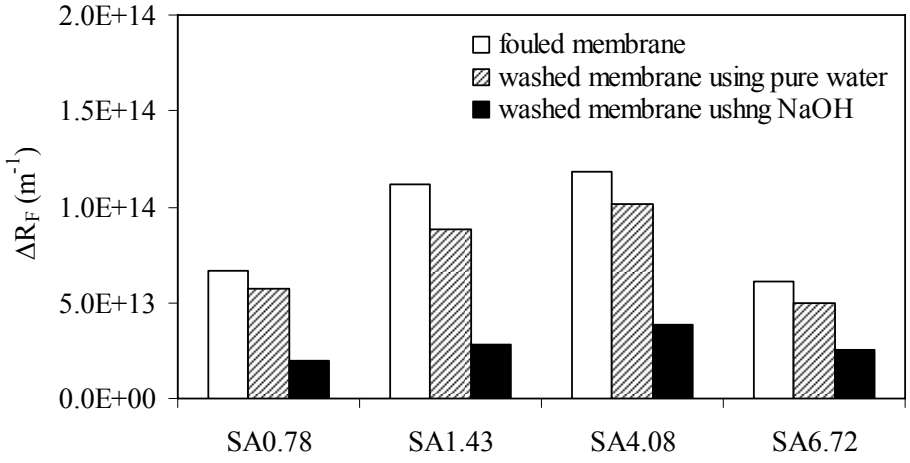

Figure 27 Foulant resistance of SA at different bulk concentration

2.2.4 Fouling of surfactant with micelle

Fouling of wastewater containing surfactant can be concluded that, at SA lower than CMC, fouling was affected by the increasing concentration. The stiff adsorption of the surfactant monomers decreases the flux even if it increases the hydrophilic property because it reduces the surface roughness and the surface area of

membrane drastically (Wilbert *et.al.*, 1998). This problem was found in the case of UF. The adsorbed surfactants, especially the non-ionic surfactant, narrow the pore of UF (Bakx *et.al.*, 2001). In addition, the hydrophobic fraction in the bulk is an important factor causing the flux decline while the hydrophilic fraction performs tiny effect (Nilson and DiGiano, 1996). Hence, at concentration lower than CMC, the higher surfactant concentration enlarges the membrane fouling by the higher hydrophobic fraction.

In contrary, at SA higher than CMC, the fouling tended to decrease. The decreasing fouling is effected by the micellisation above CMC. At concentration higher than CMC, the surfactant monomers bridge themselves by their hydrophobic part and present hydrophilic part. The micelles and the monomers in the mixture directly affect the flux decline and fouling. The aggregate equilibrium constant of surfactant with large aggregate number (n >50) can be approximated by $K_{eq} = CMC^{-n}$ (Wennerström and Lindman. 1979). The fouling mechanism of surfactant micelles are plugging and covering on membrane surface resembling a particulate fouling. According to the results, though the surfactant micelles plugged on the membrane surface, they did not decrease flux. One possible explanation is the fouling of covered surfactant micelles increase the hydrophilic property of membrane surface. Furthermore, the surfactant micelles compete in the adsorption capacity against the surfactant monomers and they decrease the adsorption capacity of surfactant monomers.

The effect of micellisation on the change in osmotic pressure at membrane surface was explained in this paragraph. In case of SA lower than CMC, $\Delta\pi_{m,\ organic}$ was affected by the monomers concentration. In contrary, when SA rose higher than CMC, $\Delta\pi_{m,\ organic}$ decreased. Since monomers bridge themselves by their hydrophobic part and present higher hydrophilic property (Schulz, 1999) this subsequently leads to the increasing hydrophilic fraction in the bulk. The hydrophilic micelles not only prefer to suspend in the bulk but also draw the monomers from the membrane surface closer to them. Consequently, the back diffusion increases judging

from the increasing mass transfer coefficient when the micelles appeared in the bulk. Leaist (1991) reported the consistent knowledge that the transport of the surfactant is influenced by diffusion of the micelles.

2.3 Effect of foulant interaction on RO fouling

Effect of the interaction between EfOMs & dye, the interaction between EfOMs & surfactant, and the interaction between dye & surfactant on the fouling of reactive dye and the fouling of surfactant were investigated. EfOMs of 0.83 mM as C was added in the synthetic wastewaters (reactive dye of 7.48 mM as C, SA of 1.43 mM as C, SA of 6.72 mM as C, TX of 5.26 mM as C, and SDS of 3.95 mM as C. Moreover, the additional foulants (dye of 1.53 mM as C, dye of 7.48 mM as C, and the mixture between EfOMs 0.83 mM as C and dye of 7.48 mM as C) were added in the synthetic wastewater containing surfactants (SA of 1.43 mM as C, SA of 6.72 mM as C, TX of 5.26 mM as C, and SDS of 3.95 mM as C).

2.3.1 Flux decline

The experimental result in **Figures 28 and 29** shows the flux profile and flux decline of the wastewater containing EfOMs, reactive dye, and surfactant. It was found that when EfOMs was added, the lower values of $\Delta J/\Delta V$ at dye of 7.48 mM as C, SA of 1.43 mM as C, SA of 6.72 mM as C and TX of 5.26 mM as C were achieved as the range from 10.62 to 40.08 m/d-m^3. Moreover, the additional dye of 1.53 mM as C, the additional dye of 7.48 mM as C, and the additional mixture between dye 7.48 mM as C and EfOMs 0.83 mM as C decreased $\Delta J/\Delta V$ of the wastewater containing SA of 1.43 mM as C from 96.69 to 16.26 m/d-m^3. In the case of the wastewater containing SA of 6.72 mM as C, the addition of dye of 1.53 mM as C increased $\Delta J/\Delta V$ from 67.92 to 95.06 m/d-m^3. When the higher dye concentration of 7.48 mM as C and the mixture between dye of 7.48 mM as C and EfOMs of 0.83 mM as C were added, $\Delta J/\Delta V$ decreased to 60.64 and to 28.09 m/d-m^3 respectively. In the case of TX at 5.26 mM as C, the same tend was obtained explicitly as SA. In the case of SDS at 3.95 mM as C, the additional dye increased

$\Delta J/\Delta V$ ranged from 30.80 to 50.40 m/d-m^3 but the additional mixture between dye 7.48 mM as C and EfOMs 0.83 mM as C decreased $\Delta J/\Delta V$ to 24.5 m/d-m^3.

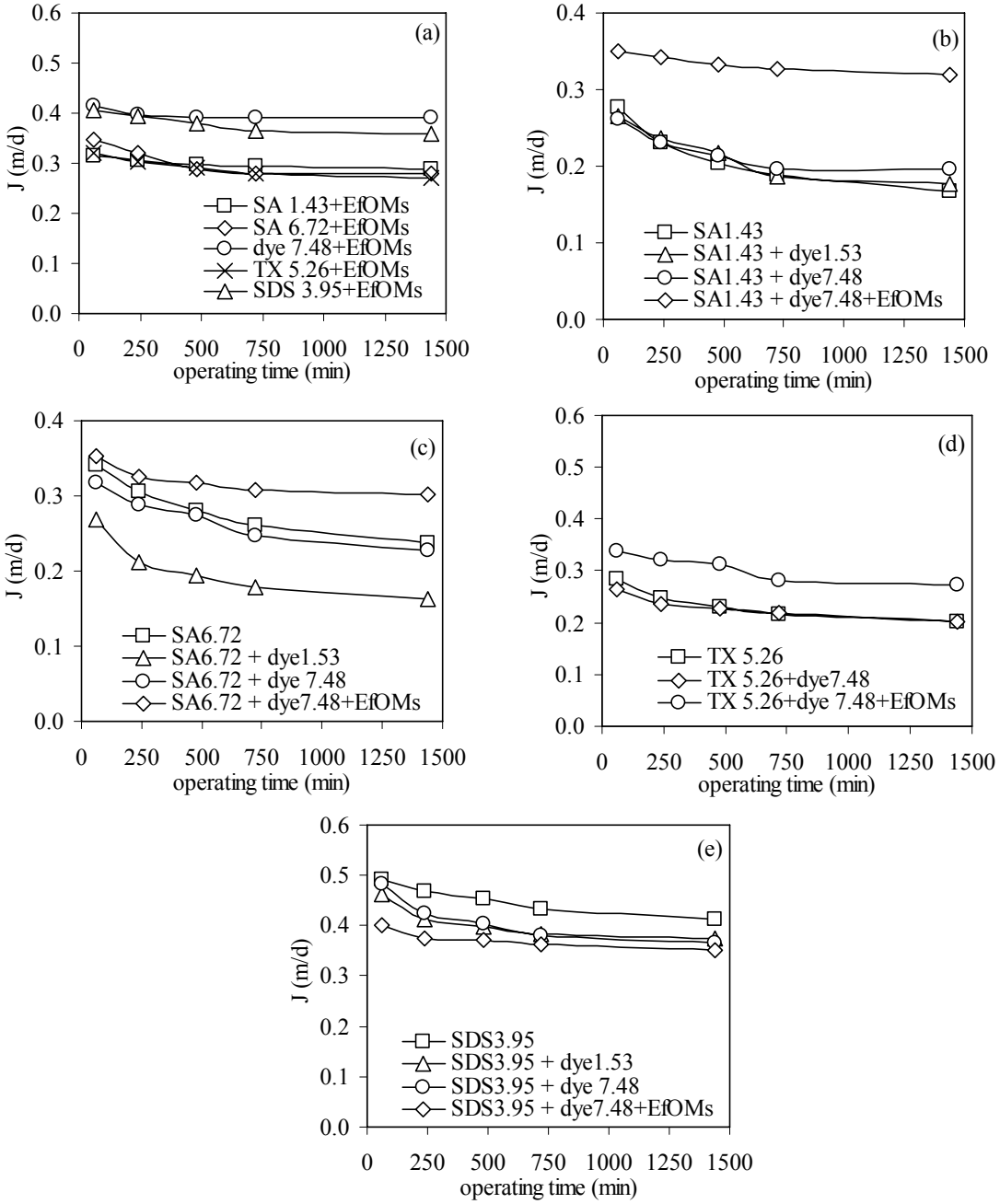

Figure 28 Flux profile of RO membrane applied to synthetic wastewater (a) single component with EfOMs, (b) SA (below CMC) + dye + EfOMs, (c), SA (above CMC) + dye + EfOMs, (d) TX + dye + EfOMs, (e) SDS + dye + EfOMs.

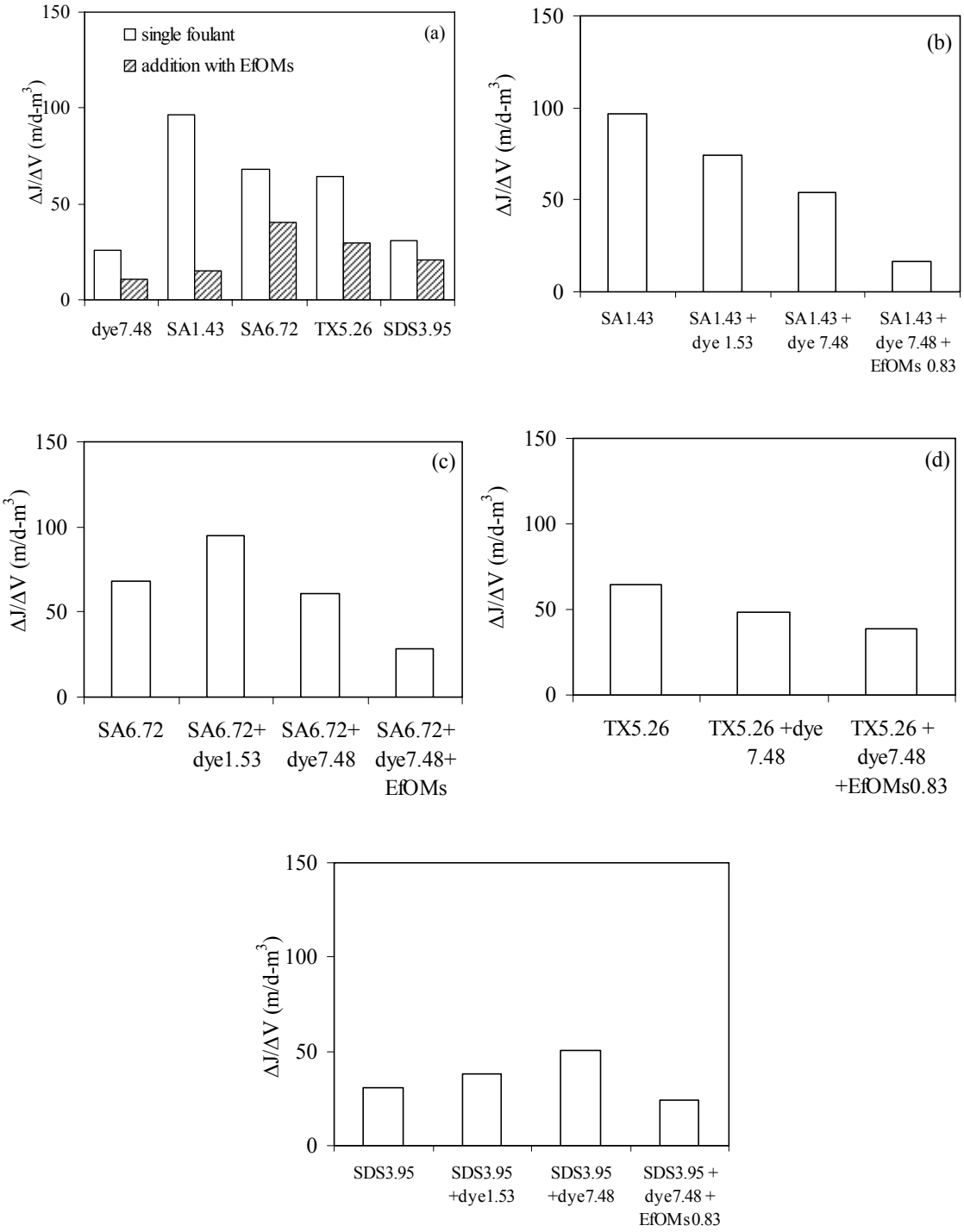

Figure 29 Flux decline of RO membrane applied to synthetic wastewater (a) single component with EfOMs, (b) SA (below CMC) + dye + EfOMs, (c) SA (above CMC) + dye + EfOMs, (d) TX + dye + EfOMs, (e) SDS + dye + EfOMs.

2.3.2 Calculated osmotic pressure at membrane surface

The experimental result in **Table 15** shows the osmotic pressure data at membrane surface of the case where EfOMs was added. The lower $\Delta\pi_{m,\ total}$ and $\Delta\pi_{m,\ organic}$ at dye of 7.48 mM as C, SA of 1.43 mM as C, SA of 6.72 mM as C, TX of 5.26 mM as C, and SDS of 3.95 mM as C were obtained ranging from 0.222 to 0.285 and from 0.021 to 0.091 MPa respectively.

Table 15 Osmotic pressure at membrane surface of wastewater containing EfOMs and other organic foulant

Wastewater	Osmotic pressure at membrane surface ($\Delta\pi_m$, MPa)		
	$\Delta\pi_{m,\ NaCl}$	$\Delta\pi_{m,\ organic}$	$\Delta\pi_{m,\ total}$
dye 7.48 mM as C + EfOMs 0.83 mM as C	0.201	0.021	0.222
SA 1.43 mM as C + EfOMs 0.83 mM as C	0.193	0.054	0.247
SA 6.72 mM as C + EfOMs 0.83 mM as C	0.195	0.053	0.248
TX 5.26 mM as C + EfOMs 0.83 mM as C	0.194	0.091	0.285
SDS 3.95 mM as C + EfOMs 0.83 mM as C	0.200	0.049	0.249

In addition, the osmotic pressure data at membrane surface of the case where the dye and the mixture between dye and EfOMs were added are shown in **Table 16**. In the case of SA of lower than CMC, the values of $\Delta\pi_{m,\ total}$ and $\Delta\pi_{m,\ organic}$ ranged from 0.268 to 0.316 and from 0.072 to 0.127 mM as C respectively. In addition, in case of SA of higher than CMC, the values of $\Delta\pi_{m,\ total}$ and $\Delta\pi_{m,\ organic}$ ranged from 0.247 to 0.300 and from 0.051 to 0.110 mM as C. In the case of TX, the values of $\Delta\pi_{m,\ total}$ and $\Delta\pi_{m,\ organic}$ ranged from 0.303 to 0.310 and from 0.108 to 0.121 mM as C. Lastly, in case of SDS, the values of $\Delta\pi_{m,\ total}$ and $\Delta\pi_{m,\ organic}$ ranged from 0.248 to 0.269 and from 0.042 to 0.069 mM as C.

Table 16 Osmotic pressure at membrane surface of wastewater containing dye, EfOMs, and surfactants

Wastewater	Osmotic pressure at membrane surface ($\Delta\pi_m$, MPa)		
	$\Delta\pi_{m,\ NaCl}$	$\Delta\pi_{m,\ organic}$	$\Delta\pi_{m,\ total}$
In case of SA 1.43 mM as C			
+ dye 1.53 mM as C	0.190	0.120	0.310
+ dye 7.48 mM as C	0.189	0.127	0.316
+ dye 7.48 mM as C + EfOMs 0.83 mM as C	0.196	0.072	0.268
In case of SA 6.72 mM as C			
+ dye 1.53 mM as C	0.190	0.110	0.300
+ dye 7.48 mM as C	0.193	0.061	0.254
+ dye 7.48 mM as C + EfOMs 0.83 mM as C	0.196	0.051	0.247
In case of TX 5.26 mM as C			
+ dye 7.48 mM as C	0.189	0.121	0.310
+ dye 7.48 mM as C + EfOMs 0.83 mM as C	0.195	0.108	0.303
In case of SDS 3.95 mM as C			
+ dye 1.53 mM as C	0.204	0.044	0.248
+ dye 7.48 mM as C	0.206	0.042	0.248
+ dye 7.48 mM as C + EfOMs 0.83 mM as C	0.200	0.069	0.269

It can be suggested that, the additional EfOMs decreased the osmotic pressure at membrane surface and flux decline of the wastewater containing multiple foulants significantly. In addition, the additional dye in wastewater tended to increase the osmotic pressure at membrane surface of the wastewater but decrease the fouling potential of wastewater excluding the case of SDS. Moreover, the addition of EfOMs in the wastewater containing surfactant and dye decreased the osmotic pressure at membrane surface and decreased flux decline.

2.3.3 Foulant interaction in wastewater

The interaction between EfOMs, dye, and surfactant contained in wastewater i.e., EfOMs & reactive dye, EfOMs & surfactant, and dye & surfactant were investigated. In this study, the mixed surfactant as SA was selected to study the interaction between surfactant and other organic foulants. The experiment conducted by filtration with UF using C40-B cell and the result can be summarized as following.

The interaction between reactive dye and EfOMs was conducted by the addition of EfOMs with concentration of 0.29 and 0.47 mM as C in the solution containing dye of 1.57, 3.05, and 3.79 mM as C. The interaction between dye and surfactant was conducted by the addition of dye at 1.57 and 4.53 mM as C in the solution containing SA of 0.77, 1.62, 2.75, and 4.07 mM as C. The interaction between EfOMs and surfactant was conducted by addition of SA at 1.43 and 4.07 mM as C in the solution containing EfOMs of 0.30, 0.38, and 0.58 mM as C. The amount of aggregated concentration due to the interaction between EfOMs & reactive dye, EfOMs & surfactant, and dye & surfactant is shown in **Figure 30**. It can be suggested that the aggregate concentration increased when the amounts of monomer increased.

In accordance with the interaction study and the filtration study, it can be suggested that the addition of EfOMs into the wastewater lead to the formation of aggregates and the decreasing foulant monomer. EfOMs associated with the reactive dye and the surfactant by their hydrophobic part and present the hydrophilic part aligned with water molecule. Subsequently, the addition of EfOMs decreased the hydrophobic adhesion of foulant. The decrease in active organic foulants (monomer) at the membrane surface leaded to a drop off of fouling potential. Moreover, when these aggregates presenting high hydrophilic adhesion plugged on the membrane surface, they increased hydrophilic condition and permeability of membrane surface. Consequently, the flux decline decreased similar to the case where fouling the surfactant aggregate was appeared.

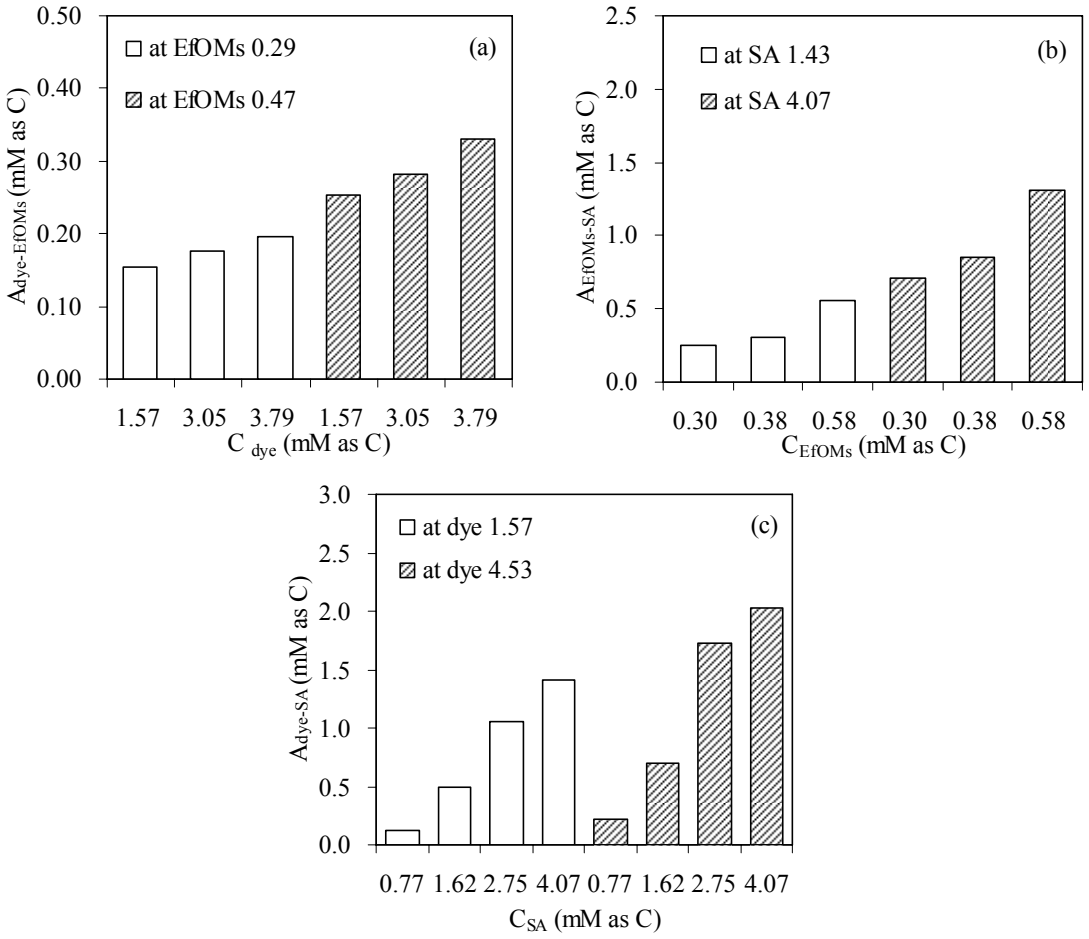

Figure 30 (a) Aggregated concentration formed between EfOMs and dye,
(b) Aggregated concentration formed between EfOMs and SA,
(c) Aggregated concentration formed between SA and dye.

The additional dye in the wastewater containing SA and TX also lead to the formation of aggregates and subsequently the flux decline decreases even if the osmotic pressure increased. In addition, the additional dye in the wastewater containing SDS increased the osmotic pressure at membrane surface and flux decline.

2.3.4 Foulant resistance

The resistance of fouled membranes, cleaned membrane by pure water, and cleaned membrane by alkaline solution were determined to evaluate the

irreversible fouling potential of wastewater containing multiple foulants. The results from **Figure 31** show the foulant resistance the mixture between EfOMs-surfactants and EfOMs-dye. It was found that, the additional EfOMs slightly increased irreversible foulant resistance on membrane surface in only case of SDS. Its permeability of washed membrane using alkaline solution decreased 8.33%. In other cases, the additional EfOMs did not considerably affect the permeability of washed membrane.

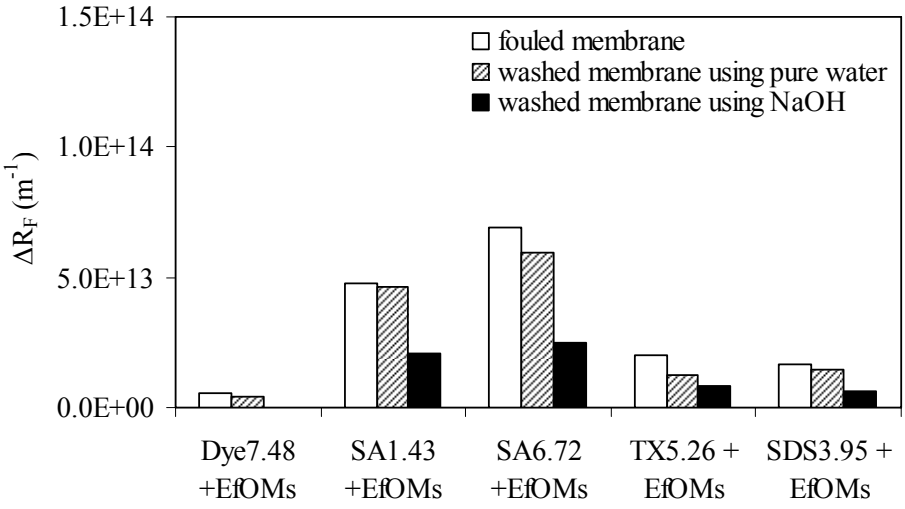

Figure 31 Foulant resistances of wastewater containing EfOMs-surfactants and EfOMs-dye mixture

In case of wastewater containing SA, and wastewater containing TX, the additional dye and the additional mixture between EfOMs and dye did not change the irreversible fouling judging from the uniform foulant resistance from **Figures 32 and 33**. The decreasing permeability of wastewater containing SA ranged between 29.22-31.33 %. In contrary, in case of SDS, the increasing irreversible fouling occurred when the high concentration of dye and EfOMs were added (**Figure 34**). The decreasing permeability of wastewater containing SDS slightly increased up to 8.73 %.

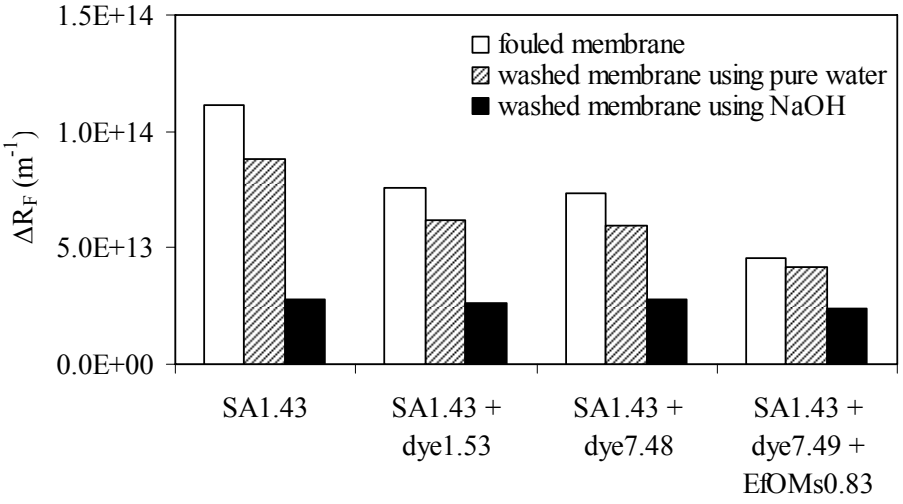

Figure 32 Effect of EfOMs and reactive dye on foulant resistance of surfactant concentration lower than CMC

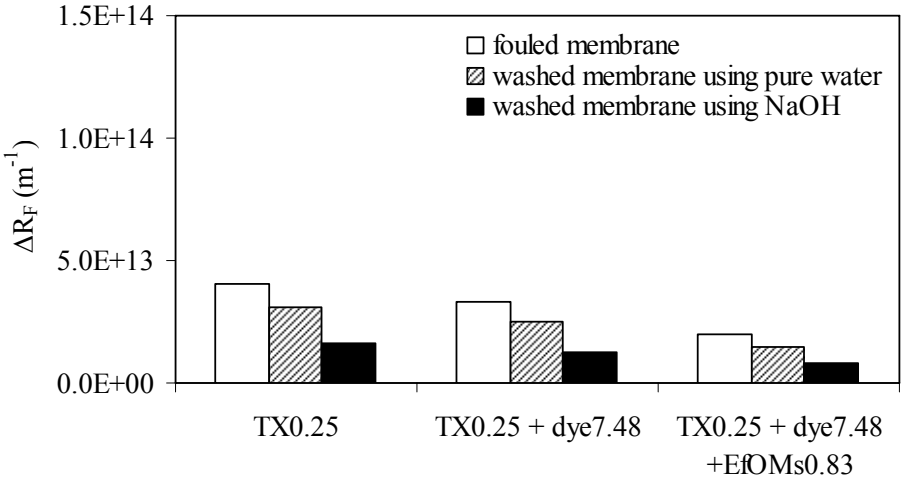

Figure 33 Effect of EfOMs and reactive dye on foulant resistance of non-ionic surfactant

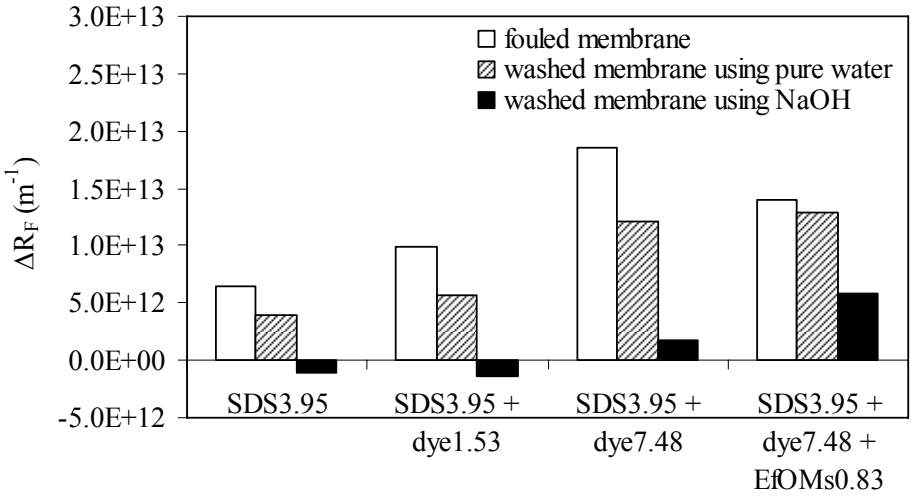

Figure 34 Effect of EfOMs and reactive dye on foulant resistance of anionic surfactant

2.3.5 Fouling of membrane applied to wastewater

The aggregate between reactive dye and SA is influenced by both of the hydrophobic adhesion and the ionic bond. In case of ionic dye and non-ionic surfactant, they aggregate themselves by the hydrophobic interaction between hydrophobic chains of surfactants within micelles with the hydrophobic part of dye (Nemoto and Funahashi, 1977; Wennerström and Lindman, 1979). Simončič and Kert (2008) reported that the stability of aggregation between dye and surfactant increases when their hydrophobic property increases. Cationic dye prefers to aggregate with anionic surfactant than non-ionic surfactant. In that case, the ionic bond plays an important role for their aggregate (Sarkar1 and Poddar, 2000). Moreover, the mixture containing anionic dye and non-ionic surfactant and anionic surfactant, non-ionic surfactant aggregate anionic dye with hydrophobic interaction better than anionic surfactant (Kartal and Akbaş, 2005). Afterward, within the aggregation between dye and mixed surfactant like SA, dye was retained in the core of aggregate. This interaction decreases the amount of monomer. Consequently, when high aggregation level became perceptibly active, the aggregates decreased the adsorption capacity of the monomers resulting in the increasing flux. In this study, the high aggregation level

occurred when the high concentration of dye was added and especially when the mixture between EfOMs and dye was added. In the case of wastewater containing anionic surfactant as SDS and anionic dye, little aggregation occurred imperceptible hence; the additional dye did not decrease fouling.

The additional dye at high concentration generated irreversible fouling of the wastewater containing anionic surfactant as SDS but did not affect the wastewater containing non-ionic surfactant as TX and mixed surfactant as SA. In addition, the additional EfOMs and the additional mixture between dye and EfOMs performed equivalent result as the additional dye.

3. Modeling of organic foulant interaction and RO fouling

Modeling investigation on foulant interaction and fouling of RO membrane was studied to explain the effect of the deposition of interacted foulant on flux decline of RO membrane. The aggregate equilibrium constant as shown in **Equation 42** ($K_{eq} = [A_{organic_1-organic_2}].[C_{organic_1}]^{-x}[C_{organic_2}]^{-y}$) was determined to quantify the concentration of monomer and aggregate forms contained in wastewater. In addition, modeling of flux decline with time dependency were proposed and model parameters were determined to investigate relationship between the deposition of interacted foulant and flux decline of RO membrane.

The mathematical modeling proposed by Braeken *et.al.* (2006) ($1-\frac{J}{J_o} = 1-\frac{J}{L_o x TMP} = b\ln(t)-b\ln(t_o)$) was modified to assess flux decline profile of wastewater containing multiple foulants. The reduction of available site (b) is proposed as a function of concentration (C_i) and fouling coefficient (β_i) as $b = C_i\beta_i$. Therefore, the relationship between occupied site by foulant (θ_i) and filtration time can be rewritten as $\theta_i = C_i\beta_i \ln(t+t_o) - C_i\beta_i \ln t_o$

3.1 Quantification of monomers and aggregates due to foulant interaction

Three types of foulant interaction, dye-EfOMs, dye-SA, EfOMs-SA, were examined by determining the aggregate equilibrium constant (K_{eq}) as following

3.1.1 Interaction between reactive dye and EfOMs

According to the chemical equilibrium, the amounts of reactive dye and EfOMs i.e., the total dye ($[C_{dye}]$), the total EfOMs ($[C_{EfOMs}]$), dye aggregate ($[A_{dye}]$), EfOMs aggregate ($[A_{EfOMs}]$), dye monomer ($[S_{dye}]$), EfOMs monomer (S_{EfOMs}), and the aggregate between EfOMs and dye ($[A_{dye\text{-}EfOMs}]$) were used to calculate the aggregated equilibrium constant (K_{eq}) between reactive dye and EfOMs. It was found that K_{eq} was 0.434 and $[A_{dye\text{-}EfOMs}]$ can be calculated from **Equation 50**. Prediction of the aggregated concentration due to the interaction between EfOMs and dye is shown in **Figure 35**. It can be suggested that the concentration of aggregation between dye and EfOMs (Adye-EfOMs) was effected by EfOMs more than dye.

$$[A_{dye-EfOMs}] = 0.434\,[C_{dye}]^{0.18}[C_{EfOMs}]^{0.82} \qquad 50)$$

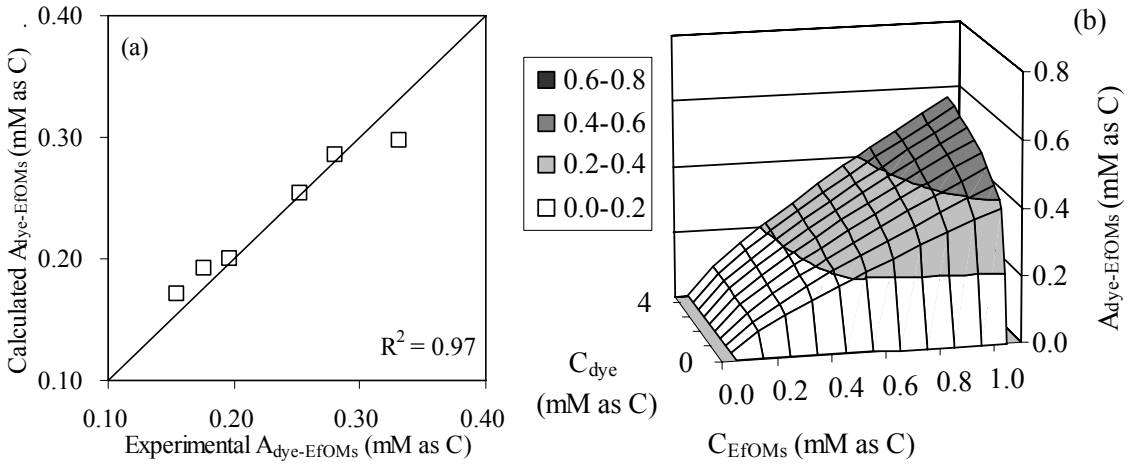

Figure 35 (a) Correlation between $A_{dye\text{-}EfOMs}$ from calculation and experiment, (b) Prediction of the $A_{dye\text{-}EfOMs}$ due to the interaction between EfOMs and dye

3.1.2 Interaction between EfOMs and surfactant

SA was selected in this study. According to the chemical equilibrium, the amounts of SA and EfOMs i.e., the total SA ($[C_{SA}]$), the total EfOMs ($[C_{EfOMs}]$), SA aggregate ($[A_{SA}]$), EfOMs aggregate ($[A_{EfOMs}]$), SA monomer ($[S_{SA}]$), EfOMs monomer (S_{EfOMs}), and the aggregate between EfOMs and SA ($[A_{EfOMs-SA}]$) were used to calculate the aggregated equilibrium constant (K_{eq}) between reactive SA and EfOMs. The value of K_{eq} at SA concentration lower than CMC was 0.672 and K_{eq} at SA concentration higher than CMC was 1.578 respectively. $[A_{EfOMs-SA}]$ can be determined from **Equations 51 and 52**. Prediction of the aggregated concentration due to the interaction between EfOMs and SA is shown in **Figure 36**. It can be suggested that a large aggregation was occurred when the mixture contained surfactant micelle and its occurrence was influenced by EfOMs more than SA.

In case of SA $\leq$ 1.62 mM as C

$$[A_{EfOMs-SA}] = 0.672\,[C_{EfOMs}]^{0.8}[C_{SA}]^{0.2} \quad 51)$$

In case of SA >1.62 mM as C

$$[A_{EfOMs-SA}] = 1.578\,[C_{EfOMs}]^{0.8}[C_{SA}]^{0.2} \quad 52)$$

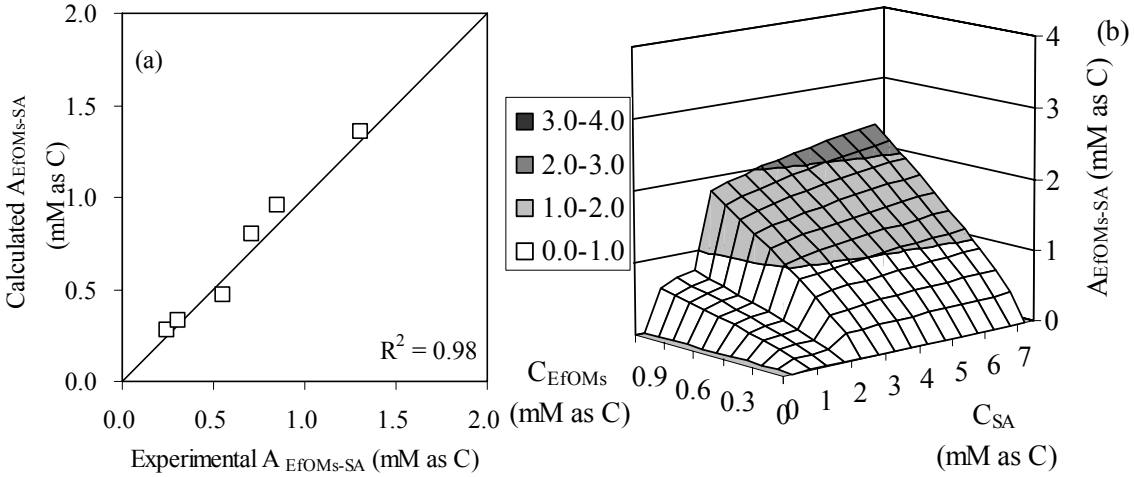

Figure 36 (a) Correlation between $A_{EfOMs-SA}$ from calculation and experiment, (b) Prediction of the $A_{EfOMs-SA}$ due to the interaction between EfOMs and SA

3.1.2 Interaction between dye and surfactant

Prediction of the aggregated concentration due to interaction between dye and SA is shown in **Figure 37**. In the case of SA lower than CMC (<1.62 mM as C), K_{eq} was 0.304 and $[A_{dye\text{-}SA}]$ can be calculated from **Equation 53**. In addition, when concentration higher than CMC (> 1.62 mM as C), K_{eq} was 0.500 and $[A_{SA\text{-}dye}]$ can be calculated from **Equation 54**. It can be suggested that when surfactant micelle appeared in the mixture, the aggregation between dye and SA ($A_{dye\text{-}SA}$) occurred more than the mixture without surfactant micelle. In addition, the aggregation was affected by SA more than dye.

In case of SA $\leq$ 1.62 mM as C

$$[A_{dye-SA}] = 0.304\,[C_{Dye}]^{0.33}[C_{SA}]^{0.67} \quad 53)$$

In case of SA >1.62 mM as C

$$[A_{dye-SA}] = 0.500\,[C_{Dye}]^{0.465}[C_{SA}]^{0.535} \quad 54)$$

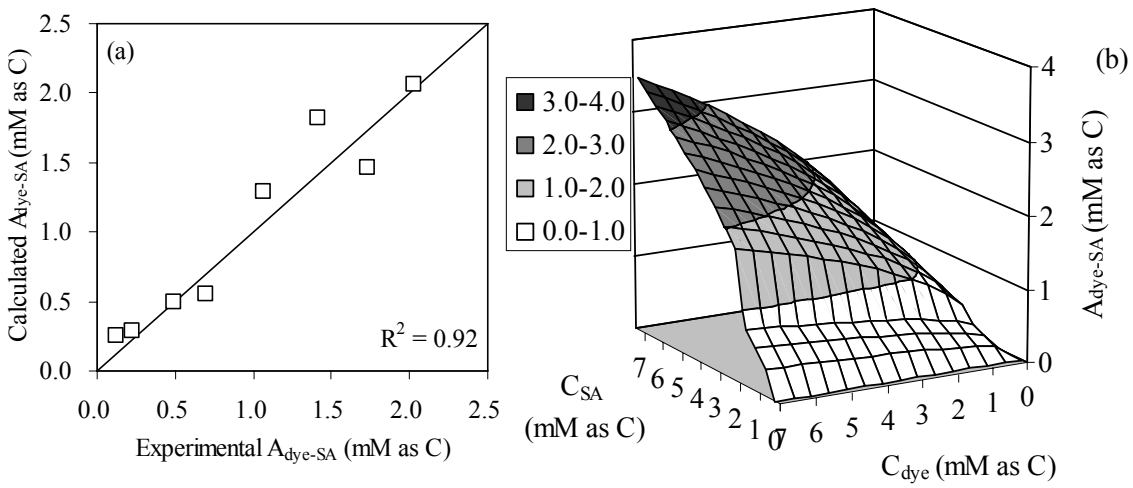

Figure 37 (a) Correlation between $A_{dye\text{-}SA}$ from calculation and experiment,
(b) Prediction of $A_{dye\text{-}SA}$ due to the interaction between SA and dye

3.2 Reduction of available site due to deposition of foulants

The normalized flux decline $(1-\frac{J}{L_o x TMP})$ data were plotted against $\ln(t+t_o)$ to determine the model parameters. The reduction of available site (b) and the initial fouling time (t_o) of synthetic wastewater (single foulant without aggregation, surfactant with and without micellisation, multiple foulant with EfOMs, and multiple foulant with dye) are shown in **Figure 38**.

It was found that, in case of single foulant without aggregation, ES-20 provided higher reduction of available site than LF-10 indicating a range from 0.029 to 0.095 and 0 to 0.083 min^{-1}, respectively. In contrary, the initial fouling time of ES-20 lower than LF-10 showing a range from 4.62 to 159.26 and 12.40 to 496.16 min. The slowest t_o was found in the membrane where SDS was applied. Nevertheless, the lowest fouling potential in term of b was found in the membrane where EfOMs were applied. In contrary, the most severe fouling potential judging from the highest b and fastest t_o was provided by SA. Higher b and lower t_o of ES-20 than LF-10 suggests that severe fouling occurs on the membrane with lower hydrophilic property.

In the case of surfactant without micellisation (SA < 1.62 mM as C), b slightly increased from 0.087 to 0.095 min^{-1} related to the increasing concentration. When the micellisation was apparent (SA > 1.62 mM as C), b slightly decreased from 0.088 to 0.084 min^{-1} conflicting with the increasing concentration. The initial fouling times of all cases were not different. Hence, the appearance of surfactant micelles tended to decrease fouling potential.

In cases of the multiple foulant with EfOMs, it was found that the additional EfOMs lowered b significantly to a range of 0.046 to 0.016 min^{-1} but it did not change t_o. The interaction between EfOMs & dye and the interaction between EfOMs & surfactants decreased b consistent with the study of $\Delta J/\Delta V$.

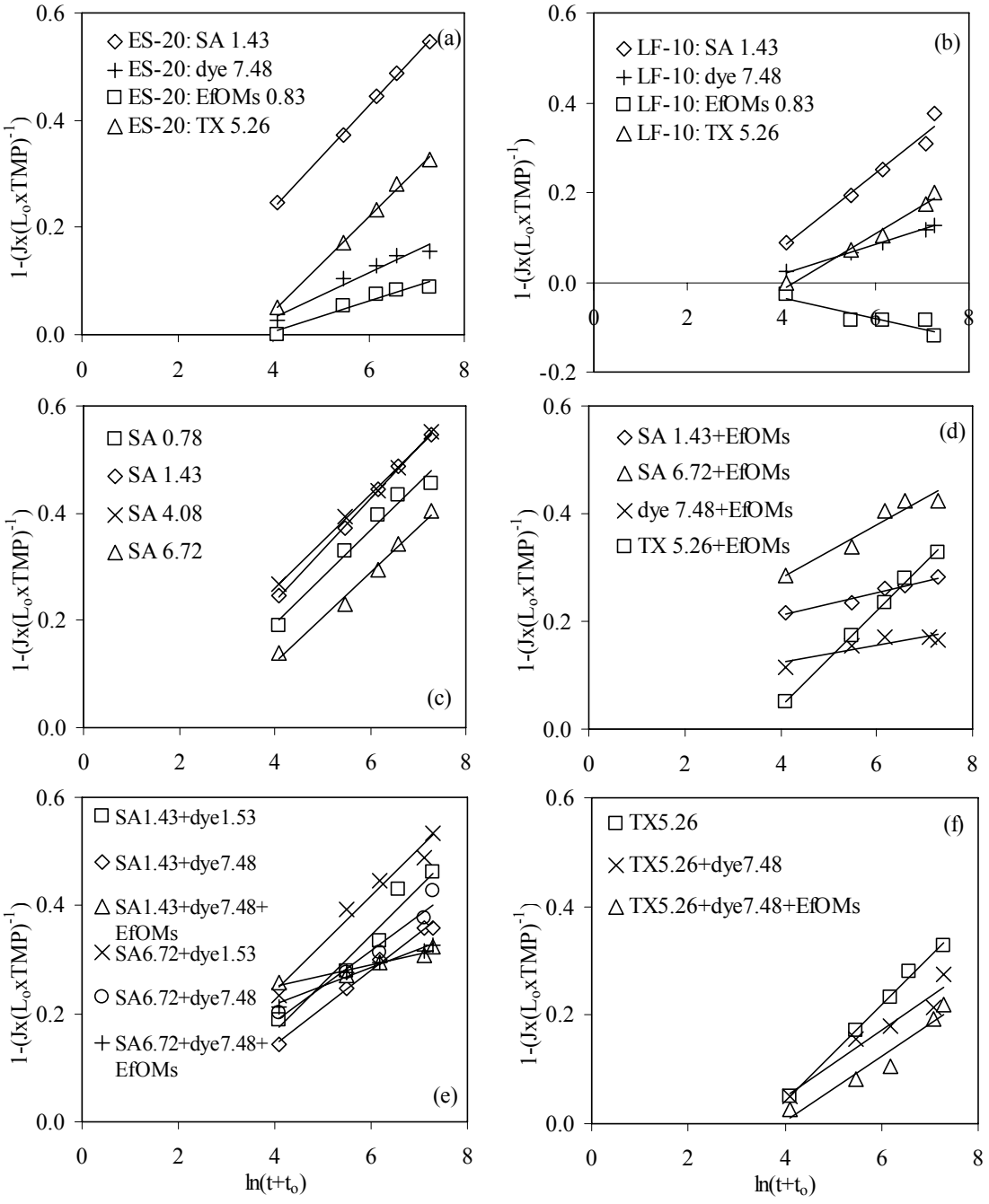

Figure 38 Normalized flux decline of (a) single organic foulant on ES-20, (b) single organic foulant on LF-10, (c) SA at different concentration on ES-20, (d) mixed wastewater between organic foulant and EfOMs on ES-20, (e) mixed wastewater between SA, dye, and EfOMs on ES-20, (f) mixed wastewater between TX, dye, and EfOMs on ES-20.

In cases of multiple foulant with dye, at SA lower than CMC, the additional dye and the additional mixture between dye and EfOMs decreased the reduction of available site significantly at a range from 0.095 to 0.020 min^{-1}. In cases where SA is higher than CMC (6.72 mM as C), the addition of dye at high concentration as 7.48 mM as C and the mixture between dye of 7.48 mM as C and EfOMs of 0.83 mM as C, b were decreased dramatically. The initial fouling times of all cases were not changed significantly. In the case of TX, the addition of dye, EfOMs, and the mixture between dye and EfOMs decreased the reduction of available site. In cases of SDS, the addition of dye increased the reduction of available site while the addition of EfOMs gave a conflicting effect. It can be concluded that the addition of dye decreased fouling potential of non-ionic surfactant, but increased the fouling potential of anionic surfactant. Fouling of the mixed surfactant as SA observed the same trend as TX mainly because composition of SA is non-ionic surfactant.

3.3 Prediction of RO flux from the deposition of monomers and aggregates

According to the experimental data of flux decline, the concentrations of aggregates, the concentration of monomers, the reduction of available site, and the initial time of fouling, it can be suggested that the monomers play an important role in the reducing flux. In contrary, the aggregates produced by foulants interaction increase flux even if they deposit on the membrane surface as well as the monomers because they increase the hydrophilic property of membrane. Moreover, the deposition of aggregates reduce the adsorption capacity of monomers from taking place on the membrane surface therefore, they decrease fouling potential of monomers.

The experimental data of the wastewater containing SA were studied in the modeling investigation on foulant interaction and RO fouling. In relation to the previous assumption, the total occupied site due to fouling (θ_T) can be equated according to the difference between the summation of occupied site due to fouling of

monomers ($\theta_{monomer,i}$) and the summation of occupied site due to aggregates ($\theta_{aggregate,i}$) as shown in **Equations 55-57**. The calculated concentrations of aggregates and monomers from **Equations 19-23** and the calculated parameters of b and t_o from **Table 17** were used in the modeling. The model parameters of fouling coefficient (β) and t_o are shown in **Table 18**.

$$\theta_T = \sum \theta_{monomer,i} - \sum \theta_{Aggregate,i} \quad 55)$$

$$\theta_{monomer,i} = \beta_i[S_i]\ln(t + t_{o,i}) - \beta_i[S_i]\ln(t_{o,i}) \quad 56)$$

$$\theta_{Agrregate,i} = \beta_i[A_i]\ln(t + t_{o,i}) - \beta_i[A_i]\ln(t_o) \quad 57)$$

where $[S_i]$ represents the concentration of monomers in unit of mM as C (S_{dye}, S_{EfOMs}, and S_{SA}) and $[A_i]$ represents the concentration of aggregates in unit of mM as C ($A_{dye\text{-}EfOMs}$, $A_{EfOMs\text{-}SA}$, $A_{dye\text{-}SA}$ and M_{SA}).

The flux profiles calculating from model were compared with the experimental data as shown in **Figures 39**. The R-square of the correlation between calculated flux profiles and experimental flux profiles ranged from 0.83 to 0.90. Hence, the model derived from the deposition of monomers and interacted foulants is successfully for prediction of flux during textile wastewater reclamation.

Table 17 Model parameters b and t_o from different wastewater

Wastewater (mM as C)	Membrane	Model parameters	
		b (min^{-1})	t_o (min)
single foulant without aggregation			
SA 1.43	ES-20	0.095	4.62
SA 1.43	LF-10	0.083	21.88
TX 5.26	ES-20	0.082	30.91
TX 5.26	LF-10	0.062	70.78
SDS 3.95	ES-20	0.048	159.26
SDS 3.95	LF-10	0.035	496.16
dye 7.48	ES-20	0.042	25.71
dye 7.48	LF-10	0.032	30.19
EfOMs 0.83	ES-20	0.029	45.49
EfOMs 0.83	LF-10	0.000[1]	12.40
surfactant with and without micellization			
SA 0.78	ES-20	0.087	6.07
SA 1.43	ES-20	0.095	4.62
SA 4.08	ES-20	0.088	2.89
SA 6.72	ES-20	0.084	13.15
multiple foulant with EfOMs			
SA 1.43 + EfOMs	ES-20	0.020	0.001
SA 6.72 + EfOMs	ES-20	0.046	0.12
TX 5.26 + EfOMs	ES-20	0.045	26.96
SDS 3.95 + EfOMs	ES-20	0.036	186.38
dye 7.23 + EfOMs	ES-20	0.016	0.03
multiple foulant with EfOMs and dye			
SA 1.43 + dye 1.53	ES-20	0.085	7.60
SA 1.43 + dye 7.48	ES-20	0.069	6.93
SA 1.43 + dye 7.48 + EfOMs	ES-20	0.020	3.38
SA 6.72 + dye 1.53	ES-20	0.089	3.63
SA 6.72 + dye 7.48	ES-20	0.066	3.37
SA 6.72 + dye 7.48 + EfOMs	ES-20	0.034	0.10
TX 5.26 + dye 7.48	ES-20	0.062	24.14
TX 5.26 + dye 7.48 + EfOMs	ES-20	0.059	49.94
SDS 3.95+ dye 1.53	ES-20	0.056	45.49
SDS 3.95+ dye 7.48	ES-20	0.072	51.50
SDS 3.95+ dye 7.48 + EfOMs	ES-20	0.035	32.79

Note: [1] The parameter b was adjusted to zero due to there was no flux decline during RO filtration.

Table 18 Model parameters β and t_o

Foulants	Fouling coefficient, β (mM as C- min)$^{-1}$	Initial fouling time, t_o (min)
S_{SA}	0.089	6.7
S_{dye}	0.002	25.7
S_{EfOMs}	0.0342	45.5
M_{SA}	0.01	6.7
$A_{dye\text{-}SA}$	0.01	6.7
$A_{dye\text{-}EfOMs}$	0.01	6.7
$A_{EfOMs\text{-}SA}$	0.01	6.7

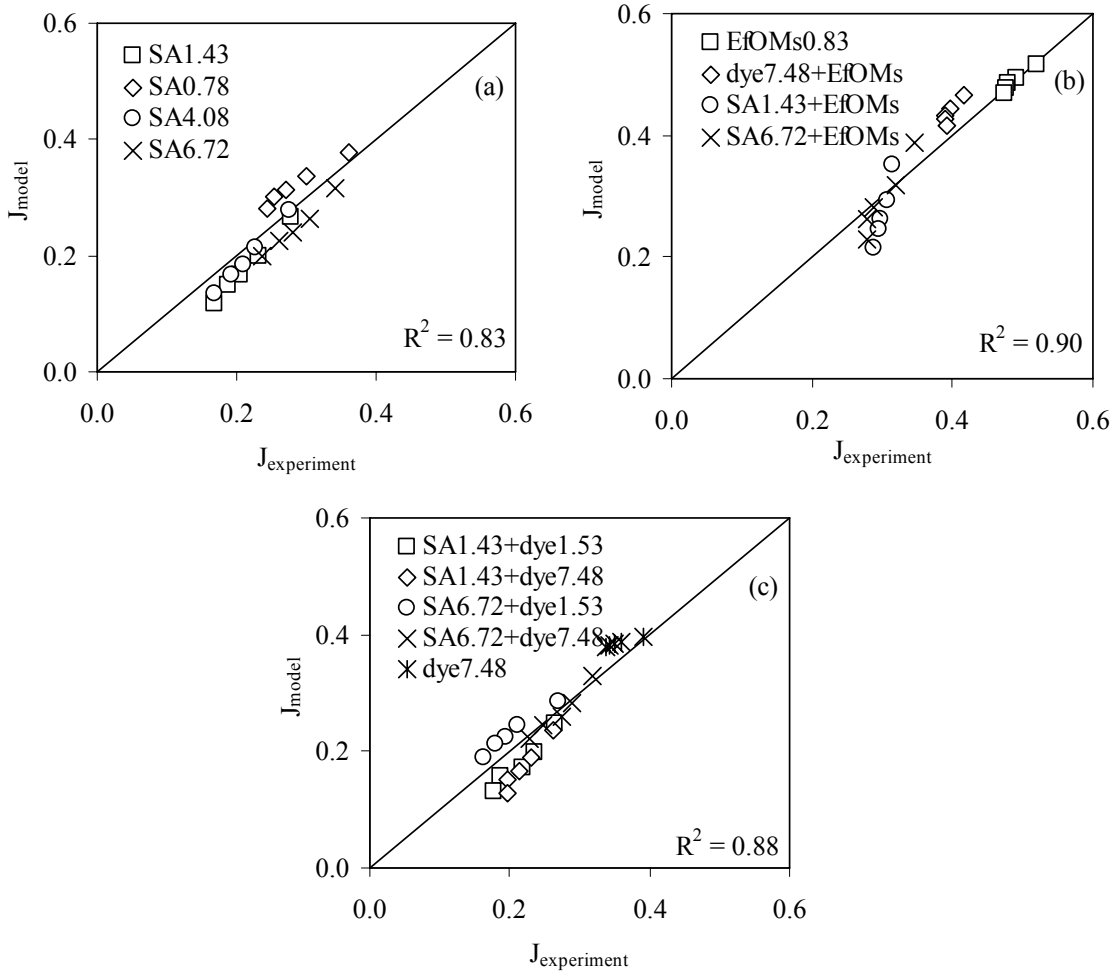

Figure 39 Correlation between permeate flux from experiment and predicted model

CONCLUSIONS AND RECOMMENDATION

Conclusions

The experimental and modeling investigation on the fouling of RO membrane treating textile wastewater lead to the conclusions:

1) Flux of RO membrane treating the secondary effluent rapidly declined at the beginning of operation (24 hours) and slightly decreased further in long-term of (~30 days). The addition of antiscalant and biocide slightly reduced the fouling and increased membrane rejection efficiency. The scaling and biofilm were observed by SEM micrographs suggesting that addition of antiscalant and biocide did not completely prevent the scaling and biofouling.

2) RO flux profile could be simulated by a mathematical expression derived from variable fouling index concept. The change in permeate flux was affected by the initial fouling index (I_o), fouling reduction rate (γ), and cumulative volume flux (V/A). The operation data of 7 days or more from bench-scale provided a promising result for estimation of flux decline in long-term operation of larger scale system using proposed model. Comparatively, it provided more accurate results than the constant fouling index model.

3) Sequential cleaning using alkaline solution (NaOH pH 12) followed by acid solution (HCl pH 2) was the most effective procedure for removing the foulant resistance caused by the secondary effluent (of MBR). The main cause of RO fouling was the organic foulants as determined by high hydraulic resistance recovery (RR) by alkaline solution.

4) An experimental investigation of RO membrane applied to synthetic wastewater showed that the non-ionic surfactant was the main cause of organic fouling. Increasing surfactant concentration above CMC did not yield further flux

decline due to the micellisation. When surfactant, EfOMs, and dye appeared in wastewater, these organic foulants aggregated with each other. Aggregation between EfOMs & dye, EfOMs & surfactants, and dye & non-ionic surfactant enhanced permeate flux of RO membrane. However, a small amount of dye could aggregate with anionic surfactant due to their repulsive force by anionic charge and they did not enhance permeate flux.

5) A mathematical model derived from the assumption that the deposited monomer was the main cause of flux decline, but the aggregates decreased the fouling potential of monomers, could successfully predict RO flux. The important model parameters were the initial fouling time (t_o) and the reduction of available site (b) which was proposed corresponding to the foulant concentration and fouling coefficient (β). According to the model, commercial soaping agent presented the highest fouling coefficient whereas the reactive dye yielded lowest fouling coefficient. The surfactant micelles and the aggregates between surfactant, dye, and EfOMs presented the same level of fouling coefficient.

Recommendation

1. Long-term operation of RO membrane applied to textile wastewater is needed to confirm the applicability of proposed model to seriously fouled membrane. Moreover, the other types of surfactant and dye should be investigated.

2. In order to reveal the change in hydrophobic/hydrophilic properties of membrane surface due to the deposition of aggregate and monomer form, other parameter such as interfacial free energy analysis should be conducted and incorporated into the model.

LITERATURE CITED

Adamson, A.W. 1990. **Physical chemistry of surfaces**. 5th ed. John Wiley & Sons, Inc., Singapore.

Al-Ahmad, M., F.A.A. Aleem, A. Mutiri and A. Ubaisy. 2000. Biofouling in RO membrane systems part1: Fundamentals and control. **Desalination** 132: 173-179.

Al-Amoudi A. and R.W. Lovitt. 2007. Fouling strategies and the cleaning system of NF membranes and factors affecting cleaning efficiency. **J. Membr. Sci.** 303: 4-28.

Amjad, Z. 1993. **Reverse osmosis: Membrane technology, water chemistry, and industrial applications**. Van Nostrand Reinhold, New York.

_____, J. Pugh and R.W. Zuhl. 1996. Membranes: Reverse osmosis element cleaning. **Ultrapure Water** 13(7): 27-28.

Ang, W.S., S. Lee and M. Elimelech. 2006. Chemical and physical aspects of cleaning of organic-fouled reverse osmosis membrane. **J. Membr. Sci.** 272: 198-210.

Baker, J.S. and L.Y. Dudley. 1998. Biofouling in membrane systems-A review. **Desalination** 118: 81-90.

Bakx, A., A.M.D.E. Timmerman and G. Frens. 2001. Shear stimulated adsorption of surfactants from micellar solutions. **Coll. Surf. A: Physicochemical Eng. Aspects** 183-185: 149-157.

Bian, R., K. Yamamoto and Y. Watanabe. 2000. The effect of shear rate on controlling the concentration polarization and membrane fouling, pp. 421-432. *In* **Proc. of the Conf. on Membranes in Drinking and Industrial Water Production**, Desalination Publications, L' Aquila, Italy.

Boerlage, S.F.E., M.D. Kennedy, M.P. Aniye, E.M. Abogrean, D.E.Y. El-Hodali, Z.S. Tarawneh and J.C. Schippers. 2000. Modified fouling index$_{ultrafiltration}$ to compare pretreatment process of reverse osmosis feed water. **Desalination** 131: 201-214.

Braeken, B. van der Bruggen and C. Vandecasteele. 2006. Flux decline in nanofiltration due to adsorption of dissolved organic compounds: Model prediction of time dependency. **J. Phys. Chem. B.** 110: 2957-2962.

Brauns, E., E. Van Hoof, B. Molenberghs, C. Dotremont, W. Doyen and R. Leysen. 2002. A new method of measureing and presenting the membrane fouling potential. **Desalination** 150: 31-162.

Buckley, C.A. 1992. Membrane technology for the treatment of dyehouse effluents. **Water Sci. Technol.** 25: 203-209.

Butt, F.H., F. Rahman and U. Baduruthamal. 1997. Characterization of foulants by autopsy of RO desalination membranes. **Desalination** 114: 51-64.

Carvalho, G., J.M. Novais, P.A. Vanrolleghem and H.M. Pinheiro. 2002. Optimal operation for timely adaptation of activated sludge plants to changes in the surfactant composition of wastewater, **Water Sci. Technol.**, 45 (4-5): 345-353.

Chakraborty, S., M.K. Purkait, S. Dasgupta, S. De and J.K. Basu. 2003. Nanofiltration of textile plant effluent for color removal and reduction in COD. **Sep. Purif. Technol.** 31: 141-151.

Chang, I.S, P.L. Clech, B. Jefferson and S. Judd. 2002. Membrane fouling in membrane bioreactors for wastewater treatment. **J. Env. Eng. *ASCE*.** 128: 1018-1029.

Chen, G., X. Chai, P. Yue and Y. Mi. 1997. Treatment of Textile Desizing wastewater by pilot scale nanofiltration membrane separation. **J. Membr. Sci.** 127: 93-99.

Chen, V., A.G. Fane and C.J.D. Fell. 1992. The use of anionic surfactants for reducing fouling of ultrafiltration membranes: their effects and optimization. **J. Membr. Sci.** 67: 249-261.

Chidambaram, N. and D.J. Burgess. 2000. Effect of non-ionic surfactant on transport of surfactant –active and non-surfactant-active model drugs and emulsion stability in triphasic systems. **AAPS Pharmsci.** 2(3).

Chiemchaisri, C. and K. Yamamoto. 1994. Performance of membrane separation bioreactor at various temperatures for domestic wastewater treatment. **J. Membr. Sci.** 87: 119-129.

Childress, A.E. and M. Elimelech. 2000. Relating Nanofiltration membrane performance to membrane charge (electrokinetic) characteristics, **Environ. Sci. Technol.** 34: 3710-3716.

Chilukuri, V.V.S., A.D. Marshall, P.A. Munro and H. Singh. 2001. Effect of sodium dodecyl sulphate and cross-flow velocity on membrane fouling during cross-flow microfiltration of lactoferrin solutions. **Chem. Eng. Processing** 40: 321-328.

Cornelis, G., K. Boussu, B. Van der Bruggen, I. Devreese and C. Vandecasteele. 2005. Nanofiltration of nonionic surfactants: Effect of the molecular weight cutoff and contact angle on flux behavior, **Ind. Eng. Res.** 44: 7652-7658.

Donlan, D.M. 2002. Biofilms: Microbial Life on Surface. **Emerging Infections Diseases.** 8 (9): 881-890.

Doulia, D., G. Trägårdh and V. Gekas. 1997. Interaction behavior in ultrafiltration of non-ionic surfactants Part II. Static adsorption below CMC. **J. Membr. Sci.** 123: 133-142.

Epolitoa, W.J., Y.H. Lee, L.A. Bottomleyb and S.G. Pavlostathis. 2005. Characterization of the textile anthraquinone dye Reactive Blue 4. **Dyes and pigments** 67: 35-46.

Gharibi, H., B. Sohrabi, S. Sohrabi, S. Javadian and M. Hashemianzadeh. 2004. Study of the electrostatic and steric contributions to the free energy of ionic/ non-ionic mixed micellization. **Colloids and Surfaces A: Physicochem. Eng. Aspects.** 244: 187-196.

Ghayeni, S.B.S., S.S. Madaeni, A.G. Fane and R.P. Schneider. 1996. Aspects of microfiltration and reverse osmosis in municipal wastewater reuse. **Desalination** 106: 25-29.

Griebe, T. and H.C. Flemming. 1998. Biocide-free antifouling strategy to protect RO membranes from biofouling. **Desalination** 118: 153-156.

Hamann, S.D. 1978. The dependence of the free energy of micelle formation on aggregation number and critical micelle concentration. **Aust. J. Chem.** 31: 919-921.

Hydranautics. 1998. **Technical Survice Bulletin TSB113.02.** Nitto Denko corp.

Jiraratananon, R., A. Sungpet and P. Luangsowan. 2000. Performance evaluation of membranes for treatment of effluents containing reactive dye and salt. **Desalination** 130: 177-183.

Jőnsson, A.S. and B. Jőnsson. 1991. The influence of non-ionic and ionic surfactants on hydrophobic and hydrophilic ultrafiltration membranes. **J. Membr. Sci.** 56: 49-76.

Judd, S. and B. Jefferson. 2003. **Membrane for Industrial Wastewater Recovery and Re-use**. Elsevier Science Ltd. UK.

Kartal, Ç. and H. Akbaş. 2005. Study on the interaction of anionic dye-nonionic surfactants in a mixture of anionic and nonionic surfactants by absorption spectroscopy. **Dyes and Pigments** 65: 191-195.

Kaya, Y., C. Aydiner, H. Barlas and B. Keskinler. 2006. Nanofiltration of single and mixture solutions containing anionic and non-ionic surfactants below their critical micelle concentration (CMC_s). **J. Membr. Sci.** 282: 401-412.

Khedr, M. G. 1998. A case study of RO plant failure due to membrane fouling, analysis and diagnosis. **Desalination** 120: 107-113.

Khirani, S. M.H. Manero and R. Ben Aim. 2006. Improving the measurement of the Modified Fouling Index by using nanofiltration membrane (NF-MFI). **Desalination** 191: 1-7.

Kim, C.K., S.S. Kim, D.W. Kim, J.C. Lim and J.J. Kim. 1998. Removal of aromatic compounds in the aqueous solution via micellar enhanced ultrafiltration part 1: Behaviors of nonionic surfactants. **J. Membr. Sci**. 147: 13-22.

Knoell, T., J. Safarik, T. Cormark, R. Riley, S.W. Lin and H. Ridgway. 1999. Biofouling potentials of microporus Polysulfone membrane containing a Sulfonated Polyether-Ethersulfone/ Polyethersulfone Block Copolymer: Correlation of membrane surface properties with bacterial attachment. **J. Membr. Sci.** 157: 117-138.

Koyuncu, I. 2002. Reactive dye removal in dye/ salt mixtures by nanofiltration membranes containing Vinylsulphon dyes: Effect of feed concentration and cross flow velocity. **Desalination** 143: 243-253.

Kreft, J.U. and J.W.T. Wimpenny. 2001. Effect of EPS on biofilm structure and function as revealed by an individual-based model of biofilm growth. **Water Sci. Technol**. 43(6): 135-141.

Leaist, D.G. 1991. A moving-boundary technique for the measurement of diffusion in liquids. Triton X-100 in water. **J. Solution Chem.** 20 (2): 187-197.

Li, H., A.G. Fane, H.G.L. Coster and S. Vigneswaran. 1998. Direct observation of particle deposition on the membrane surface during crossflow microfiltration. **J. Membr. sci.** 149: 83-97.

Madaeni, S.S., T. Mohamamdi and M.K. Moghadam. 2001. Chemical cleaning of reverse osmosis membranes. **Desalination** 134: 77-82.

Marcucci, M., G. Nosenzo, G. Capanelli, I. Ciabatti, D. Corrieri and G. Ciardelli. 2001. Treatment and reuse of textile effluents based on new ultrafiltration and other membrane technologies. **Desalination** 138: 75-82.

Metcalf & Eddy. 2003. **Wastewater Engineering Treatment and Reuse 4th ed**. Int. ed. McGraw-Hill, Inc., New York.

Mietton-Peuchot, M. and O. Ranisio. 1997. Study of Behaviour of Membranes in the Presence of Anionic or Nonionic Surfactants. **Filtration & Separation** October: 883-886.

Mulder, M. 2000. **Basic Principles of Membrane Technology**. Kluwer Academic publishers, Netherlands.

Muller, P. 1994. Glossary of terms used in physical organic chemistry. **Pure & Appl. Chem.** 66 (5): 1077-1184.

Møller, J.V. and M. le Mare. 1993. Detergent binding as a measure of hydrophobic surface area of integral membrane proteins. **J. Biol. Chem.** 265 (25): 18659-18672.

Nemoto, Y. and H. Funahashi. 1977. The interaction between acid dye and nonionic surfactant. **J. Coll. Interf. Sci.** 62 (1): 95-100.

Nilson, J.A. and F.A. DiGiano. 1996. Influence of NOM composition on nanofiltration. **J. Am. Water Works Assoc.** 88 (5): 53–66.

Nitto Denko Corp. 1998. **Low Fouling Spiral Wound Type Reverse Osmosis Element LF10 Technical Data**. Japan.

Osmonic, inc. 2003. **Automated Silt Density Index Tester Built to ASTM D4189-95, Operation and Maintenance Manual**. USA.

Pisárčik, M., F. Devinsky, and I. Lacko. 2003. Critical micelle concentration, ionization degree and micellisation energy of cationic dimeric (Gemini) surfactants in aqueous solution and mixed micelles with anionic surfactant. **Acta. Facult. Pharm. Univ. Comenianae.** 50: 119-131.

Purhait, M.K., S. DasGupta and S. De. 2004. Removal of dye from wastewater using micellar-enhanced ultrafiltration and recovery of surfactant. **Sep. Purif. Technol.** 37: 81-92.

Rabie, H.R., P. Côté and N. Adams. 2001. A method for assessing membrane fouling in pilot and full systems. **Desalination** 141: 247-243.

Saiviwat N. and T. Fujioka. 2004. Experiments of Wastewater Reuse in Textile and Finishing/ Dyeing Factories. pp. 7-10 – 7-19. *In* The Seminar on Wastewater Reuse Project in Thailand, Entitled **"The Development of Environmental Wastewater Reuse Technology"**. Department of Industrial Works, Century Park Hotel, Bangkok.

Sarkar1, M. and S. Poddar. 2000. Studies on the tnteraction of surfactants with cationic dye by absorption spectroscopy. **J. Coll. Interf. Sci.** 221: 81-85.

Schafer, A.L., A.G. Fane and T.D. Waite. 2005. **Nanofiltration – Principles and Applications**. Elesvier Advanced Technology, UK.

Schulz, R. 1999**. Titrimetric determination of surfactants and pharmaceuticals**, Motrohm Ltd., Switzerland.

Simončič, B. and M. Kert. 2008. Influence of the chemical structure of dyes and surfactants on their interactions in binary and ternary mixture. **Dyes and Pigments** 76: 104-112.

Sirisongthum, N., Y. Sikarinkul and T. Fujioka. 2004. Experiments of Wsatewater Reuse in Textile and Finishing/ Dyeing Factories. pp. 7-4 – 7-9. *In* The Seminar on Wastewater Reuse Project in Thailand, Entitled **"The Development of Environmental Wastewater Reuse Technology"**. Department of Industrial Works, Century Park Hotel, Bangkok.

Sójka-Ledakowicz, J., T. Koprowski, W. Machnowski and H.H. Knudsen. 1998. Membrane filtration of textile dyehouse wastewater for technological water reuse. **Desalination** 119: 1-10.

Sostar-Turk, S., M. Simonic and I. Petrinic. 2005. Wastewater treatment reactive printing. **Dyes and Pigments** 64: 147-152.

Subramani, A. and E.M.V. Hoek. 2008. Direct observation of initial microbial deposition onto reverse osmosis and nanofiltration membranes. **J. Membr. sci.** 319:111-125.

Suksaroj, C., M. Héran, C. Allègre and F. Persin. 2005. Treatment of textile plant effluent by nanofiltration and/or reverse osmosis for water reuse. **Desalination** 178: 333-341.

Sutzkover, I., D. Hasson and R. Semiat. 2000. Simple technique for measuring the concentration polarization level in a reverse osmosis system. **Desalination** 131: 117-127.

Tang, C. and V. Chen. 2002. Nanofiltration of textile wastewater for water reuse. **Desalination** 143: 11-20.

Tansel, B., J. Sager, J. Garland, S. Xu, L. Levine and P. Bisbee. 2006. Decomposition of extracellular polymeric substances (EPS) and microtopographical changes on membrane surfaces during intermittent filtration conditions. **J. Membr. Sci.** 285: 225-231.

Thanuttamavong, M. 2002. **Ultra Low Nanofiltration of River Water of Drinking Water Treatment**. Ph.D. Thesis, The University of Tokyo.

_____, K. Yamamoto, J.I. Oh, K.H. Choo and S.J. Choi. 2002. Rejection characteristics of organic and inorganic pollutants by ultra low-pressure nanofiltration of surface water for drinking water treatment. **Desalination** 145: 257-264.

Van der Bruggen B., G. Cornelis, C. Vandecasteele and I. Devreese. 2005. Fouling of nanofiltration and ultrafiltration membranes applied for wastewater regeneration in the textile industry. **Desalination** 175: 111-119.

_____, B. Daems and C. Vandecasteele. 2001. Mechanisms of retention and flux decline for the nanofiltration of dye baths from the textile industry. **Sep. Purif. Technol.** 22-23: 519-528.

Van Loosdercht, M.C.M., J.J. Heijnen, H. Eberl, J. Kreft and C. Picioreanu. 2002. Mathematical modeling of biofilm Structures. **Antonie van Leeuwenhoek** 81: 245-256.

Visvanathan, C., N. Boonthanon, A. Sathasivan and V. Jegatheesan. 2002. Pretreatment of seawater for biodegradable organic content removal using membrane bioreactor. **Desalination** 153: 133-140.

Vrouwenvelder, J.S. and D. van der Kooij, 2001. Diagnosis, Prediction and Prevention of Biofouling of NF and RO Membranes, pp. 1-7. *In* **Proc. AWWA Membr. Technol. Conf.**, San Antonio.

_____, J.W.N.M. Kappelhof, S.G.J. Heijman, J.C. Schippers and D. Van der Kooij. 2003. Tools for fouling diagnosis of NF and RO membranes and assessment of the fouling potential of feed water. **Desalination** 157: 361-365.

Wennerström, H. and B. Lindman. 1979. Micelles. **Phys. chem. surfactant assoc.** 52 (1): 1-86.

Wijmans, J.G., S. Nakao, F.R. van der Berg, F. R. Trelstra and C.A. Smolders. 1985. Hydrodynamic resistance of concentration polarization boundary layers in ultrafiltration, **J. Membr. Sci.** 22: 117-135.

Wilbert, M.C., J. Pellegrino and A. Zydney. 1998. Bench-scale testing of surfactant-modified reverse osmosis/nanofiltration membranes. **Desalination** 115: 15-32.

APPENDICES

Appendix A

Characteristic of raw wastewater and MBR effluent

Appendix Table A1 The characteristic of raw and treated wastewater

Date	Raw wastewater						Membrane tank	MBR effluent							
	COD (mg/L)	BOD (mg/L)	SS (mg/L)	TKN (mg/L)	TP (mg/L)	Color (Pt-Co unit)	MLSS (mg/L)	COD (mg/L)	BOD (mg/L)	SS (mg/L)	TKN (mg/L)	TP (mg/L)	Color (Pt-Co unit)	EC (µS/cm)	SDI (%/min)
4-Aug-05	315	89	36	9.6	5.8	379	20,300	34.9	ND	ND	12.5	6.4	125	4,030	4.7
15-Aug-05	345	149	32	9.6	10.9	345	21,700	42.3	1.3	ND	6.6	8.2	133	4,895	3.6
31-Aug-05	372	142	55	10.7	5.2	305	25,100	35.8	ND	ND	3	5.9	90	4,080	3.9
13-Sep-05	353	132	32	10.7	9.2	33	28,000	45	ND	ND	4.8	7.2	169	4,360	1.9
30-Sep-05	476	202	36	12.5	5.9	45	25,600	46.7	ND	ND	2.4	7.4	154	3,580	1.9
13-Oct-05	385	150	24	20.8	6.1	32	26,100	48.6	1.6	ND	2.7	6.6	143	4,430	4.5
8-Nov-05	406	174	26	13.4	6	36	23,500	44.8	ND	ND	2.7	6.5	143	3,960	3.7
23-Nov-05	436	160	32	14.9	7.7	36	30,000	64.8	2.5	ND	3.6	6.1	273	4,630	3.7
30-Nov-05	368	167	27	8.9	6.3	35	32,600	52.2	2.1	ND	3.6	5.8	111	4,400	3.7
3-Dec-05	229	90	24	8.9	1.8	18	24,900	27.6	ND	ND	2.1	1.5	43	5,150	4.1
10-Dec-05	350	146	27	12.7	6	26	24,600	45.8	ND	ND	5.1	5.8	138	4,260	3.4
Average	367	146	32	12.1	6.5	117	25673	44.4	ND	ND	4.5	6.1	138	4,343	3.6
SD	64.2	33.4	8.8	3.5	2.3	146	3518	9.8	0.5	#DIV/0!	3.0	1.7	56.3	441.8	0.9

Appendix B

Operating data of spiral wound membrane filtration unit

Appendix Table B1 The operating data of the spiral wound membrane filtration unit from the case where without chemical addition

Operating Time (d)	Sample point	pH	EC (µs/cm)	Rejection (%)	Temp. (°C)	Flow (L/min)	Flux 25 °C (m/d)	Flow 25 °C (L/min)	Recovery (%)	Flux/P (m/d.MPa)
4 Aug 05	Feed	7.00	4770		38.5	1.687		1.132		
1 h	Permeate	6.60	237	72.6	36.2	0.087	0.22	0.062	5.52	0.64
	Concentrate	7.36	4890		38.3	1.600		1.080		
4 Aug 05	Feed	6.70	4250		38.3	1.688		1.139		
12 h	Permeate	6.52	140	93.7	36.0	0.030	0.08	0.022	1.90	2138
	Concentrate	6.67	4300		38.2	1.658		1.122		
5 Aug 05	Feed	6.68	4000		39.0	1.683		1.113		
1 d	Permeate	6.68	136	93.3	38.9	0.033	0.08	0.022	1.97	0.23
	Concentrate	6.33	4060		36.0	1.650		1.192		
8Aug 05	Feed	6.58	2600		35.9	1.773		1.285		
4 d	Permeate	7.10	76.9	94.4	35.6	0.033	0.09	0.024	1.88	0.25
	Concentrate	6.30	2680		32.3	1.740		1.402		
9 Aug 05	Feed	6.95	4778		40.7	1.706		1.073		
5 d	Permeate	6.23	343	92.5	34.6	0.015	0.04	0.011	1.04	0.12
	Concentrate	6.96	4950		46.5	1.691		0.896		
11 Aug 05	Feed	7.26	4310		38.3	1.689		1.140		
7 d	Permeate	7.00	266	88.2	34.7	0.029	0.08	0.022	1.91	0.22
	Concentrate	7.08	4410		39.7	1.660		1.075		
15 Aug 05	Feed	6.85	3520		32.7	1.620		1.290		
11 d	Permeate	6.20	184.4	90.0	31.2	0.030	0.09	0.025	1.90	0.25
	Concentrate	6.87	3580		32.5	1.590		1.274		
19 Aug 05	Feed	6.81	4160		39.2	1.592		1.046		
15 d	Permeate	6.23	120.1	93.7	36.4	0.032	0.08	0.023	2.18	0.23
	Concentrate	7.11	4200		38.5	1.560		1.047		
24 Aug 05	Feed	6.51	2900		34.1	1.599		1.222		
20 d	Permeate	5.60	97.1	91.6	32.9	0.039	0.11	0.030	2.50	0.31
	Concentrate	6.82	2930		33.9	1.560		1.199		
25 Aug 05	Feed	7.27	4030		39.1	1.599		1.054		
21 d	Permeate	6.48	85	94.7	37.7	0.039	0.10	0.026	2.51	0.27
	Concentrate	7.03	4120		39.3	1.560		1.022		
26 Aug 05	Feed	7.23	4190		40.0	1.623		1.041		
22 d	Permeate	6.54	105.1	94.7	38.1	0.033	0.08	0.022	2.12	0.23
	Concentrate	7.18	4280		39.8	1.590		1.027		
31 Aug 05	Feed	7.13	4390		38.0	1.528		1.040		
27 d	Permeate	6.55	86.4	96.1	35.2	0.028	0.07	0.021	1.99	0.21
	Concentrate	7.08	4440		38.1	1.500		1.018		

Note : 1. Membrane area of BW-PA-2012-60 GPD is 0.4 m^2.

2. Feed flow rate was 1.6 L/min.

3. Applied pressure was 0.35 MPa

Appendix Table B2 The operating data of the spiral wound membrane filtration unit from the case where antiscalant was added

Operating Time (d)	Sample point	pH	EC (µs/cm)	Rejection (%)	Temp. (^{o}C)	Flow (L/min)	Flux 25 ^{O}C (m/d)	Flow 25 ^{O}C (L/min)	Recovery (%)	Flux/P (m/d.MPa)
8 Nov 05	Feed	6.28	3680		37.2	1.623		1.132		
1 h	Permeate	5.83	196.8	89.1	33.5	0.033	0.08	0.023	2.03	0.24
	Concentrate	6.36	3800		36.1	1.590		1.109		
9 Nov 05	Feed	6.57	4180		37.9	1.631		1.114		
1 d	Permeate	6.04	126.5	92.5	35.1	0.041	0.10	0.028	2.48	0.28
	Concentrate	6.53	4250		38.5	1.590		1.086		
12 Nov 05	Feed	6.65	4150		39.4	1.630		1.065		
4 d	Permeate	6.06	123.7	92.8	37.2	0.040	0.09	0.026	2.42	0.27
	Concentrate	6.65	4260		40.3	1.590		1.039		
21 Nov 05	Feed	6.07	3570		34.2	1.690		1.288		
7 d	Permeate	6.00	135.3	91.0	32.4	0.040	0.11	0.030	2.37	0.31
	Concentrate	6.12	3600		34.5	1.650		1.257		
23 Nov 05	Feed	6.31	4100		35.9	1.674		1.213		
9 d	Permeate	5.97	134	92.7	32.8	0.038	0.10	0.027	2.24	0.28
	Concentrate	6.30	4170		37.0	1.636		1.186		
25 Nov 05	Feed	6.21	4170		35.2	1.686		1.247		
11 d	Permeate	5.96	152	92.3	33.7	0.036	0.09	0.026	2.11	0.27
	Concentrate	6.31	4200		37.1	1.650		1.221		
28 Nov 05	Feed	6.10	4200		35.0	1.654		1.231		
14 d	Permeate	5.85	156.1	92.4	33.0	0.034	0.09	0.025	2.06	0.26
	Concentrate	6.19	4280		36.0	1.620		1.205		
30 Nov 05	Feed	6.30	4300		38.5	1.629		1.093		
16 d	Permeate	5.97	166	90.9	36.0	0.039	0.09	0.026	2.36	0.27
	Concentrate	6.28	4460		40.4	1.590		1.067		
3 Dec 05	Feed	6.16	4320		39.2	1.566		1.029		
19 d	Permeate	5.58	132.1	93.0	36.0	0.036	0.09	0.024	2.30	0.24
	Concentrate	6.20	4350		39.9	1.530		1.006		
06 Dec 05	Feed	6.50	2140		31.9	1.602		1.306		
23 d	Permeate	5.55	60.2	92.7	30.0	0.042	0.12	0.034	2.61	0.35
	Concentrate	6.66	2200		31.6	1.560		1.272		
08 Dec 05	Feed	6.64	4070		38.0	1.598		1.088		
25 d	Permeate	6.12	95.7	94.4	34.3	0.038	0.09	0.026	2.38	0.27
	Concentrate	6.64	4180		38.3	1.560		1.062		
10 Dec 05	Feed	6.58	4440		38.3	1.595		1.077		
27 d	Permeate	6.15	146.2	92.8	36.3	0.035	0.09	0.024	2.19	0.24
	Concentrate	6.62	4560		39.2	1.560		1.053		
13 Dec 05	Feed	6.60	3990		37.9	1.628		1.112		
30 d	Permeate	6.08	115	93.4	36.0	0.038	0.09	0.026	2.30	0.26
	Concentrate	6.71	4120		38.0	1.590		1.086		

Note : 1. Membrane area of BW-PA-2012-60 GPD is 0.4 m^2.

2. Feed flow rate was 1.6 L/min.

3. Applied pressure was 0.35 MPa

Appendix Table B3 The operating data of the spiral wound membrane filtration unit from the case where antiscalant and biocide were added

Operating Time (d)	Sample point	pH	EC (µs/cm)	Rejection (%)	Temp. (^{o}C)	Flow (L/min)	Flux 25 ^{O}C (m/d)	Flow 25 ^{O}C (L/min)	Recovery (%)	Flux/P (m/d.MPa)
13 Sep 05	Feed	6.45	2660		34.1	1.608		1.229		
1 h	Permeate	5.72	85.1	84.5	33.3	0.078	0.21	0.060	4.85	0.61
	Concentrate	6.63	2740		34.3	1.530		1.169		
14 Sep 05	Feed	6.85	3960		35.8	1.727		1.255		
1 d	Permeate	5.75	94.3	93.6	31.0	0.047	0.12	0.034	2.70	0.35
	Concentrate	6.89	4060		36.5	1.680		1.221		
16 Sep 05	Feed	7.06	4110		39.3	1.603		1.050		
3 d	Permeate	6.68	119.3	92.2	37.1	0.043	0.10	0.028	2.68	0.29
	Concentrate	7.22	4190		38.5	1.560		1.022		
17 Sep 05	Feed	6.36	4210		39.0	1.543		1.020		
4 d	Permeate	5.90	124.6	91.8	37.0	0.043	0.10	0.028	2.76	0.29
	Concentrate	6.90	4260		38.9	1.500		0.992		
20 Sep 05	Feed	6.96	3780		34.1	1.569		1.199		
7 d	Permeate	6.37	78.7	94.9	32.2	0.039	0.11	0.029	2.45	0.30
	Concentrate	6.92	3860		34.3	1.530		1.169		
22 Sep 05	Feed	6.84	3710		37.4	1.572		1.089		
9 d	Permeate	6.35	83.5	94.1	34.1	0.042	0.10	0.029	2.64	0.30
	Concentrate	6.87	3800		38.7	1.530		1.060		
24 Sep 05	Feed	6.75	4070		40.2	1.661		1.060		
11 d	Permeate	6.17	128.1	92.2	37.0	0.041	0.09	0.026	2.48	0.27
	Concentrate	6.70	4150		38.8	1.620		1.034		
27 Sep 05	Feed	6.54	4210		39.9	1.535		0.988		
14 d	Permeate	5.83	166.6	88.9	36.9	0.043	0.10	0.028	2.80	0.28
	Concentrate	6.35	4340		39.9	1.492		0.960		
30 Sep 05	Feed	6.51	4270		39.5	1.598		1.041		
17 d	Permeate	6.48	222	87.8	34.6	0.038	0.09	0.024	2.35	0.25
	Concentrate	6.56	4370		39.4	1.560		1.016		
03 Oct 05	Feed	6.45	3170		33.2	1.629		1.278		
20 d	Permeate	5.93	86.8	93.4	31.5	0.039	0.11	0.031	2.39	0.31
	Concentrate	6.48	3260		33.2	1.590		1.248		
07 Oct 05	Feed	6.62	4090		39.5	1.601		1.043		
24 d	Permeate	6.19	118.4	92.7	36.0	0.041	0.09	0.026	2.53	0.27
	Concentrate	6.80	4220		39.5	1.560		1.016		
11 Oct 05	Feed	6.66	3900		38.6	1.660		1.111		
27 d	Permeate	6.07	113	93.0	36.0	0.040	0.10	0.027	2.41	0.28
	Concentrate	6.68	3990		38.8	1.620		1.084		
13 Oct 05	Feed	6.52	4190		39.1	1.659		1.093		
29 d	Permeate	6.15	130.6	92.8	37.5	0.039	0.09	0.025	2.32	0.26
	Concentrate	6.57	4280		40.7	1.620		1.068		

Note : 1. Membrane area of BW-PA-2012-60 GPD is 0.4 m^2.

2. Feed flow rate was 1.6 L/min.

3. Applied pressure was 0.35 MPa

Appendix C

Cleaning results

Appendix Table C1 Effect of CFV on cleaning

CFV (cm/s)	Flow (mL/min)	Temp (^{O}C)	Flow 25 ^{O}C (mL/min)	J_W (m/d)	R_F (m^{-1})	RR (%)
Case 1: without addition						
Fouled mambrane				0.49	1.712E+14	
5	0.310	28.3	0.281	0.504	1.610E+14	5.98
15	0.335	30.3	0.286	0.513	1.556E+14	9.12
25	0.315	28.3	0.286	0.512	1.563E+14	8.71
35	0.325	29.2	0.287	0.514	1.549E+14	9.49
45	0.320	28.8	0.286	0.512	1.560E+14	8.87
55	0.330	29.8	0.286	0.513	1.557E+14	9.08
Case 2: addition with antiscalant						
Fouled mambrane				0.536	1.433E+14	
5	0.320	24.9	0.321	0.575	1.245E+14	13.16
15	0.330	25.5	0.325	0.582	1.211E+14	15.50
25	0.350	27.1	0.329	0.589	1.182E+14	17.54
35	0.355	27.6	0.329	0.589	1.184E+14	17.43
45	0.355	27.6	0.329	0.589	1.184E+14	17.43
55	0.355	27.6	0.329	0.589	1.184E+14	17.43
Case 3: addition with antiscalant and biocide						
Fouled mambrane				0.504	1.608E+14	
5	0.329	26.2	0.318	0.570	1.269E+14	23.65
15	0.345	27.0	0.325	0.582	1.211E+14	27.66
25	0.348	27.2	0.327	0.585	1.200E+14	28.41
35	0.360	28.4	0.326	0.583	1.208E+14	27.87
45	0.350	27.4	0.326	0.584	1.204E+14	28.12
55	0.355	27.9	0.326	0.584	1.206E+14	28.01

Note : 1. pure water was fed with flow rate of 1 mL/min.
2. Washing time of all cases were 1 hour

Appendix Table C2 Resistance removal efficiency of chemical solutions for the case where without chemical was added

Cleaning solution	R_{Fw} (m^{-1})			*RR* (%)		
	Feed side	Permeate side	Average	Feed side	Permeate side	Average
pure water	1.639E+14	1.575E+14	1.639E+14	4.25	8.03	4.25
NaOH pH 12	1.208E+14	1.016E+14	1.112E+14	29.42	40.64	35.03
HCl pH 2	1.304E+14	1.309E+14	1.306E+14	23.83	23.55	23.69
Citric 2%	1.423E+14	1.326E+14	1.374E+14	16.89	22.55	19.72
Oxalic 0.2%	1.358E+14	1.350E+14	1.354E+14	20.70	21.16	20.93
EDTA 2%	1.636E+14	1.560E+14	1.598E+14	4.44	8.87	6.66
SBS 0.2%	1.597E+14	1.549E+14	1.573E+14	6.69	9.50	8.10
NaOH+HCl	7.885E+13	6.846E+13	7.844E+13	53.94	60.01	54.18
HCl+NaOH	8.444E+13	8.025E+13	8.234E+13	50.68	53.13	51.90
Citric2%+NaOH	1.303E+14	8.075E+13	1.055E+14	23.88	52.84	38.36

Appendix Table C3 Resistance removal efficiency of chemical solutions for the case where without chemical was added

Case	Cleaning solution	R_{Fw} (m^{-1})			*RR* (%)		
		Feed side	Permeate side	Average	Feed side	Permeate side	Average
1	pure water	1.639E+14	1.575E+14	1.607E+14	4.25	8.03	6.14
	NaOH pH 12	1.208E+14	1.016E+14	1.112E+14	29.42	40.64	35.03
	HCl pH 2	1.304E+14	1.309E+14	1.306E+14	23.83	23.55	23.69
	NaOH pH12+HCl pH2	7.746E+13	7.942E+13	7.844E+13	54.76	53.61	54.18
	HCl pH2+NaOH pH12	8.444E+13	8.025E+13	8.234E+13	50.68	53.13	51.90
2	pure water	1.426E+14	1.351E+14	1.388E+14	0.49	5.78	3.14
	NaOH pH 12	8.141E+13	6.059E+13	7.100E+13	43.21	57.73	50.47
	HCl pH 2	9.266E+13	9.443E+13	9.354E+13	35.36	34.12	34.74
	NaOH pH12+HCl pH2	5.775E+13	5.392E+13	5.584E+13	59.71	62.38	61.04
	HCl pH2+NaOH pH12	7.601E+13	6.784E+13	7.192E+13	46.97	52.67	49.82
3	pure water	1.293E+14	1.252E+14	1.273E+14	19.54	22.09	20.82
	NaOH pH 12	7.749E+13	8.837E+13	8.293E+13	51.80	45.03	48.41
	HCl pH 2	8.910E+13	8.573E+13	8.742E+13	44.57	46.67	45.62
	NaOH pH12+HCl pH2	4.459E+13	4.489E+13	4.474E+13	72.26	72.08	72.17
	HCl pH2+NaOH pH12	5.543E+13	6.797E+13	6.170E+13	65.52	57.72	61.62

Note: case 1: without chemical addition, R_{Ff} = 1.712E+14 m^{-1}

case 2: addition with antiscalant, R_{Ff} = 1.433E+14 m^{-1}

case 3: addition with antiscalant and biocide, R_{Ff} = 1.6E+14 m^{-1}

Appendix D

Operating data of cross-flow membrane filtration unit

Appendix Table D1 Fouling potential of wastewater containing single fouling

Run no	Feed water	Membrane	Time (h)	Flux 30^{O}C (m/d)	R_M	R_T	R_F
1	dye 500 mg/L	ES-20	0	0.79	6.85E+13	6.85E+13	0.00E+00
			1	0.39	6.85E+13	1.39E+14	7.01E+13
			4	0.36	6.85E+13	1.50E+14	8.20E+13
			8	0.35	6.85E+13	1.55E+14	8.64E+13
			12	0.34	6.85E+13	1.58E+14	8.94E+13
			24	0.34	6.85E+13	1.60E+14	9.14E+13
2	soaping agent 50 mg/L	ES-20	0	0.95	5.68E+13	5.68E+13	0.00E+00
			1	0.36	5.68E+13	1.50E+14	9.29E+13
			4	0.30	5.68E+13	1.81E+14	1.24E+14
			8	0.27	5.68E+13	2.01E+14	1.44E+14
			12	0.25	5.68E+13	2.14E+14	1.57E+14
			24	0.24	5.68E+13	2.23E+14	1.66E+14
3	soaping agent 100 mg/L	ES-20	0	0.85	6.39E+13	6.39E+13	0.00E+00
			1	0.28	6.39E+13	1.95E+14	1.31E+14
			4	0.23	6.39E+13	2.34E+14	1.71E+14
			8	0.20	6.39E+13	2.65E+14	2.01E+14
			12	0.19	6.39E+13	2.88E+14	2.24E+14
			24	0.17	6.39E+13	3.24E+14	2.60E+14
4	soaping agent 300 mg/L	ES-20	0	0.84	6.46E+13	6.46E+13	0.00E+00
			1	0.27	6.46E+13	1.97E+14	1.33E+14
			4	0.23	6.46E+13	2.38E+14	1.73E+14
			8	0.21	6.46E+13	2.58E+14	1.93E+14
			12	0.19	6.46E+13	2.81E+14	2.16E+14
			24	0.17	6.46E+13	3.22E+14	2.58E+14
5	soaping agent 500 mg/L	ES-20	0	0.81	6.68E+13	6.68E+13	0.00E+00
			1	0.34	6.68E+13	1.58E+14	9.15E+13
			4	0.31	6.68E+13	1.77E+14	1.10E+14
			8	0.28	6.68E+13	1.93E+14	1.26E+14
			12	0.26	6.68E+13	2.08E+14	1.41E+14
			24	0.24	6.68E+13	2.29E+14	1.62E+14
6	TX 100 mg/L	ES-20	0	0.76	7.15E+13	7.15E+13	0.00E+00
			1	0.29	7.15E+13	1.90E+14	1.19E+14
			4	0.25	7.15E+13	2.18E+14	1.47E+14
			8	0.23	7.15E+13	2.36E+14	1.64E+14
			12	0.22	7.15E+13	2.51E+14	1.79E+14
			24	0.20	7.15E+13	2.68E+14	1.97E+14
7	SDS 100 mg/L	ES-20	0	0.86	6.27E+13	6.27E+13	0.00E+00
			1	0.49	6.27E+13	1.10E+14	4.74E+13
			4	0.47	6.27E+13	1.16E+14	5.33E+13
			8	0.45	6.27E+13	1.19E+14	5.66E+13
			12	0.43	6.27E+13	1.25E+14	6.27E+13
			24	0.41	6.27E+13	1.31E+14	6.82E+13
8	EfOMs	ES-20	0	0.95	5.67E+13	5.67E+13	0.00E+00
			1	0.52	5.67E+13	1.04E+14	4.76E+13
			4	0.49	5.67E+13	1.10E+14	5.34E+13
			8	0.48	5.67E+13	1.13E+14	5.61E+13
			12	0.48	5.67E+13	1.14E+14	5.69E+13
			24	0.47	5.67E+13	1.14E+14	5.76E+13

Appendix Table D2 Effect of reactive dye on fouling potential of surfactant

Run no	Feed water	Membrane	Time (h)	Flux 30^{O}C (m/d)	R_M	R_T	R_F
9	dye 100 mg/L + soaping agent 100 mg/L	ES-20	0	0.86	6.28E+13	6.28E+13	0.00E+00
			1	0.27	6.28E+13	2.04E+14	1.41E+14
			4	0.24	6.28E+13	2.29E+14	1.66E+14
			8	0.22	6.28E+13	2.43E+14	1.80E+14
			20	0.20	6.28E+13	2.67E+14	2.04E+14
			24	0.18	6.28E+13	3.07E+14	2.44E+14
10	dye 100 mg/L + soaping agent 500 mg/L	ES-20	0	0.83	6.55E+13	6.55E+13	0.00E+00
			1	0.27	6.55E+13	2.01E+14	1.36E+14
			4	0.21	6.55E+13	2.55E+14	1.89E+14
			8	0.19	6.55E+13	2.79E+14	2.14E+14
			20	0.18	6.55E+13	3.02E+14	2.36E+14
			24	0.16	6.55E+13	3.32E+14	2.67E+14
11	dye 500 mg/L + soaping agent 100 mg/L	ES-20	0	0.83	6.51E+13	6.51E+13	0.00E+00
			1	0.26	6.51E+13	2.07E+14	1.42E+14
			4	0.23	6.51E+13	2.35E+14	1.70E+14
			8	0.21	6.51E+13	2.53E+14	1.88E+14
			20	0.20	6.51E+13	2.76E+14	2.11E+14
			24	0.20	6.51E+13	2.76E+14	2.11E+14
12	dye 500 mg/L + soaping agent 500 mg/L	ES-20	0	0.81	6.69E+13	6.69E+13	0.00E+00
			1	0.32	6.69E+13	1.70E+14	1.03E+14
			4	0.29	6.69E+13	1.87E+14	1.21E+14
			8	0.27	6.69E+13	1.98E+14	1.31E+14
			12	0.25	6.69E+13	2.18E+14	1.52E+14
			24	0.23	6.69E+13	2.38E+14	1.71E+14
13	dye 500 mg/L + TX 100 mg/L	ES-20	0	0.74	7.36E+13	7.36E+13	0.00E+00
			1	0.26	7.36E+13	2.05E+14	1.32E+14
			4	0.24	7.36E+13	2.30E+14	1.57E+14
			8	0.23	7.36E+13	2.38E+14	1.64E+14
			12	0.22	7.36E+13	2.47E+14	1.74E+14
			24	0.20	7.36E+13	2.68E+14	1.95E+14
14	dye 100 mg/L + SDS 100 mg/L	ES-20	0	0.89	6.08E+13	6.08E+13	0.00E+00
			1	0.46	6.08E+13	1.17E+14	5.64E+13
			4	0.41	6.08E+13	1.31E+14	7.07E+13
			8	0.40	6.08E+13	1.36E+14	7.56E+13
			20	0.38	6.08E+13	1.41E+14	8.03E+13
			24	0.38	6.08E+13	1.44E+14	8.36E+13
15	dye 500 mg/L + SDS 100 mg/L	ES-20	0	0.96	5.65E+13	5.65E+13	0.00E+00
			1	0.48	5.65E+13	1.12E+14	5.59E+13
			4	0.42	5.65E+13	1.28E+14	7.16E+13
			8	0.40	5.65E+13	1.34E+14	7.76E+13
			20	0.38	5.65E+13	1.43E+14	8.61E+13
			24	0.37	5.65E+13	1.48E+14	9.15E+13

Appendix Table D3 Effect of reactive dye and EfOMs on fouling potential of surfactant

Run no	Feed water	Membrane	Time (h)	Flux 30^{O}C (m/d)	R_M	R_T	R_F
16	dye 500 mg/L + EfOMs	ES-20	0	0.85	6.40E+13	6.40E+13	0.00E+00
			1	0.42	6.40E+13	1.30E+14	6.62E+13
			4	0.40	6.40E+13	1.36E+14	7.24E+13
			8	0.39	6.40E+13	1.39E+14	7.49E+13
			20	0.39	6.40E+13	1.39E+14	7.49E+13
			24	0.39	6.40E+13	1.38E+14	7.41E+13
17	soaping agent 100 mg/L + EfOMs	ES-20	0	0.80	6.80E+13	6.80E+13	0.00E+00
			1	0.31	6.80E+13	1.72E+14	1.04E+14
			4	0.31	6.80E+13	1.76E+14	1.08E+14
			8	0.30	6.80E+13	1.83E+14	1.15E+14
			20	0.29	6.80E+13	1.84E+14	1.16E+14
			24	0.29	6.80E+13	1.88E+14	1.20E+14
18	soaping agent 500 mg/L + EfOMs	ES-20	0	0.96	5.62E+13	5.62E+13	0.00E+00
			1	0.35	5.62E+13	1.57E+14	1.00E+14
			4	0.32	5.62E+13	1.69E+14	1.13E+14
			8	0.29	5.62E+13	1.88E+14	1.32E+14
			20	0.28	5.62E+13	1.94E+14	1.38E+14
			24	0.28	5.62E+13	1.94E+14	1.38E+14
19	TX 100 mg/L + EfOMs	ES-20	0	0.77	7.00E+13	7.00E+13	0.00E+00
			1	0.32	7.00E+13	1.69E+14	9.92E+13
			4	0.30	7.00E+13	1.78E+14	1.08E+14
			8	0.29	7.00E+13	1.86E+14	1.15E+14
			12	0.28	7.00E+13	1.95E+14	1.25E+14
			24	0.27	7.00E+13	2.00E+14	1.30E+14
20	SDS 100 mg/L + EfOMs	ES-20	0	0.79	6.90E+13	6.90E+13	0.00E+00
			1	0.41	6.90E+13	1.33E+14	6.44E+13
			4	0.39	6.90E+13	1.38E+14	6.89E+13
			8	0.39	6.90E+13	1.39E+14	6.99E+13
			20	0.37	6.90E+13	1.48E+14	7.90E+13
			24	0.31	6.90E+13	1.76E+14	1.07E+14
21	dye 500 mg/L + soaping agent 100 mg/L + EfOMs	ES-20	0	1.02	5.33E+13	5.33E+13	0.00E+00
			1	0.35	5.33E+13	1.55E+14	1.01E+14
			4	0.34	5.33E+13	1.58E+14	1.05E+14
			8	0.33	5.33E+13	1.63E+14	1.10E+14
			20	0.33	5.33E+13	1.66E+14	1.13E+14
			24	0.32	5.33E+13	1.70E+14	1.16E+14
22	dye 500 mg/L + soaping agent 500 mg/L + EfOMs	ES-20	0	0.89	6.08E+13	6.08E+13	0.00E+00
			1	0.35	6.08E+13	1.53E+14	9.26E+13
			4	0.33	6.08E+13	1.67E+14	1.06E+14
			8	0.32	6.08E+13	1.71E+14	1.10E+14
			20	0.31	6.08E+13	1.76E+14	1.16E+14
			24	0.30	6.08E+13	1.79E+14	1.19E+14
23	dye 500 mg/L + TX 100 mg/L + EfOMs	ES-20	0	0.88	6.12E+13	6.12E+13	0.00E+00
			1	0.34	6.12E+13	1.60E+14	9.86E+13
			4	0.32	6.12E+13	1.69E+14	1.08E+14
			8	0.31	6.12E+13	1.74E+14	1.12E+14
			20	0.28	6.12E+13	1.93E+14	1.32E+14
			24	0.27	6.12E+13	1.99E+14	1.38E+14
24	dye 500 mg/L + SDS 100 mg/L + EfOMs	ES-20	0	0.90	6.02E+13	6.02E+13	0.00E+00
			1	0.40	6.02E+13	1.35E+14	7.45E+13
			4	0.37	6.02E+13	1.45E+14	8.46E+13
			8	0.37	6.02E+13	1.46E+14	8.54E+13
			20	0.36	6.02E+13	1.49E+14	8.93E+13
			24	0.35	6.02E+13	1.55E+14	9.46E+13

Appendix Table D4 Fouling potential of organic foulants on membrane model LF-10

Run no	Feed water	Membrane	Time (h)	Flux 30^{O}C (m/d)	R_M	R_T	R_F
25	dye 500 mg/L	LF-10	0	0.56	9.69E+13	9.69E+13	0.00E+00
			1	0.32	9.69E+13	1.70E+14	7.29E+13
			4	0.31	9.69E+13	1.78E+14	8.07E+13
			8	0.30	9.69E+13	1.82E+14	8.49E+13
			12	0.29	9.69E+13	1.88E+14	9.12E+13
			24	0.29	9.69E+13	1.90E+14	9.32E+13
26	soaping agent 100 mg/L	LF-10	0	0.61	8.88E+13	8.88E+13	0.00E+00
			1	0.31	8.88E+13	1.74E+14	8.48E+13
			4	0.28	8.88E+13	1.96E+14	1.07E+14
			8	0.26	8.88E+13	2.11E+14	1.22E+14
			12	0.24	8.88E+13	2.28E+14	1.40E+14
			24	0.21	8.88E+13	2.53E+14	1.64E+14
27	TX 100 mg/L	LF-10	0	0.44	1.22E+14	1.22E+14	0.00E+00
			1	0.23	1.22E+14	2.40E+14	1.17E+14
			4	0.21	1.22E+14	2.59E+14	1.37E+14
			8	0.20	1.22E+14	2.68E+14	1.46E+14
			12	0.19	1.22E+14	2.91E+14	1.69E+14
			24	0.18	1.22E+14	3.01E+14	1.78E+14
28	SDS 100 mg/L	LF-10	0	0.43	1.25E+14	1.25E+14	0.00E+00
			1	0.28	1.25E+14	1.95E+14	6.96E+13
			4	0.26	1.25E+14	2.05E+14	8.00E+13
			8	0.26	1.25E+14	2.11E+14	8.56E+13
			12	0.26	1.25E+14	2.11E+14	8.56E+13
			24	0.24	1.25E+14	2.22E+14	9.68E+13
29	dye 500 mg/L + TX 100 mg/L	LF-10	0	0.53	1.03E+14	1.03E+14	0.00E+00
			1	0.27	1.03E+14	2.04E+14	1.02E+14
			4	0.24	1.03E+14	2.30E+14	1.27E+14
			8	0.22	1.03E+14	2.46E+14	1.44E+14
			20	0.21	1.03E+14	2.64E+14	1.62E+14
			24	0.19	1.03E+14	2.82E+14	1.80E+14
30	EfOMs	LF-10	0	0.45	1.20E+14	1.20E+14	0.00E+00
			1	0.28	1.20E+14	1.94E+14	7.41E+13
			4	0.30	1.20E+14	1.84E+14	6.36E+13
			8	0.30	1.20E+14	1.84E+14	6.36E+13
			20	0.30	1.20E+14	1.84E+14	6.36E+13
			24	0.30	1.20E+14	1.78E+14	5.82E+13
31	dye 500 mg/L + TX 100 mg/L + EfOMs	LF-10	0	0.51	1.06E+14	1.06E+14	0.00E+00
			1	0.27	1.06E+14	2.04E+14	9.77E+13
			4	0.25	1.06E+14	2.13E+14	1.07E+14
			8	0.24	1.06E+14	2.28E+14	1.22E+14
			20	0.23	1.06E+14	2.32E+14	1.27E+14
			24	0.23	1.06E+14	2.34E+14	1.28E+14

Appendix Table D5 The values of ΔJΔV

Run no	Feed water	Membrane	ΔJ/ΔV
1	dye 500 mg/L	ES-20	26.0
2	soaping agent 50 mg/L	ES-20	77.4
3	soaping agent 100 mg/L	ES-20	96.7
4	soaping agent 300 mg/L	ES-20	92.6
5	soaping agent 500 mg/L	ES-20	67.9
6	TX 100 mg/L	ES-20	64.4
7	SDS 100 mg/L	ES-20	30.8
8	dye 100 mg/L + soaping agent 100 mg/L	ES-20	71.5
9	dye 100 mg/L + soaping agent 500 mg/L	ES-20	95.1
10	dye 500 mg/L + soaping agent 100 mg/L	ES-20	53.8
11	dye 500 mg/L + soaping agent 500 mg/L	ES-20	60.6
12	dye 500 mg/L + TX 100 mg/L	ES-20	48.7
13	dye 100 mg/L + SDS 100 mg/L	ES-20	38.0
14	dye 500 mg/L + SDS 100 mg/L	ES-20	50.4
15	EfOMs	ES-20	16.2
16	dye 500 mg/L + EfOMs	ES-20	10.6
17	soaping agent 100 mg/L + EfOMs	ES-20	15.4
18	soaping agent 500 mg/L + EfOMs	ES-20	40.1
19	TX 100 mg/L + EfOMs	ES-20	29.9
20	SDS 100 mg/L + EfOMs	ES-20	45.3
21	dye 500 mg/L + soaping agent 100 mg/L + EfOMs	ES-20	16.3
22	dye 500 mg/L + soaping agent 500 mg/L + EfOMs	ES-20	28.1
23	dye 500 mg/L + TX 100 mg/L + EfOMs	ES-20	38.7
24	dye 500 mg/L + SDS 100 mg/L + EfOMs	ES-20	24.5
25	dye 500 mg/L	LF-10	20.1
26	soaping agent 100 mg/L	LF-10	69.5
27	TX 100 mg/L	LF-10	62.3
28	SDS 100 mg/L	LF-10	23.1
29	dye 500 mg/L + TX 100 mg/L	LF-10	58.3
30	EfOMs	LF-10	-14.8
31	dye 500 mg/L + TX 100 mg/L + EfOMs	LF-10	25.0

Appendix Table D6 ΔR and the hydraulic resistance removal efficiency (RR, %)

Run no	Feed water	Membrane	ΔR (m^{-1}) fouled membrane	ΔR (m^{-1}) cleaned with water	ΔR (m^{-1}) cleaned with alkaline	RR (%) water	RR (%) alkaline
1	dye 500 mg/L	ES-20	1.459E+13	1.328E+13	1.073E+12	9.0	92.6
2	soaping agent 50 mg/L	ES-20	6.696E+13	5.744E+13	2.004E+13	14.2	70.1
3	soaping agent 100 mg/L	ES-20	1.115E+14	8.838E+13	2.796E+13	20.7	74.9
4	soaping agent 300 mg/L	ES-20	1.186E+14	1.014E+14	3.842E+13	14.6	67.6
5	soaping agent 500 mg/L	ES-20	6.148E+13	4.968E+13	2.515E+13	19.2	59.1
6	TX 100 mg/L	ES-20	4.039E+13	3.056E+13	1.587E+13	24.3	60.7
7	SDS 100 mg/L	ES-20	6.437E+12	3.946E+12	-1.118E+12	38.7	117.4
8	dye 100 mg/L + soaping agent 100 mg/L	ES-20	7.585E+13	6.195E+13	2.594E+13	18.3	65.8
9	dye 100 mg/L + soaping agent 500 mg/L	ES-20	1.079E+14	8.633E+13	6.722E+13	20.0	37.7
10	dye 500 mg/L + soaping agent 100 mg/L	ES-20	7.357E+13	5.968E+13	2.813E+13	18.9	61.8
11	dye 500 mg/L + soaping agent 500 mg/L	ES-20	7.976E+13	6.250E+13	2.297E+13	21.6	71.2
12	dye 500 mg/L + TX 100 mg/L	ES-20	3.330E+13	2.518E+13	1.286E+13	24.4	61.4
13	dye 100 mg/L + SDS 100 mg/L	ES-20	9.840E+12	5.711E+12	-1.361E+12	42.0	113.8
14	dye 500 mg/L + SDS 100 mg/L	ES-20	1.852E+13	1.217E+13	1.740E+12	34.3	90.6
15	EfOMs	ES-20	3.867E+12	-3.512E+11		109.1	
16	dye 500 mg/L + EfOMs	ES-20	5.321E+12	4.358E+12	1.442E+11	18.1	97.3
17	soaping agent 100 mg/L + EfOMs	ES-20	4.772E+13	4.601E+13	2.077E+13	3.6	56.5
18	soaping agent 500 mg/L + EfOMs	ES-20	6.935E+13	5.923E+13	2.505E+13	14.6	63.9
19	TX 100 mg/L + EfOMs	ES-20	1.988E+13	1.230E+13	8.146E+12	38.1	59.0
20	SDS 100 mg/L + EfOMs	ES-20	1.677E+13	1.437E+13	6.265E+12	14.3	62.6
21	dye 500 mg/L + soaping agent 100 mg/L + EfOMs	ES-20	4.583E+13	4.208E+13	2.433E+13	8.2	46.9
22	dye 500 mg/L + soaping agent 500 mg/L + EfOMs	ES-20	4.922E+13	3.459E+13	3.351E+12	29.7	93.2
23	dye 500 mg/L + TX 100 mg/L + EfOMs	ES-20	1.332E+13	4.741E+12	-5.070E+12	64.4	138.1
24	dye 500 mg/L + SDS 100 mg/L + EfOMs	ES-20	1.392E+13	1.286E+13	5.755E+12	7.6	58.7
25	dye 500 mg/L	LF-10	1.646E+13	1.478E+13	-2.109E+12	10.2	112.8
26	soaping agent 100 mg/L	LF-10	6.596E+13	5.638E+13	1.615E+13	14.5	75.5
27	TX 100 mg/L	LF-10	3.037E+13	2.328E+13	-4.533E+12	23.4	114.9
28	SDS 100 mg/L	LF-10	-2.746E+12				
29	dye 500 mg/L + TX 100 mg/L	LF-10	2.908E+13	1.921E+13	-3.665E+12	33.9	112.6
30	EfOMs	LF-10	-1.562E+13				
31	dye 500 mg/L + TX 100 mg/L + EfOMs	LF-10	1.332E+13	4.741E+12	-5.070E+12	64.4	138.1

Note : 1. ΔR (fouled membrane) = R (fouled membrane) - R (new membrane)
2. ΔR (cleaned with water) = R (cleaned with water) - R (new membrane)
3. ΔR (cleaned with alkaline) = R (cleaned with alkaline) - R (new membrane)
4. Alkaline solution was NaOH pH 10.5

Appendix E

Temperature coefficient factor

Temperature coefficient factor

The temperature coefficient factor (TCF) was investigated for standardization of the error due to a viscosity at different temperature. Two relationships were studied i.e., pressure versus pure water flow rate, and temperature versus pure water flow rate, respectively. The relationship between TCF and temperature are shown in **Equations E1 and E2** (ASTM D 4516-00).

$$Q_T = Q_{25^oC} \text{x} TCF \quad \text{E1)}$$

$$TCF = \theta^{(T-25)} \quad \text{E2)}$$

where $Q_{25°C}$ is the pure water flow rate at 25 ^{O}C (mL/min), Q_T is the pure water flow rate at operating temperature (mL/min).

In order to investigate TCF-value, two relationships were studied i.e., trans-membrane pressure versus pure water flow rate, and temperature versus pure water flow rate, respectively. The relationship between TMP and pure water flow rate is shown in **Appendix Table E1 and Figure E1**.

Appendix Table E1 The relationship between transmembrane pressure and pure water flow rate

Transmembrane pressure (MPa)	Temperature (^{O}C)	Pure water flow rate (mL/min)
0.35	25	0.210
	35	0.251
	40	0.305
1.00	25	0.545
	35	0.752
	40	0.890
1.50	25	0.850
	35	1.090
	40	1.327

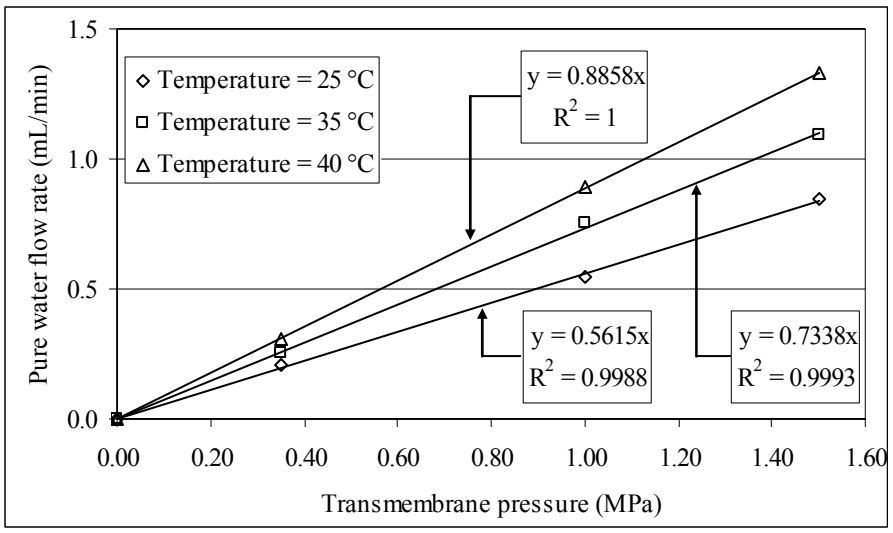

Appendix Figure E1 Effect of temperature and transmembrane pressure on pure water flow rate

An average Θ value of 1.029 was calculated from flow rate data in **Appendix Figure E1** as showed in **Appendix Table E2**. The Θ values from calculation and ASTM recommendation (Θ = 1.030) were compared by sum of squared error (SSE). Subsequently, SSE valued of ASTM recommendation showed higher superiority than the average value. Then, Θ value of 1.030 was used in this research.

Appendix Table E2 Comparison of pure water flow rate between measuring method and ASTM equation.

TMP (MPa)	Temperature (^{O}C)	Pure water flow rate(mL/min)				
		Equation from figure 1	Θav	ASTM equation		
				Θ = 1.029	Θ = 1.030	Θ = 1.031
0.35	25	0.197	1.029	0.197	0.197	0.197
	35	0.257		0.262	0.264	0.267
	40	0.310		0.302	0.306	0.311
1.00	25	0.562	1.029	0.562	0.562	0.562
	35	0.734		0.747	0.755	0.762
	40	0.886		0.864	0.875	0.888
1.50	25	0.842	1.029	0.842	0.842	0.842
	35	1.101		1.121	1.132	1.143
	40	1.329		1.293	1.312	1.331
SSEav				0.0008	0.0006	0.0009

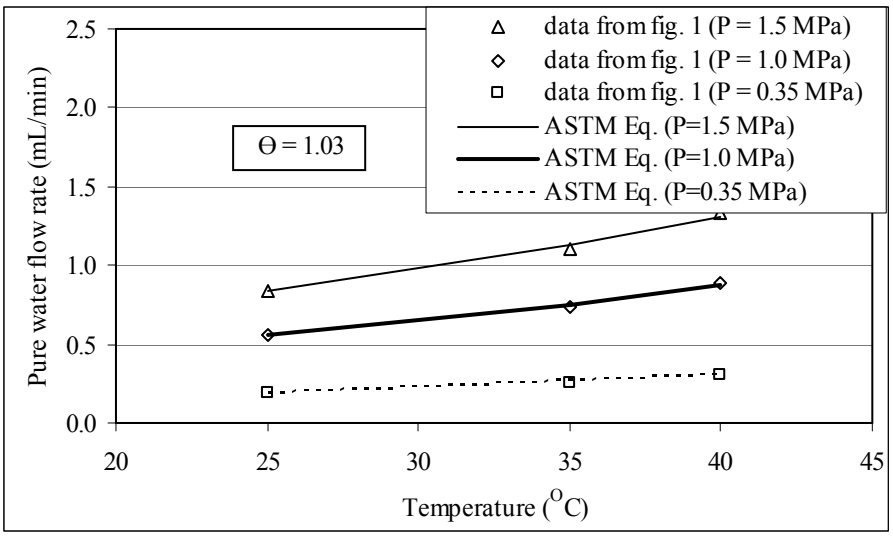

Appendix Figure E2 Comparison of pure water flow rate between measuring method and ASTM equation (Θ = 1.03)

Appendix F

Calculation of cross flow velocity in spiral wound membrane filtration unit

Calculation of cross flow velocity in spiral wound membrane filtration unit

The cross flow velocity above membrane surface was controlled at 0.86 cm/s by controlling feed flow rate. The cross section of spiral wound membrane (BW-2012) and the technical data are shown in appendix Figure F1 and Appendix Table F1.

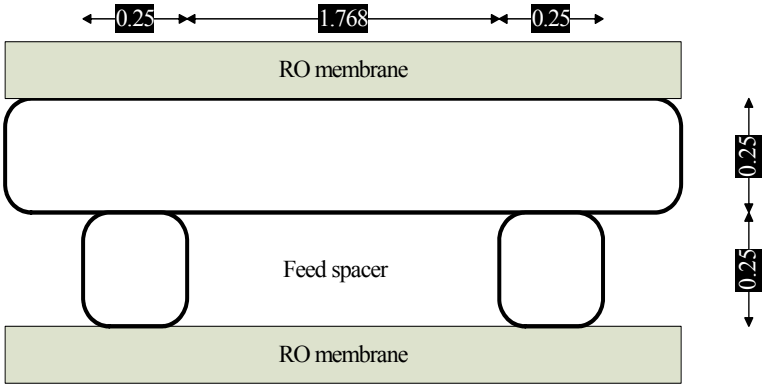

Appendix Figure F1 Cross section of spiral wound membrane (BW-2012)

Appendix Table F1 Technical data of spiral wound membrane BW-2012

Item	Data
Membrane area	0.40 m^2/module
Number of flat sheet	4 sheets/module
length of flat sheet	475 mm
Number of feed spacer	3 channels/module
Height of feed spacer	0.5 mm

The calculation is shown as follows.

Feed flow rate	=	1.6	L/min
Number of transverse filament $475/(1.768+0.25)$	=	235	lines
Area of feed flow $(475-(235x0.25))x0.25x3x10^{-6}$	=	$3.12x10^{-4}$	m^2
Cross flow velocity $(1.6x10^{-3})/(3.12x10^{-4}x60)$	=	0.086	m/s

CIRRICULUM VITAE

NAME Mr. Thirdpong Srisukphun

BIRTH DATE 5 November 1974

BIRTH PLACE Bangkok, Thailand

EDUCATION	**YEAR**	**INSTITUTE**	**DEGREE**
	1997	King Mongkut Univ. Technol.	B. Eng. (Environmental Engineering)
	2002	Kasetsart Univ.	M. Eng. (Environmental Engineering)

WORK PLACE Department of Environmental Health, Faculty of Public and Environmental Health, Huachiew Chalermprakiet University

SCHOLARSHIP 1) The Japan Society for the Promotion of Science (JSPS)
2) Kasetsart University Research and Development